Spatiotemporal variability of the fraction of Photosynthetically Active Radiation (fPAR) in a mixed coniferous forest using Wireless sensor networks

by

Yuhui Ke

A thesis submitted in partial fulfillment of the requirements for the degree of

Master of Science

Earth and Atmospheric Sciences
University of Alberta

Abstract

Contemporary climate change has become rapid, and its impacts affect forest growth and productivity directly and indirectly through changes in temperature, precipitation, carbon dioxide, and other factors. Forest ecosystem plays an essential role in carbon exchange between the atmosphere and terrestrial. Green plants absorb carbon from the atmosphere through photosynthesis, whereas degradation and deforestation release carbon. Given appropriate and efficient management, forest can be a beneficial asset in climate mitigation. The fraction of photosynthetically active radiation (fPAR) is a fundamental term to quantifying light used by plants in photosynthesis. This term has been mainly derived from satellite data, but some inherent issues of satellite data limit the quality of long-term fPAR estimation. Advances in technology and the emergence of wireless sensor networks have allowed for long-term, continuous, high spatial and temporal fPAR measurements. In Chapter 1, the general methods of estimating fPAR are reviewed, and the importance of accurate fPAR estimation and factors that can cause measurement bias are explored. Needs for long-term fPAR study and its role in forest dynamics are proposed, and the research questions and hypotheses of this thesis are then posed.

In Chapter 2, forest structure metrics, such as leaf area index (LAI), were extracted from the 3D point cloud developed by terrestrial laser scanning (TLS). In situ wireless sensor networks (WSNs) were used to collect continuous photosynthetically active radiation (PAR) in the mixed coniferous Graswang forest site and were calculated into fPAR. The spatial distribution of fPAR from 2016 to 2019 was compared and analyzed using Kriging

interpolation to determine the spatiotemporal variation of fPAR in the mixed wood forest. Chi-square statistical test was performed to assess the significance of fPAR variation. To better understand the vertical forest structure of the study site, metrics such as LAI, centroid (Cx, Cy), and radius of gyration (RG) were interpolated to explore and understand the spatial forest structure variation. Forest inventory included tree species, diameter breast height (DBH), and mortality was documented. To assess the influence factors on fPAR, multiple correlation analyses was used between LAI, tree species type, mortality and fPAR.

The third chapter of this thesis examined the significance of the results concluded in Chapter 2 and suggested the study's limitation. Potential future explorations are proposed, including the advance of wireless sensor networks outdoor performance and factors, such as mortality and drought, influence on the effect of LAI on fPAR in a coniferous and deciduous mixed forest.

Preface

The research conducted in this thesis is the culmination of a joint effort between the Geography department in Ludwig-Maximilians-Universitaet Muenchen under the direction of Dr. Ralf Ludwig, and the Centre for Earth Observation Sciences led by Dr. G.A. Sanchez-Azofeifa.

Terrestrial laser scanning of the Graswang forest used in Chapter 2 were collected by Ian Sharp. PAR data from wireless sensor networks was uploaded to Enviro-Net by Ludwig-Maximilians-Universitaet Muenchen. The forest inventory was collected by Birgitta Putzenlechner. The project was designed by Dr. G.A. Sanchez-Azofeifa, and I performed the data analysis and results in Chapter 2.

Acknowledgements

First and foremost, I have to thank my research supervisor Dr. Arturo Sanchez-Azofeifa for giving me the opportunity to join his lab and learn about remoting sensing. Without his assistance and profound belief in my work, this thesis would have never been accomplished. I would like to thank for his constant support and guidance over the past years. It gave me the confidence and lighten up my way forward.

I would like to extend my sincere thanks to my committee, including Dr. Ralf Ludwig and Dr. Kati Laakso, for their insightful comments and suggestions. Their kind help and dedicated involvement in every step throughout the process during the COVID year calmed my anxiety and pushed my research forward.

I take this opportunity to express gratitude to all of the CEOS members for their help and support. I also thank my parents for the unceasing encouragement and endless support.

Table of Contents

List of Tables

List of Figures

Chapter 1 - Introduction

1.1 Background and Motivation

Nowadays, climate change has become a hot topic in all kinds of disciplines. Its impacts can be seen throughout every aspect of the world we live in and are threatening the ecosystem, biodiversity, and human health (Diffey, 2004). Rapid changes of climate has induced a series of dangerous weather events. Events such as drought, storms, heatwaves, rising sea levels, melting glaciers and warming oceans are more severe and frequent than before (National Academies of Sciences and Medicine, 2016). The dominant cause of rapid climate change is widely recognized as human activities, such as burning fossil fuels and deforestation (Somerville, 2020). These anthropogenic activities emit carbon dioxide and methane in the atmosphere and have risen the dominant greenhouse gases stored in Earth's atmosphere now about 45% more than they were in the early 1800s (Somerville, 2020). The average global land and ocean temperature has also risen and caused the average thickness of glaciers decreased more than 60 feet and the sea ice cover survives the summer melt season has declined to approximately half of its extent since 1980 (Francis and Wu, 2020). Rising sea levels due to thermal expansion, in addition to melting ice sheets and glacier, put coastal areas at great risk of erosion and storm surge (Bindoff et al., 2007). The potential impacts of climate change on human lives, socioeconomics, and ecosystems highlight the importance of understanding all the components of the climate system. With this knowledge, one can simulate a better prediction of future climate scenarios and be used as a vital component to policy makers to develop climate change mitigation and adaptation strategies.

In the study of the Earth's climate system, most research focuses on the changes of more visible components such as the carbon cycle (Friedlingstein, 2015; Friedlingstein et al., 2003, 2001; Mitchard, 2018) and the water cycle (Ellison et al., 2017; Imbach et al., 2012; Tao et al., 2003). Whereas less observable climate variables, such as photosynthesis, have just started to catch more attention. Photosynthesis is a major process leading to primary production in the biosphere and is considered the fundamental life process for plants and animals (Craggs,

2016). Plants take carbon dioxide out of the atmosphere through photosynthesis and thus help reduce the greenhouse gases concentration. This process fixes more than 100bn out of 7000bn tons of carbon dioxide annually in the atmosphere (Baslam et al., 2020). Previous experimental studies show that photosynthesis can be strongly affected by climate variables such as temperature (Medlyn et al., 2002; Sieber et al., 2016) and carbon dioxide concentration (Sanz- Sáez et al., 2017; Urban, 2003). Therefore, having a good understanding of the role photosynthesis plays in climate change and the impact of changing environmental conditions on its performance can be an asset in climate mitigation, starting from carbon balance.

Photosynthetically Active Radiation (PAR) is the part of electromagnetic radiation in the spectral range from 400 nm to 700 nm that can be used as the source of energy for photosynthesis by green plants (Mõttus et al., 2012). The PAR absorbed by plants for photosynthesis (APAR) can be either measured directly using PAR sensors or estimated indirectly based on canopy gap fraction measurements. Fraction of Photosynthetically Active Radiation (fPAR) is a fundamental term in the quantification of light used by plants in photosynthesis. It is represented by the ratio of APAR relative to the incident PAR on the top of the canopy (Fensholt et al., 2004). FPAR is one of the critical biophysical variables for the quantitative analysis of many physical and biological processes related to vegetation dynamics (Knorr et al., 2005). A detailed estimation and characterization of fPAR provide information for assessing the gross primary production (GPP), terrestrial net primary production (NPP), light-use efficiency (Fan et al., 2014), the associated fixation of atmospheric carbon dioxide and the energy balance of the surface (GCOS, 2016). Thus, long-term monitoring with high temporal and spatial resolution fPAR data is required.

The estimation of fPAR can be divided into remote sensing and in situ measurements. The in situ measurement obtains high temporal resolution data, while remote sensing quantifies the spatial heterogeneity data of fPAR (Senna et al., 2005). The ability of providing spatial distribution functions of land-surface properties makes remote sensing a good asset in fPAR measurements. Regional and global fPAR datasets can now be derived from multiple sensors,

including Moderate Resolution Imaging Spectroradiometer (MODIS) (Dong et al., 2016; Li et al., 2020; Myneni et al., 2002; Yang et al., 2006), Sea-Viewing Wide Field-of-View Sensor (SeaWiFS) (Wang et al., 2001), the Medium Resolution Imaging Spectrometer (MERIS) (Myneni, 2001; Sun et al., 2014; Yang et al., 2014), Advanced Very High Resolution Radiometer (AVHRR) (Claverie et al., 2016), and Sentinel-2 (Dong et al., 2015; Putzenlechner et al., 2019a; Sun et al., 2021). Research assesses the performance of these satellite products in estimating fPAR and finds the differences are consistent over most of the land cover types excepts forests (Pickett-Heaps et al., 2014; Tao et al., 2015). The reason could be the varied assumptions in the retrieval algorithms, as well as the disparities between green and total fPAR products over forests due to tree trunks and branches absorption (Tao et al., 2015). These satellite products play an essential role in measuring and monitoring surface variables such as fPAR and provide an opportunity to gain insight into the dynamic processes within ecosystems. However, accurate estimation across broad spatial extents and long periods require efficient methods, calibration and validation for derived fPAR products (Fritsch et al., 2012; Majasalmi et al., 2014; Nestola et al., 2017; Putzenlechner et al., 2019a; Serbin et al., 2013). Issues such as weather conditions and propagation delay could extend the challenge of calibration and validation of the sensor. The weather condition, for instance atmospheric interference and cloud cover, can limit the availability and quality of satellite data (Reiche et al., 2016); its ability to monitor temporal variability is unreliable due to its propagation delay, brings the uncertainty of using satellite data in detecting small climate changes such as important phenological events (Ryu et al., 2014) and subtle changes in forest productivity. Due to these limitations and constraints, the in situ sensor has been advanced to produce high-quality time series data and has become popular in temporal observation (Moreno et al., 2014).

In situ measurements of fPAR are usually combined with satellite data and used as reference data for satellite-derived fPAR products validation (Fensholt et al., 2004; Liu et al., 2019; Putzenlechner et al., 2020; Tao et al., 2016). In situ sensors technologies are increasingly being implemented for environmental and climate monitoring. Compared with satellite-derived fPAR, in situ methods quantify the fPAR at a local scale and provide

spatially precise, continuous, and near real-time data (Kotamäki et al., 2009). In situ fPAR is generally measured by radiation monitoring or detecting directional gap fraction using hemispherical photographs (Wang et al., 2016). Some common in situ instruments are Digital Hemispherical Photography (DHP) (Baret et al., 1993; Whitmore et al., 1993), PAR ceptometer (AccuPAR) (Camacho et al., 2021), and Light Detection and Ranging (LiDAR) (Luo et al., 2014; Qin et al., 2017; Thomas et al., 2006). One of the recent improvements in in situ measurement is Wireless sensor networks (WSNs). It has gained a lot of popularity due to its ability to provide continuous, automated, and high temporal and spatial resolution data of dynamic environmental processes in remote locations with poor accessibility (Rankine et al., 2014). This technique has been widely used in environmental applications (Aslan et al., 2012; Bauer et al., 2019; Díaz-Ramírez et al., 2012; Pawlowski et al., 2009; Qu et al., 2014) and is an effective tool of measuring key micro-meteorological variables sensitive to climate change and land use/cover change (Sánchez-Azofeifa et al., 2011). WSN enables the execution of asynchronous operations according to a timetable or set of rules, as well as the construction of data collection networks with minimal wire infrastructure (Ferre et al., 2010). Regardless of the strength, the individual nodes in WSNs still has concerns with long-duration and large-scale environmental monitoring and are constrained by limited processing speed, storage capacity, and communication bandwidth (Corke et al., 2010; Matin and Islam, 2012). WSN has the advantage of increasing the observational sample area for continuous PAR data, which allows capturing spatial and temporal variation (Rankine et al., 2014). As the advancements in communication and computing technologies, WSN may become more suitable for outdoor environment as it was original designed for indoor and provides more information in responding to environment issues, for instant droughts and extreme temperature events. Hence, exploring the utility of WSN for long-term fPAR monitoring outdoor is necessary to advance the usefulness of in situ technologies in monitoring forest phenology and understanding the biosphere.

FPAR value results directly from the radiative transfer in the canopy and depends on canopy structure, vegetation element optical properties and illumination conditions (Peng et al., 2012). The estimation of fPAR, both satellite-derived and in situ, still have considerable bias.

Studies show that changes in solar zenith angle, wind speed (Putzenlechner et al., 2019b), atmospheric conditions (Liu et al., 2019), and surface roughness (Zhao et al., 2016) can create bias in fPAR estimation. Phenological conditions, such as Leaf angle distribution (LAD) (Fensholt et al., 2004), foliage clumping (Hovi et al., 2017), and canopy structure (Liang et al., 2017), could also vary fPAR estimation. Leaf Area Index (LAI), an Essential Climate Variable (ESV), is one of the most informative parameters for monitoring forest function (Culvenor et al., 2014). It is defined as one-sided green leaf area per unit ground area in broadleaf canopies (Chen and Black, 1992) and as the projected needle leaf area in coniferous canopies (Myneni et al., 2002). LAI varies with stand development, stand structure, and environmental conditions, which also affect the carbon exchange, water balance, evapotranspiration, and vegetation photosynthesis (Vose et al., 1994). Hence, the estimation of LAI becomes important in assessing vegetation phenology and climate change impact.

Direct measurements of LAI, such as harvesting, allometry and litter collection (Breda, 2003), are considered the most accurate and hence are often used as reference for calibrating or validating indirect methods (Sonnentag et al., 2007). However, all direct measurements have the disadvantage of being labor-intensive and time-consuming, making them unsuitable for long-term monitoring (Jonckheere et al., 2004). Indirect measurements require less time and labor and are more practical for collecting extensive spatial and temporal data. Most frequently used indirect methods are ground-based instruments (LAI-2000, hemispherical photography) and above-canopy methods (satellite, terrestrial and airborne laser scanning) (Goude et al., 2019). Terrestrial laser scanning (TLS), a ground-based LiDAR, provides a measurement technique that can acquire a three-dimensional detail from the surrounding area. It has been used in documenting basic tree attributes, such as DBH (Murphy et al., 2010; Vastaranta et al., 2009) and has shown to be capable of determining important tree attributes that are not directly measurable in conventional forest inventories, such as gap fraction, leaf area profile, and plant area volume density (Anderson et al., 2016; Danson et al., 2007). Some of these attributes are tightly related to climate changes and are able to provide special viewpoint of climate dynamic by document data consecutively in a time series (Liang et al.,

2012; Luoma et al., 2021; Srinivasan et al., 2014). The utility of TLS in LAI estimation still require more research.

Both fPAR and LAI are used for calculating surface photosynthesis, evapotranspiration, and net primary production, hence are the two key variables in most climatic, hydrological, biogeochemical, and ecological models. (Chen et al., 2019). Because of their linkage, a number of LAI/fPAR products have been developed from satellite data algorithms, for instance MODIS (Fu and Wu, 2017; Ranga B Myneni et al., 2002; Serbin et al., 2013; Shabanov et al., 2003; Zhu et al., 2013), MISR (Hu et al., 2007; Tao et al., 2016, 2015), VIIRS (Xiao et al., 2016; Xu et al., 2018), and Sentinel-2 (Li et al., 2015; Putzenlechner et al., 2019a). These products were extracted from non-geostationary satellite observations (Chen et al., 2019), and their uncertainties are evaluated (Hu et al., 2007; Pu et al., 2020; Xu et al., 2018). The impact of LAI on fPAR has also been studied but mainly used satellite-based data (Myneni et al., 2002; Y. Tian et al., 2004; Yang et al., 2006). However, the satellite data are not spatially and temporally continuous due to the orbital period and climate conditions (Chen et al., 2019). Hence, having a better understanding of the influence of LAI on fPAR helps monitor the impact of climate change and provide mitigation strategies by interfering with forest ecosystem.

1.2 Specific hypothesis and objectives

With the background information and some context of the previous scientific research, the state of fPAR knowledge about its spatiotemporal variability in a mixed wood forest the purpose of this thesis can be introduced. While fPAR have primarily been derived from satellite data, advanced in situ technology, Wireless Sensor Networks, still require further exploration in its long-term duration monitoring. Most studies of long-term fPAR have conducted in boreal forest (Serbin et al., 2013; Tao et al., 2016; J. L. Widlowski, 2010; Yang et al., 2021), and only a few are in temperate forest (Carrer et al., 2013; Parker, 2020; Putzenlechner et al., 2019b, 2019a). As LAI and fPAR are both recognized as Essential Cliamtic Variables (ECVs), it is necessary to continue to explore their connection and interaction with each other in the deciduous and coniferous forest. Therefore, this thesis

explores two specific hypotheses:

1. FPAR has a natural spatiotemporal change in the mixed coniferous forest and varies with forest dynamics over the time
2. Forest structure, especially LAI, is related to fPAR. It is expected to have a negative impact on fPAR as the low LAI value creates more gaps, thus leading to high fPAR.

With the context provided above, the main goal of my thesis research is

1. To explore the spatiotemporal variability of fPAR in a mixed coniferous forest using Wireless Sensor Networks (WSNs).
2. To discover the relationship between vertical forest structure and fPAR using Terrestrial Laser Scanner (TLS).

1.3 References

Anderson, K., Hancock, S., Disney, M., Gaston, K.J., 2016. Is waveform worth it? A comparison of LiDAR approaches for vegetation and landscape characterization. Remote Sens. Ecol. Conserv. 2, 5–15. https://doi.org/10.1002/rse2.8

Aslan, Y.E., Korpeoglu, I., Ulusoy, özgür, 2012. A framework for use of wireless sensor networks in forest fire detection and monitoring. Comput. Environ. Urban Syst. 36, 614–625. https://doi.org/10.1016/j.compenvurbsys.2012.03.002

Baret, F., Andrieu, B., Folmer, J.C., Hanocq, J.F., Sarrouy, C., 1993. Gap fraction measurement from hemispherical infrared photography and its use to evaluate PAR interception efficiency. Crop Struct. Microclim. Charact. Appl. INRA Ed. Paris 359–372.

Baslam, M., Mitsui, T., Hodges, M., Priesack, E., Herritt, M.T., Aranjuelo, I., Sanz-Sáez, Á., 2020. Photosynthesis in a changing global climate: Scaling up and scaling down in crops. Front. Plant Sci. 11, 882.

Bauer, J., Jarmer, T., Schittenhelm, S., Siegmann, B., Aschenbruck, N., 2019. Processing and filtering of leaf area index time series assessed by in-situ wireless sensor networks. Comput. Electron. Agric. 165, 104867. https://doi.org/10.1016/j.compag.2019.104867

Bindoff, N.L., Willebrand, J., Artale, V., Cazenave, A., Gregory, J.M., Gulev, S., Hanawa, K., Le Quere, C., Levitus, S., Nojiri, Y., 2007. Observations: oceanic climate change and sea level.

Camacho, F., Fuster, B., Li, W., Weiss, M., Ganguly, S., Lacaze, R., Baret, F., 2021. Crop specific algorithms trained over ground measurements provide the best performance for GAI and fAPAR estimates from Landsat-8 observations. Remote Sens. Environ. 260,

112453.

Carrer, D., Roujean, J.L., Lafont, S., Calvet, J.C., Boone, A., Decharme, B., Delire, C., Gastellu-Etchegorry, J.P., 2013. A canopy radiative transfer scheme with explicit FAPAR for the interactive vegetation model ISBA-A-gs: Impact on carbon fluxes. J. Geophys. Res. Biogeosciences 118, 888–903. https://doi.org/10.1002/jgrg.20070

Chen, J.M., Black, T.A., 1992. Defining leaf area index for non- flat leaves. Plant. Cell Environ. 15, 421–429.

Chen, Y., Sun, K., Chen, C., Bai, T., Park, T., Wang, W., Nemani, R.R., Myneni, R.B., 2019. Generation and evaluation of LAI and FPAR products from Himawari-8 advanced Himawari imager (AHI) data. Remote Sens. 11. https://doi.org/10.3390/rs11131517

Claverie, M., Matthews, J.L., Vermote, E.F., Justice, C.O., 2016. A 30+ year AVHRR LAI and FAPAR climate data record: Algorithm description and validation. Remote Sens. 8, 1–12. https://doi.org/10.3390/rs8030263

Corke, P., Wark, T., Jurdak, R., Hu, W., Valencia, P., Moore, D., 2010. Environmental wireless sensor networks. Proc. IEEE 98, 1903–1917. https://doi.org/10.1109/JPROC.2010.2068530

Culvenor, D.S., Newnham, G.J., Mellor, A., Sims, N.C., Haywood, A., 2014. Automated in-situ laser scanner for monitoring forest leaf area index. Sensors 14, 14994–15008.

Danson, F.M., Hetherington, D., Morsdorf, F., Koetz, B., Allgöwer, B., 2007. Forest canopy gap fraction from terrestrial laser scanning. IEEE Geosci. Remote Sens. Lett. 4, 157–160. https://doi.org/10.1109/LGRS.2006.887064

Díaz-Ramírez, A., Tafoya, L.A., Atempa, J.A., Mejía-Alvarez, P., 2012. Wireless Sensor

Networks and Fusion Information Methods for Forest Fire Detection. Procedia Technol. 3, 69–79. https://doi.org/10.1016/j.protcy.2012.03.008

Diffey, B., 2004. Climate change, ozone depletion and the impact on ultraviolet exposure of human skin. Phys. Med. Biol. 49. https://doi.org/10.1088/0031-9155/49/1/R01

Dong, T., Liu, J., Shang, J., Qian, B., Huffman, T., Zhang, Y., Champagne, C., Daneshfar, B., 2016. Assessing the impact of climate variability on cropland productivity in the Canadian Prairies using time series MODIS FAPAR. Remote Sens. 8. https://doi.org/10.3390/rs8040281

Dong, T., Meng, J., Shang, J., Liu, J., Wu, B., 2015. Evaluation of chlorophyll-related vegetation indices using simulated Sentinel-2 data for estimation of crop fraction of absorbed photosynthetically active radiation. IEEE J. Sel. Top. Appl. Earth Obs. Remote Sens. 8, 4049–4059.

Ellison, D., Morris, C.E., Locatelli, B., Sheil, D., Cohen, J., Murdiyarso, D., Gutierrez, V., Noordwijk, M. van, Creed, I.F., Pokorny, J., Gaveau, D., Spracklen, D. V., Tobella, A.B., Ilstedt, U., Teuling, A.J., Gebrehiwot, S.G., Sands, D.C., Muys, B., Verbist, B., Springgay, E., Sugandi, Y., Sullivan, C.A., 2017. Trees, forests and water: Cool insights for a hot world. Glob. Environ. Chang. https://doi.org/10.1016/j.gloenvcha.2017.01.002

Fan, W., Liu, Y., Xu, X., Chen, G., Zhang, B., 2014. A new FAPAR analytical model based on the law of energy conservation: A case study in China. IEEE J. Sel. Top. Appl. Earth Obs. Remote Sens. 7, 3945–3955.

Fensholt, R., Sandholt, I., Rasmussen, M.S., 2004. Evaluation of MODIS LAI, fAPAR and the relation between fAPAR and NDVI in a semi-arid environment using in situ

measurements. Remote Sens. Environ. 91, 490–507. https://doi.org/10.1016/j.rse.2004.04.009

Ferre, J.A., Pawlowski, A., Guzman, J.L., Rodriguez, F., Berenguel, M., 2010. A wireless sensor network for greenhouse climate monitoring, in: 2010 Fifth International Conference on Broadband and Biomedical Communications. IEEE, pp. 1–5.

Francis, J.A., Wu, B., 2020. Why has no new record-minimum Arctic sea-ice extent occurred since September 2012? Environ. Res. Lett. 15, 114034.

Friedlingstein, P., 2015. Carbon cycle feedbacks and future climate change. Philos. Trans. R. Soc. A Math. Phys. Eng. Sci. 373, 20140421.

Friedlingstein, P., Bopp, L., Ciais, P., Dufresne, J., Fairhead, L., LeTreut, H., Monfray, P., Orr, J., 2001. Positive feedback between future climate change and the carbon cycle. Geophys. Res. Lett. 28, 1543–1546.

Friedlingstein, P., Dufresne, J.-L., Cox, P.M., Rayner, P., 2003. How positive is the feedback between climate change and the carbon cycle? Tellus B Chem. Phys. Meteorol. 55, 692–700.

Fritsch, S., Machwitz, M., Ehammer, A., Conrad, C., Dech, S., 2012. Validation of the collection 5 MODIS FPAR product in a heterogeneous agricultural landscape in arid Uzbekistan using multitemporal RapidEye imagery. Int. J. Remote Sens. 33, 6818–6837.

Fu, G., Wu, J.-S., 2017. Validation of MODIS collection 6 FPAR/LAI in the alpine grassland of the Northern Tibetan Plateau. Remote Sens. Lett. 8, 831–838.

GCOS, 2016. The global observing system for climate: Implementation needs (GCOS- 200).

Geoffrey Craggs, 2016. Photosynthesis and its Role in Climate Change and Soil Regeneration

- Future Directions International.

Goude, M., Nilsson, U., Holmström, E., 2019. Comparing direct and indirect leaf area measurements for Scots pine and Norway spruce plantations in Sweden. Eur. J. For. Res. 138, 1033–1047.

Hovi, A., Lukeš, P., Rautiainen, M., 2017. Seasonality of albedo and FAPAR in a boreal forest. Agric. For. Meteorol. 247, 331–342.

Hu, J., Su, Y., Tan, B., Huang, D., Yang, W., Schull, M., Bull, M.A., Martonchik, J. V., Diner, D.J., Knyazikhin, Y., Myneni, R.B., 2007. Analysis of the MISR LAI/FPAR product for spatial and temporal coverage, accuracy and consistency. Remote Sens. Environ. 107, 334–347. https://doi.org/10.1016/j.rse.2006.06.020

Imbach, P., Molina, L., Locatelli, B., Roupsard, O., Mahé, G., Neilson, R., Corrales, L., Scholze, M., Ciais, P., 2012. Modeling potential equilibrium states of vegetation and terrestrial water cycle of Mesoamerica under climate change scenarios. J. Hydrometeorol. 13, 665–680.

Jonckheere, I., Fleck, S., Nackaerts, K., Muys, B., Coppin, P., Weiss, M., Baret, F., 2004. Review of methods for in situ leaf area index determination Part I. Theories, sensors and hemispherical photography. Agric. For. Meteorol. 121, 19–35. https://doi.org/10.1016/j.agrformet.2003.08.027

Knorr, W., Gobron, N., Scholze, M., Kaminski, T., Pinty, B., 2005. Global drought conditions causing recent atmospheric carbon dioxide increase. Eos Trans. AGU 86, 178–181.

Kotamäki, N., Thessler, S., Koskiaho, J., Hannukkala, A., Huitu, H., Huttula, T., Havento, J., Järvenpää, M., 2009. Wireless in-situ Sensor Network for Agriculture and Water

Monitoring on a River Basin Scale in Southern Finland: Evaluation from a Data User's Perspective. Sensors 9, 2862–2883. https://doi.org/10.3390/s90402862

Li, W., Weiss, M., Waldner, F., Defourny, P., Demarez, V., Morin, D., Hagolle, O., Baret, F., 2015. A generic algorithm to estimate LAI, FAPAR and FCOVER variables from SPOT4_HRVIR and landsat sensors: Evaluation of the consistency and comparison with ground measurements. Remote Sens. 7, 15494–15516. https://doi.org/10.3390/rs71115494

Li, X., Liang, H., Cheng, W., 2020. Spatio-temporal variation in AOD and correlation analysis with PAR and NPP in China from 2001 to 2017. Remote Sens. 12. https://doi.org/10.3390/rs12060976

Liang, S., Hou, X., Sui, X., Wang, M., 2017. Deciduous broadleaf forests green FPAR and its relationship with spectral vegetation indices, in: 2017 10th International Congress on Image and Signal Processing, BioMedical Engineering and Informatics (CISP-BMEI). IEEE, pp. 1–5.

Liang, X., Hyyppä, J., Kaartinen, H., Holopainen, M., Melkas, T., 2012. Detecting changes in forest structure over time with bi-temporal terrestrial laser scanning data. ISPRS Int. J. Geo-Information 1, 242–255.

Liu, L., Zhang, X., Xie, S., Liu, X., Song, B., Chen, S., Peng, D., 2019. Global white-sky and black-sky fapar retrieval using the energy balance residual method: Algorithm and validation. Remote Sens. 11, 1004.

Luo, S., Wang, C., Xi, X., Pan, F., 2014. Estimating FPAR of maize canopy using airborne discrete-return LiDAR data. Opt. Express 22, 5106–5117.

Luoma, V., Yrttimaa, T., Kankare, V., Saarinen, N., Pyörälä, J., Kukko, A., Kaartinen, H., Hyyppä, J., Holopainen, M., Vastaranta, M., 2021. Revealing changes in the stem form and volume allocation in diverse boreal forests using two-date terrestrial laser scanning. Forests 12, 835.

Majasalmi, T., Rautiainen, M., Stenberg, P., 2014. Modeled and measured fPAR in a boreal forest: Validation and application of a new model. Agric. For. Meteorol. 189, 118–124.

Matin, M.A., Islam, M.M., 2012. Overview of wireless sensor network. Wirel. Sens. networks-technology Protoc. 1–3.

Medlyn, B.E., Dreyer, E., Ellsworth, D., Forstreuter, M., Harley, P.C., Kirschbaum, M.U.F., Le Roux, X., Montpied, P., Strassemeyer, J., Walcroft, A., 2002. Temperature response of parameters of a biochemically based model of photosynthesis. II. A review of experimental data. Plant. Cell Environ. 25, 1167–1179.

Mitchard, E.T.A., 2018. The tropical forest carbon cycle and climate change. Nature 559, 527–534. https://doi.org/10.1038/s41586-018-0300-2

Moreno, Á., García-Haro, F.J., Martínez, B., Gilabert, M.A., 2014. Noise reduction and gap filling of fAPAR time series using an adapted local regression filter. Remote Sens. 6, 8238–8260. https://doi.org/10.3390/rs6098238

Mõttus, M., Sulev, M., Baret, F., Lopez-Lozano, R., Reinart, A., 2012. Photosynthetically active radiation: measurement and modeling, in: Encyclopedia of Sustainability Science and Technology. Springer, pp. 7970–8000.

Murphy, G.E., Acuna, M.A., Dumbrell, I., 2010. Tree value and log product yield determination in radiata pine (Pinus radiata) plantations in Australia: comparisons of

terrestrial laser scanning with a forest inventory system and manual measurements. Can. J. For. Res. 40, 2223–2233.

Myneni, R.B., 2001. Retrieving LAI and FPAR from MERIS Data With Advanced Algorithms.

Myneni, Ranga B, Hoffman, S., Knyazikhin, Y., Privette, J.L., Glassy, J., Tian, Y., Wang, Y., Song, X., Zhang, Y., Smith, G.R., 2002. Global products of vegetation leaf area and fraction absorbed PAR from year one of MODIS data. Remote Sens. Environ. 83, 214–231.

Myneni, R. B., Hoffman, S., Knyazikhin, Y., Privette, J.L., Glassy, J., Tian, Y., Wang, Y., Song, X., Zhang, Y., Smith, G.R., Lotsch, A., Friedl, M., Morisette, J.T., Votava, P., Nemani, R.R., Running, S.W., 2002. Global products of vegetation leaf area and fraction absorbed PAR from year one of MODIS data. Remote Sens. Environ. 83, 214–231. https://doi.org/10.1016/S0034-4257(02)00074-3

National Academies of Sciences and Medicine, E., 2016. Attribution of extreme weather events in the context of climate change. National Academies Press.

Nestola, E., Sánchez-Zapero, J., Latorre, C., Mazzenga, F., Matteucci, G., Calfapietra, C., Camacho, F., 2017. Validation of PROBA-V GEOV1 and MODIS C5 & C6 fAPAR products in a deciduous beech forest site in Italy. Remote Sens. 9, 126.

Parker, G.G., 2020. Tamm review: Leaf Area Index (LAI) is both a determinant and a consequence of important processes in vegetation canopies. For. Ecol. Manage. 477. https://doi.org/10.1016/j.foreco.2020.118496

Pawlowski, A., Guzman, J.L., Rodríguez, F., Berenguel, M., Sánchez, J., Dormido, S., 2009.

Simulation of greenhouse climate monitoring and control with wireless sensor network and event-based control. Sensors 9, 232–252. https://doi.org/10.3390/s90100232

Peng, D., Zhang, B., Liu, Liangyun, Fang, H., Chen, D., Hu, Y., Liu, Lingling, 2012. Characteristics and drivers of global NDVI- based FPAR from 1982 to 2006. Global Biogeochem. Cycles 26.

Pickett-Heaps, C.A., Canadell, J.G., Briggs, P.R., Gobron, N., Haverd, V., Paget, M.J., Pinty, B., Raupach, M.R., 2014. Evaluation of six satellite-derived Fraction of Absorbed Photosynthetic Active Radiation (FAPAR) products across the Australian continent. Remote Sens. Environ. 140, 241–256. https://doi.org/10.1016/j.rse.2013.08.037

Pu, J., Yan, K., Zhou, G., Lei, Y., Zhu, Y., Guo, D., Li, H., Xu, L., Knyazikhin, Y., Myneni, R.B., 2020. Evaluation of the MODIS LAI/FPAR algorithm based on 3D-RTM simulations: A case study of grassland. Remote Sens. 12, 3391.

Putzenlechner, B., Castro, S., Kiese, R., Ludwig, R., Marzahn, P., Sharp, I., Sanchez-Azofeifa, A., 2019a. Validation of Sentinel-2 fAPAR products using ground observations across three forest ecosystems. Remote Sens. Environ. 232, 111310. https://doi.org/10.1016/j.rse.2019.111310

Putzenlechner, B., Marzahn, P., Kiese, R., Ludwig, R., Sanchez-Azofeifa, A., 2019b. Assessing the variability and uncertainty of two-flux FAPAR measurements in a conifer-dominated forest. Agric. For. Meteorol. 264, 149–163. https://doi.org/10.1016/j.agrformet.2018.10.007

Putzenlechner, B., Marzahn, P., Sanchez-azofeifa, A., 2020. Accuracy assessment on the number offlux terms needed to estimate in situ fAPAR. Int J Appl Earth Obs Geoinf. 88,

102061. https://doi.org/10.1016/j.jag.2020.102061

Qin, H., Wang, C., Pan, F., Lin, Y., Xi, X., Luo, S., 2017. Estimation of FPAR and FPAR profile for maize canopies using airborne LiDAR. Ecol. Indic. 83, 53–61.

Qu, Y., Zhu, Y., Han, W., Wang, J., Ma, M., 2014. Crop leaf area index observations with a wireless sensor network and its potential for validating remote sensing products. IEEE J. Sel. Top. Appl. Earth Obs. Remote Sens. 7, 431–444. https://doi.org/10.1109/JSTARS.2013.2289931

Rankine, C.J., Sanchez-Azofeifa, G.A., Macgregor, M.H., 2014. Seasonal wireless sensor network link performance in boreal forest phenology monitoring. 2014 11th Annu. IEEE Int. Conf. Sensing, Commun. Networking, SECON 2014 302–310. https://doi.org/10.1109/SAHCN.2014.6990366

Reiche, J., Lucas, R., Mitchell, A.L., Verbesselt, J., Hoekman, D.H., Haarpaintner, J., Kellndorfer, J.M., Rosenqvist, A., Lehmann, E.A., Woodcock, C.E., Seifert, F.M., Herold, M., 2016. Combining satellite data for better tropical forest monitoring. Nat. Clim. Chang. 6, 120–122. https://doi.org/10.1038/nclimate2919

Ryu, Y., Lee, G., Jeon, S., Song, Y., Kimm, H., 2014. Monitoring multi-layer canopy spring phenology of temperate deciduous and evergreen forests using low-cost spectral sensors. Remote Sens. Environ. 149, 227–238.

Sánchez-Azofeifa, G.A., Rankine, C., Do Espirito Santo, M.M., Fatland, R., Garcia, M., 2011. Wireless sensing networks for environmental monitoring: Two case studies from tropical forests. Proc. - 2011 7th IEEE Int. Conf. eScience, eScience 2011 70–76. https://doi.org/10.1109/eScience.2011.18

Sanz- Sáez, Á., Koester, R.P., Rosenthal, D.M., Montes, C.M., Ort, D.R., Ainsworth, E.A., 2017. Leaf and canopy scale drivers of genotypic variation in soybean response to elevated carbon dioxide concentration. Glob. Chang. Biol. 23, 3908–3920.

Senna, M.C.A., Costa, M.H., Shimabukuro, Y.E., 2005. Fraction of photosynthetically active radiation absorbed by Amazon tropical forest: A comparison of field measurements, modeling, and remote sensing. J. Geophys. Res. Biogeosciences 110.

Serbin, S.P., Ahl, D.E., Gower, S.T., 2013. Spatial and temporal validation of the MODIS LAI and FPAR products across a boreal forest wildfire chronosequence. Remote Sens. Environ. 133, 71–84. https://doi.org/10.1016/j.rse.2013.01.022

Shabanov, N. V., Wang, Y., Buermann, W., Dong, J., Hoffman, S., Smith, G.R., Tian, Y., Knyazikhin, Y., Myneni, R.B., 2003. Effect of foliage spatial heterogeneity in the MODIS LAI and FPAR algorithm over broadleaf forests. Remote Sens. Environ. 85, 410–423. https://doi.org/10.1016/S0034-4257(03)00017-8

Sieber, M.H., Thomsen, M.B., Spradling, A.C., 2016. Electron transport chain remodeling by GSK3 during oogenesis connects nutrient state to reproduction. Cell 164, 420–432.

Somerville, R.C.J., 2020. Facts and opinions about climate change. Bull. At. Sci. 76, 331–335.

Sonnentag, O., Talbot, J., Chen, J.M., Roulet, N.T., 2007. Using direct and indirect measurements of leaf area index to characterize the shrub canopy in an ombrotrophic peatland. Agric. For. Meteorol. 144, 200–212.

Srinivasan, S., Popescu, S.C., Eriksson, M., Sheridan, R.D., Ku, N.-W., 2014. Multi-temporal terrestrial laser scanning for modeling tree biomass change. For. Ecol. Manage. 318,

304–317.

Sun, B., Gao, Z., Li, Z., Wang, B., Bai, L., Wu, J., Li, C., Ding, X., 2014. Construction of Monthly Time-Series NPP Datasets over Chinese Terrestrial Based on MERIS FPAR Data During 2002-2012. Dragon 3Mid Term Results 724, 140.

Sun, Y., Qin, Q., Ren, H., Zhang, Y., 2021. Decameter Cropland LAI/FPAR Estimation From Sentinel-2 Imagery Using Google Earth Engine. IEEE Trans. Geosci. Remote Sens.

Tao, F., Yokozawa, M., Hayashi, Y., Lin, E., 2003. Terrestrial water cycle and the impact of climate change. AMBIO A J. Hum. Environ. 32, 295–301.

Tao, X., Liang, S., He, T., Jin, H., 2016. Estimation of fraction of absorbed photosynthetically active radiation from multiple satellite data: Model development and validation. Remote Sens. Environ. 184, 539–557. https://doi.org/10.1016/j.rse.2016.07.036

Tao, X., Liang, S., Wang, D., 2015. Assessment of five global satellite products of fraction of absorbed photosynthetically active radiation: Intercomparison and direct validation against ground-based data. Remote Sens. Environ. 163, 270–285. https://doi.org/10.1016/j.rse.2015.03.025

Thomas, V., Finch, D.A., McCaughey, J.H., Noland, T., Rich, L., Treitz, P., 2006. Spatial modelling of the fraction of photosynthetically active radiation absorbed by a boreal mixedwood forest using a lidar–hyperspectral approach. Agric. For. Meteorol. 140, 287–307.

Tian, Y., Dickinson, R.E., Zhou, L., Zeng, X., Dai, Y., Myneni, R.B., Knyazikhin, Y., Zhang, X., Friedl, M., Yu, H., Wu, W., Shaikh, M., 2004. Comparison of seasonal and spatial variations of leaf area index and fraction of absorbed photosynthetically active radiation

from Moderate Resolution Imaging Spectroradiometer (MODIS) and Common Land Model. J. Geophys. Res. D Atmos. 109, 1–14. https://doi.org/10.1029/2003jd003777

Urban, O., 2003. Physiological impacts of elevated CO 2 concentration ranging from molecular to whole plant responses. Photosynthetica 41, 9–20.

Vastaranta, M., Melkas, T., Holopainen, M., Kaartinen, H., Hyyppä, J., Hyyppä, H., 2009. Laser-based field measurements in tree-level forest data acquisition. Photogramm. J. Finl 21, 51–61.

Vose, J.M., Dougherty, P.M., Long, J.N., Smith, F.W., Gholz, H.L., Curran, P.J., 1994. Factors influencing the amount and distribution of leaf area of pine stands. Ecol. Bull. 102–114.

Wang, Y., Tian, Y., Zhang, Y., El-Saleous, N., Knyazikhin, Y., Vermote, E., Myneni, R.B., 2001. Investigation of product accuracy as a function of input and model uncertainties: Case study with SeaWiFS and MODIS LAI/FPAR algorithm. Remote Sens. Environ. 78, 299–313.

Wang, Y., Xie, D., Liu, S., Hu, R., Li, Y., Yan, G., 2016. Scaling of FAPAR from the Field to the Satellite. Remote Sens. 8, 310.

Whitmore, T.C., Brown, N.D., Swaine, M.D., Kennedy, D., Goodwin-Bailey, C.I., Gong, W.-K., 1993. Use of hemispherical photographs in forest ecology: measurement of gap size and radiation totals in a Bornean tropical rain forest. J. Trop. Ecol. 9, 131–151.

Widlowski, J.L., 2010. On the bias of instantaneous FAPAR estimates in open-canopy forests. Agric. For. Meteorol. 150, 1501–1522. https://doi.org/10.1016/j.agrformet.2010.07.011

Xiao, Z., Liang, S., Wang, T., Jiang, B., 2016. Retrieval of leaf area index (LAI) and fraction of absorbed photosynthetically active radiation (FAPAR) from VIIRS time-series data.

Remote Sens. 8. https://doi.org/10.3390/rs8040351

Xu, B., Park, T., Yan, K., Chen, C., Zeng, Y., Song, W., Yin, G., Li, J., Liu, Q., Knyazikhin, Y., Myneni, R.B., 2018. Analysis of global LAI/FPAR products from VIIRS and MODIS sensors for spatio-temporal consistency and uncertainty from 2012-2016. Forests 9, 1–21. https://doi.org/10.3390/f9020073

Yang, F., Ren, H., Li, X., Hu, M., Yang, Y., 2014. Assessment of MODIS, MERIS, GEOV1 FPAR products over Northern China with ground measured data and by analyzing residential effect in mixed pixel. Remote Sens. 6, 5428–5451.

Yang, W., Huang, D., Tan, B., Stroeve, J.C., Shabanov, N. V, Knyazikhin, Y., Nemani, R.R., Myneni, R.B., 2006. Analysis of leaf area index and fraction of PAR absorbed by vegetation products from the terra MODIS sensor: 2000-2005. IEEE Trans. Geosci. Remote Sens. 44, 1829–1842.

Yang, Z.I., Zhang, T. bin, Yi, G. hua, Li, J. ji, Qin, Y. bin, Chen, Y., 2021. Spatio-temporal variation of Fraction of Photosynthetically Active Radiation absorbed by vegetation in the Hengduan Mountains, China. J. Mt. Sci. 18, 891–906. https://doi.org/10.1007/s11629-020-6465-9

Zhao, P., Fan, W., Liu, Y., Mu, X., Xu, X., Peng, J., 2016. Study of the remote sensing model of FAPAR over rugged terrains. Remote Sens. 8, 10–12. https://doi.org/10.3390/rs8040309

Zhu, Z., Bi, J., Pan, Y., Ganguly, S., Anav, A., Xu, L., Samanta, A., Piao, S., Nemani, R.R., Myneni, R.B., 2013. Global data sets of vegetation leaf area index (LAI)3g and fraction of photosynthetically active radiation (FPAR)3g derived from global inventory modeling

and mapping studies (GIMMS) normalized difference vegetation index (NDVI3G) for the period 1981 to 2. Remote Sens. 5, 927–948. https://doi.org/10.3390/rs5020927

Chapter 2 - The Spatiotemporal Variability of the Fraction of Photosynthetically Active Radiation (fPAR) in a Mixed Coniferous Forest

Abstract

The fraction of photosynthetically active radiation (fPAR) quantifies the fraction of the solar radiation absorbed by plants for the photosynthesis activity. Long-term fPAR variation is required to monitor forest function and climate dynamics, but it is challenging to estimate in a complex and heterogeneous canopy. Leaf area index (LAI), a parameter of vertical forest structure, is often studied along with fPAR as both of them are crucial biophysical variables in most climatic and ecological models. Their relationship has been previously studied mainly using satellite-derived data. In this context, this study investigates the long-term spatiotemporal variability of fPAR and the relationship between LAI and fPAR in a mixed coniferous forest using terrestrial laser scanner (TLS) and advanced wireless sensor networks (WSNs). The study was conducted in the Graswang forest station, where the WSN was installed with PAR sensor. Waveform metrics (LAI, centroid and radius of gyration) were estimated through TLS data. We performed Kriging interpolation for fPAR to determine its variation and multiple correlations to explore fPAR response to LAI, tree species, and tree mortality. Results show that fPAR has a natural spatiotemporal variation over a year and a significant change from 2016 to 2019. LAI and tree species present a significant positive correlation with fPAR, whereas mortality has an insignificant small influence on fPAR. Our work contributes to the study of long-term fPAR variation in mixed coniferous forest and shows the potential for WSNs monitoring long-term fPAR observations. This study lays the groundwork for the relationship between vertical forest structure and fPAR in a mixed coniferous forest, as well as providing a potential project for the influence of tree species and mortality rate on LAI impacts on fPAR.

Keywords: Fraction of photosynthetically active radiation (fPAR); Wireless sensor networks (WSNs); Leaf area index (LAI).

2.1 Introduction

Over the past century, functions inherent to forests have been implemented in many different

disciplines to help gain a stronger understanding of these fields and the processes that drive them. Forests couple the biosphere to other components of the Earth system and are connected to and influenced by climate dynamics (Khaine and Woo, 2015a). Changes in canopy structure, composition, and functional processes in a forest ecosystem would impact climatic variables and in turn, the resulting changes in the environmental conditions would disturb forest growth, affecting net primary productivity and habitat functions (Khaine and Woo, 2015b; Mo et al., 2018). Based on this ecological interrelationship between forest and climate, studying the interaction and response between climate dynamics and forest ecosystems has become essential for climate mitigation and adaptation.

In 2003, the Global Climate Observing System (GCOS) program introduced a set of essential climatic variables (ECVs) critical to the characterization of Earth's climate (GCOS, 2016). The fraction of photosynthetically active radiation (fPAR) and leaf area index (LAI) are examples of ECVs that characterize vegetation canopy functioning and energy absorption capacity (Myneni et al., 2002). FPAR is the fraction of incident photosynthetically active radiation (400- 700 nm) absorbed by the vegetation (Fensholt et al., 2004). It characterizes the energy used in the process of photosynthesis (Myneni et al., 2002) , and thus expresses a canopy's energy absorption capacity (Tian et al., 2015). Quantifying fPAR provides vital information for estimating the vegetation net primary productivity, carbon balance, ecosystem energy and mass exchanges over a range of temporal and spatial resolution (Gobron and Verstraete, 2009; Sánchez-Azofeifa et al., 2011).

Estimation of fPAR can be categorized into in situ and satellite-derived. FPAR derived from polar orbit satellites, such as MODIS (Dong et al., 2016; Li et al., 2020), Landsat-TM (Li and Fang, 2015), and Sentinel-2 (Putzenlechner et al., 2019a), has the advantages in monitoring large-scale spatial variability, but at the same time observations are constrained by weather conditions (Reiche et al., 2016) and temporal delay. Atmospheric interference and cloud cover can limit the quality and availability of satellite-derived data (Reiche et al., 2016). The propagation delay of satellites brings uncertainty in detecting small temporal changes (Ryu et al., 2014). As such, in situ sensor technologies fill the gaps of temporal resolution and have

become widely used for long-term environmental and climate monitoring (Kotamäki et al., 2009).

Long-term observations of fPAR are required to monitor global vegetation dynamics and assess global carbon balances in the context of climate variability and change studies (Xiao et al., 2018, 2016; Zhu et al., 2013). However, accurately measuring fPAR over a long period tends to be problematic in large complex vegetative stands because of the spatial heterogeneity of these environments (Sánchez-Azofeifa et al., 2011). Both in situ and satellite-derived fPAR can be influenced by changes in phenological and meteorological conditions and create estimation bias. This bias the sampling error and the transfer error (J.-L. Widlowski, 2010) on the estimation can be strongly affected by solar zenith angle, wind speed (Putzenlechner et al., 2019b), atmospheric conditions (Liu et al., 2019), as well as surface roughness (Zhao et al., 2016). Since the satellite-based data are often not continuous and consistent in space and time (Ryu et al., 2014), filtering methods are required to fill in gaps and produce high-quality time series (Moreno et al., 2014). The in situ sensors have been advanced and become popular in climate variables observation.

Wireless sensor networks (WSNs) are new in situ technologies that bring advances in sensor technology, wireless communications, digital electronics and computer networks to the realm of environmental monitoring (Takruri et al., 2008). Compared with satellite sensors, WSNs use low-cost, low-power, multi-functional small-size sensor nodes (Takruri et al., 2008) to collect continuous, automated, and high temporal and spatial resolution data of dynamic environmental processes in remote locations with poor accessibility (Rankine et al., 2014). These strengths make WSNs a beneficial asset in in situ monitoring forest micro-meteorological variables (Rankine et al., 2014), especially for assessing long-term fPAR spatiotemporal variability.

Along with fPAR, LAI is another ECV generally defined as one-sided green leaf area per unit ground area in broadleaf canopies (Chen and Black, 1992) and the projected needle leaf area in coniferous canopies (Myneni et al., 2002). It is one of the most informative parameters for monitoring mass and energy exchange processes in the forest (Culvenor et al., 2014), and

hence was recommended as a promising indicator of climate change impacts on vegetation (IPCC, 1998). Dense canopies with high LAI can intercept 95% solar radiation from reaching the Earth's surface (Bonan, 2015), decreasing the amount of energy that penetrates through to the soil (Hardwick et al., 2015). The estimation of LAI can be done using direct and indirect methods. Direct methods are the most accurate, but they are destructive in nature and can be time-consuming and labor-intensive; thus, they are not compatible with the long-term monitoring of spatial and temporal dynamics (Jonckheere et al., 2004). Indirect methods are non-destructive measurements that extrapolate LAI from measurements of another variable and are faster and thus suitable for extensive spatial data collection.

Digital hemispherical photography (DHP) is an in situ optical method that estimates LAI from the measurement of the gap fraction of an image taken from ground level looking up at the canopy using a wide angle lens (Chianucci and Cutini, 2012). However, it is limited by user subjectivity and the sky condition. AccuPAR LP-80, another indirect instrument, estimates LAI using the amount of light energy transmitted by a plant canopy (PAR) (Breda, 2003). However, it is not helpful in very tall and dense forest canopies and can be affected by foliage clumping (Adeboye et al., 2019). These methods are advanced from direct methods but are still labor-intensive, time-consuming, and difficult to implement over large areas.

Terrestrial laser scanners (TLS) use ground-based LiDAR technology to provide a permanent 3D record of forest structure and detailed information about forest canopy architecture (Wang and Fang, 2020). They can capture high precision and spatial resolution data with promising accuracy on large scales in a short time. A TLS emits laser pulses and classifies them into the discrete return and full-waveform models, from which vertical profile information such as LAI, plant area volume density (PAVD), and shape-metrics (centroid and radius of gyration) can be extracted. The centroid (Cx, Cy) assesses the shape of a waveform, and RG captures how the waveforms are distributed around the centroid (Muss et al., 2013). These shape-based metrics can be well related to forest structures and biomass (Muss et al., 2013), and are useful for differentiating forest successional stages (Gu et al., 2018).

Most long-term fPAR studies have conducted in the boreal forest (Serbin et al., 2013; Tao et

al., 2016; J. L. Widlowski, 2010; Yang et al., 2021), and only a few are in mixed coniferous forest (Carrer et al., 2013; Parker, 2020; Putzenlechner et al., 2019b, 2019a). As the severe growth reduction and mortality in European forest (Pretzsch et al., 2014), a better understanding of the fPAR variation and how it varies with LAI in a temperate forest would provide a critical insight in restore and protect forest ecosystem and mitigate climate impacts. In this context, the specific objective of this paper is to explore the spatiotemporal variability of fPAR, as well as study the influence of LAI on fPAR in a mixed wood temperate forest using WSNs and TLS.

2.2 Materials and methods

2.2.1 Study Site

Measurements of fPAR were carried out at the Graswang forest station located in Bavaria, Germany (47.571^0 N, 11.033^0 E, 864 m a.s.l) (Figure 1). Graswang is a temperate mixed coniferous forest and it comprises a mid-age spruce-dominated forest stand with Norway spruce, European beech, and Sycamore maple (Putzenlechner et al., 2019a). The Graswang forest station is situated on a flat alluvial plain in a sub-alpine valley, and it is the highest elevated site in the Ammer catchment. The climate is classified as a warm-temperate, fully humid climate with warm summers and cold winters (Köppen Classification). The study area has a mean annual air temperature of 6.8 ^{0}C and a mean annual precipitation of 1300 mm (Putzenlechner et al., 2019b). The site is part of Germany's Terrestrial Environmental Observatories (TERENO) project to conduct long-term environmental research on the impacts of climate change on terrestrial ecosystems in Upper Bavaria Germany (Zacharias et al., 2011).

The Graswang site is currently equipped with a WSN for continuous fPAR ground observations (Putzenlechner et al., 2019b). This WSN has been in operation since 2015 by Ludwig Maximillian University – Munich and the University of Alberta. A forest inventory was collected in 2017 at the WSN site. A total of 350 trees were documented, including position, diameter breast height (DBH), radius, species, and vitality. The latitude and

longitude were also recorded for each tree. The tree species within the study area are combined with Norway spruce and European beech. The vitality of trees was categorized as healthy, damaged or sick, or dying or dead.

2.2.2 Vertical Forest Structure Data Collection

The RIEGL VZ-400i terrestrial laser scanner (TLS) was deployed at the study site from September 11th to 13th, 2018. This instrument is a 3D real-time laser scanning system and has a 100^{o} *360^{o} field of view (RIEGL, 2019). It collects simultaneous scan and image data with 5 mm accuracy per 3 mm repeatability and a measurement range of up to 800 m (Kamnik et al., 2020). The TLS was mounted on the tripod at a 90^{o} angle. Both a vertical and horizontal scan were performed at each point to avoid the blind spots of the instrument. A total of 69 scans were collected on the study site using the RIEGL TLS and organized and stored in RISCAN Pro's project structure (Figure 2). These TLS data include scans, digital images, coordinates of control points, and transformation matrices needed to transform the data of multiple scans into a standard, well-defined coordinate system (Krelling et al., 2012).

Digital Hemispherical Photographs (DHPs) were captured early in the morning at each WSN node in 2018 using a digital camera equipped with a fisheye Sigma 8mm lens. The camera was leveled at 1.50 m by using a tripod and facing towards magnetic north to ensure photographic standardization. The resulting circular images are analyzed by Gap Light Analyzer (GLA) (Frazer et al., 1999), image processing software to extract canopy structure data such as effective LAI and canopy openness (Frazer et al., 1999).

2.2.3 Processing of TLS and DHP Data and Analysis of Forest Structure Estimates

Each TLS scan was exported as an individual point cloud and then processed using the R-package "rTLS"(Guzmán Q., 2021). The resulting waveforms illuminate different canopy elements to present and describe the 3D structure of vegetation canopies (Anderson et al., 2016). Parameters, such as the gap fraction, LAI, PAVD, Cx, Cy and the radius of gyration (RG), can be extracted from the waveforms for each scan. The height was calculated as the cosine of the laser zenith angle (57.5^{o}) multiplied by the laser distance measurement,

assuming that the terrain is flat as described by Culvenor et al. (2014). With an estimate of the probability of gap, leaf area profile can be calculated and thus the PAVD which is the derivative of the leaf area profile (Lovell et al., 2011). Plant area density is calculated as the cumulative of PAVD for each scan to determine the LAI.

The LAI, Cx, Cy and RG from TLS data are further spatially interpolated to extract the spatial information of forest structure in the study area, using the Kriging method (Kiš, 2016) in Surfer® from Golden Software, LLC (Software, 2021). Kriging is a geostatistical approach that depends on expressing the spatial variation of the property in terms of its variogram. It considers that the originated data process has a deterministic trend and an autocorrelated error (Oliver and Webster, 1990). The variogram is a discrete function computed through a measure of the variability between pairs of points at different distances (Said and Yurtal, 2019). The model's graph type, sill, nugget, and range are changed based on the distribution of points (Franklin, 2014). A Block Kriging technique was used over Point Kriging since it can estimate the average value of the rectangular blocks centred on the grid nodes (Oliver and Webster, 1990). In addition, this technique provides better variance estimates and has the effect of smoothing interpolated results (Franklin, 2014). The block size (cell size) is set to 1 m *1 m to present the most spatial detail for analysis and to capture the spatial variations. The spatial information of LAI and shape-metrics are used to describe the vertical structure of the Graswang site.

A total of 16 Digital Hemispherical Photographs were taken on the WSN site and analyzed using GLA. Images are registered in GLA so that both the orientation and circular extent of the exposure are known (Frazer et al., 1999). A threshold is chosen for each image to accurately classify the sky (white) and non-sky (black) pixels. The estimation of LAI at each node can be calculated.

2.2.4 Wireless Sensor Networks for Permanent PAR Observation

Graswang has been equipped with a WSN for continuous PAR ground observations since 2015 (Putzenlechner et al., 2019b). The experimental setup for the fPAR measurements

consisted of self-powered nodes (model ENV-Link-Mini-LXRS, LORD MicroStrain, Cary, NC, USA) equipped with quantum PAR sensors (Model SQ-110, Apogee, Logan, UT, USA; field of view 180^{o}; uncertainty estimates: cosine response ± 5% at 75^{o} solar zenith angle, temperature response 0.06 ± 0.06% per ^{o}C, calibration uncertainty ± 5% and long-term drift < 2% y^{-1}). Additional information can be found in Putzenlechner et al. (2020). Sensors are mounted at 1.3m from the ground and deployed in a hexagonal topology (Figure 3). This sampling scheme maximizes the sensing area covered by a given number of sensors while ensuring signal quality and connectivity, and provides the least error compared with other localization algorithms for WSNs (García et al., 2007; Mortazavi et al., 2014; Younis and Akkaya, 2008). At Graswang, the incoming PAR is measured approximately 300 m from the forest edge. The final configuration consists of 16 PAR nodes spaced 10 m apart and covers a site area of 35 m *43.3 m (Figure 3).

PAR data was downloaded using a portable aggregator with frequencies ranging from 2.4 GHz to 2.5 GHz and equipped with a USB interface (model WSDA-Base-104 USB Base Station, MicroStrain, Cary, NC, USA). The aggregator is connected to a portable computer for data download and is equipped with the software "Node Commander" (version 2.17.0, LORD MicroStrain, Cary, NC, USA) (Putzenlechner et al., 2020). The WSN nodes are configured to measure the instantaneous PAR every 10 min synchronously (∼1 ns).

2.2.5 Processing of PAR Data and Calculation of FPAR Estimates

The PAR data was uploaded to "Enviro-Net" (Pastorello et al., 2011), a web platform for sensor data management, near real-time visualization and analysis (Pastorello et al. 2011). The sensors have been operational at the study site since 2015 and experience both random and systematic bias problems. Many studies assume that PAR sensor calibration is valid during the setup of PAR sensors (Li and Fang, 2015; Majasalmi, 2015; Majasalmi et al., 2014), but even when the sensors are calibrated at their deployment, they develop drift in their records, leading to erroneous inferences being made by the network (Takruri et al., 2008). The drift in this context is a slow, directional, long-term change in the sensor measurements (Takruri et al., 2008). The manufacturer states 5% radiometric uncertainty with

approximately 2% drift per year (Apogee Instrument, 2003). Therefore, a drift term of 2% per year is applied to calibrated PAR sensors for 2016, 2017, 2018 and 2019 analyses. To eliminate the influence of high wind speed conditions on the bias of fPAR estimation, we removed the PAR data in which the wind speed is greater than 5 m/s based on Putzenlechner et al. (2020) study. The wind speed records on open grassland are from the TERENO meteorological station (model WXT520, Vaisala, Vantaa, Finland).

At the sub-alpine site Graswang, topographic shadowing periodically affects the WSNs (Putzenlechner et al., 2020). A digital elevation model (DEM 5 m, Free State of Bavaria, https://www.ldbv.bayern.de) and the solar position were used to determine the PAR data affected by topographic shadowing and excluded them from dataset. Sensors for incoming PAR (PAR_{in}) and transmitted PAR (PAR_{trans}) are separated by 300 m in the site (Putzenlechner et al., 2019a). Considering the shadowing effect of moving clouds, we excluded data where PAR_{trans} exceeded PAR_{in} to eliminate the impact of cloud shadows for sensors outside the forest, and data acquired during mixed illumination conditions for sensors in the forest (Putzenlechner et al., 2019b).

PAR data were further processed and analyzed using the statistical programming language R to calculate the fPAR. Measurements of PAR_{in} and PAR_{trans} carried out at 10 min temporal resolution were processed to fPAR estimates and calculated individually at each (i) of the 16 (n) sensor locations in the forest following equation (Putzenlechner et al., 2019a):

$$\mathrm{fPAR} = 1 - \frac{\mathrm{PAR_{trans}}}{\mathrm{PAR_{in}}}$$

The resulting daily fPAR at noontime was used for fPAR analysis. The variation of the mean fPAR value in the growing season (June, July and August) of Graswang forest during 2016 to 2019 is then plotted and interpolated using the Kriging interpolation algorithm method to represent the spatial distribution of fPAR using Surfer® from Golden Software, LLC (Software, 2021). Spatiotemporal variability of the fPAR was compared using the resulting interpolations for 2016, 2017, 2018 and 2019. A raster calculation was performed to determine the spatiotemporal change of fPAR in the WSN site between each year.

2.2.6 Relationship between Vertical Forest Structure, Tree Inventory, and FPAR

To better understand the vertical forest structure in the study site, raster correlation was used to determine the spatiotemporal relationship between each factor's interpolation map (LAI, Cx, Cy, and RG). Three scans with different RG level (high, medium and low) are selected and their waveforms are compared to determine the difference of vertical profile.

The DHPs were taken in September 2019. The resulting LAI values and the mean daily fPAR over this period are calculated and were used for the analysis. Both LAI and fPAR are interpolated for spatial analysis using the Kriging interpolation (cell size of 1m) in Surfer.

Montgomery et al. (2001) found that light transmission becomes independent when the lag distance between two points increases to approximate 5 m. To determine the factors of the fPAR value, a 5m buffer is applied at each node in ArcGIS software and the number of healthy and unhealthy trees (damaged/sick and dying/dead) are counted within each buffer. A Pearson correlation analysis is performed between LAI from DHP, tree mortality, tree species and fPAR (mean value of September 2019 for each node).

2.2.7 Statistical Analysis

The chi-squared test is a non-parametric statistical test to analyze group difference when the dependent variable is measured at a nominal level (Mchugh, 2013). This statistical test was used to determine whether there is a significant temporal change of fPAR between years in the study area. This test was performed in RStudio with a 5% significance level. The mean values of fPAR for each node from June to August on a yearly basis are used in the test.

2.3 Results

2.3.1 Forest Inventory

The WSN site comprises 84% Norway spruce and 16% European beech (Figure 4a) of which 84% of the trees have a DBH less than 20 cm, 13% have a DBH between 20 cm to 30 cm, and 3% have a DBH greater than 30 cm (Figure 4e). Spruce has a DBH range from 0 cm to

45 cm with a median of 8cm, whereas beech has a DBH range from 2 cm to 26 cm with a median of 7 cm (Figure 4c). Both species have the most DBH distribution between 0 cm and 10 cm (Figure 4c).

In this mixed coniferous forest, 53% of trees were healthy, 11% were damaged or sick, and 36% were dying or dead when the inventory was gathered in 2017 (Figure 4b,d). The medians are 13 cm, 8 cm, and 5 cm, respectively. Norway spruce was 49% healthy, 11% sick, and 40% dead; European beech had 73% healthy and 27% unhealthy (Figure 4f). The healthy trees had a DBH range from 0 cm to 45 cm and were well distributed along the range with a median of 13 cm, and unhealthy trees had a DBH maximum at 20 cm and were concentrated below 10 cm (Figure 4d). The median of DBH for unhealthy trees was 6 cm.

2.3.2 Spatial Variation of Vertical Forest Structure

A combination of all resulting waveforms from TLS data is presented in Figure 5. The waveform includes the probability of gap (Pgap), PAVD, and plant area density. LAI presents as the value at maximum height in plant area density. The centroid (Cx, Cy) and radius of gyration (RG) can be extracted from the PAVD profile. Figure 6 presents the spatial variation of the vertical forest structure (LAI, centroid and RG) in the study site in 2018. Information shows LAI ranges from 0.8 to 4.2 with a median of 2.1 and a standard deviation of 1.0 (Figure 6a). High LAI (LAI>2.8) is mainly concentrated in the WSN covered area, and varies between 0.8-4.2 with a median of 2.6. Cx varies between 0.01 and 0.18 with a median 0.06 and a standard deviation of 0.01 (Figure 6b). Cy fluctuates from 3.9 to 20.6 with a median of 11.6 and a standard deviation of 0.5 (Figure 6c). The WSN covered area experienced mostly high Cy with two low Cy spots. RG ranges from 5.7 to 22.4 with a median value of 8.1 and a standard deviation of 0.3 (Figure 6d). The forest has relative low RG except for Scan 21 where the RG is around 20. Scan 6 (medium RG) and Scan 64 (low RG) are selected to compare with Scan 21 (high RG) to explore the profile of vertical forest structure at locations with different RG levels (Figure 7). In the PAVD profile, the biomass in Scan 64 is mostly distributed at the bottom and at relatively higher heights for Scans 6 and 21. However, Scan 6 has more biomass than Scan 21 in general. Among three scans, Scan 6 showed the highest

LAI and Scan 21 showed the lowest LAI.

The relationship between centroid, RG and LAI is presented in Figure 8. The scatterplot shows that LAI has a significant positive correlation with Cx and Cy, but is negatively correlated with RG (Figure 8). The grey area presents the 95% confidence interval for the linear regression. Data are mostly concentrated between 0.05-0.12 Cx, 10-13 Cy, and 1-3 LAI in the Graswang forest site (Figure 8).

2.3.3 FPAR Ground Observations

Seasonal changes of mean fPAR among 16 sensors at noontime are depicted on a yearly basis in Figure 9. The period from April to September has the most complete continuous PAR data recorded for all 16 sensors from 2016 to 2019. Therefore, the fPAR data in this period was used for the analysis. During these four years, the mean fPAR for 16 nodes in the summer varied between 0.89 (+/- 1 STD) to 0.99 (+/- 1 STD) (Figure 9). Relatively lower fPAR values are observed in April, and higher fPAR values occur between June to September (Figure 9). The growing season (June, July, and August) is highlighted for each year where fPAR has the least fluctuation through the year (Figure 9). The 7-day moving average shows an increasing trend from April to May and then becomes relatively steady in June, July, and August except for 2017, where fPAR shows a gradual decrease in September (Figure 9).

Over the course of four years, the observations of fPAR consist of 92 sampling days in the growing season (June, July and August) at the Graswang study site, where 16 point measurements were continuously collected on a daily basis, resulting in a total of 4351 PAR measurements (Table 1). In the growing season, fPAR varies between 0.83 and 1.0, and the minimum value increased from 0.85 to 0.89 then decreased to 0.83 (Table 1). They are mostly distributed in the range of 0.95 to 0.99 in the first three years and 0.96 to 1.0 in 2019, where the frequency is over 100 (Figure 10). The highest frequency of fPAR appears between 0.96 and 0.97 in 2016, 0.97 and 0.98 in 2017, 0.98 and 0.99 in 2018 and 2019 (Figure 10). The summary of the descriptive statistics of fPAR for all sampling days in the growing season is presented in Table 1. The fPAR data are all follow a negatively skewed distribution over four

years and have a Platykurtic distribution in the first three years and a Leptokurtic distribution in the last year (Table 1). The average fPAR is estimated to be 0.96, 0.97, 0.97 and 0.97, respectively, and the standard deviation is 0.02 for all four years (Table 1).

2.3.4 Spatiotemporal Variability of FPAR

The spatial distributions of fPAR from 2016 to 2019 are shown in Figure 11, respectively. The map shows that the majority of the fPAR in the WSN covered area is above 0.96 in all four years. In 2016, the center (Node 4 and Node 10) and bottom (Node 15) regions of the WSN site experienced a high fPAR where the value was over 0.98 (Figure 11a). Node 1, Node 9, and Node 13 are within the low-value region where fPAR is below 0.95. In 2017, the locations of two high and two low areas stayed the same as 2016. Nodes 3 and 14 are included in the high fPAR region, and Node 16 is added as one of the low fPAR sensors (Figure 11b). The range of high fPAR, from 2017 to 2018, only included Node 4, and fPAR at Node 14 and 15 was classified as moderate (0.95-0.98) (Figure 11c). Node 9 also experienced an increase in fPAR since 2017. In 2019, two high fPAR regions appeared in the WSN site around Node 4 and Node 15, and two low fPAR areas were located around Node 1 and 13 (Figure 11d). Overall, high fPAR distributes into two regions, and low fPAR is concentrated in three regions and their locations have not been distinctly relocated spatially (Figure 11). From 2016 to 2019, fPAR varied between 0.90 and 1.0, increasing skewness towards 1.0 (Table 1). As for 2017, the fPAR in the Node 9 area and central regions increased in value, but fPAR around Node 1 remained constant (Figure 11). FPAR at Node 15 decreased before increasing since 2017.

Figure 12 presents the spatial change of mean fPAR in the growing season between years. Through the years, the mean fPAR varied between -0.019 to 0.011. From 2016 to 2017, the WSN-covered area mainly experienced increasing fPAR except for the regions around Node 14 and Nodes 4, 5, 6, 7, and 10 (Figure 12a). In 2018, most areas experienced an increasing fPAR except for the areas around Nodes 1 and 2 (Figure 12b). Since 2018, the WSN area has shown a declining fPAR, except for Nodes 2, 9, 11, and 15, where fPAR rose more than 0.005 (Figure 12c). Since 2017, Node 9 has been one of the cold spots over the years and has been

growing, as well as Node 15 and Node 4 which are the hot spots of fPAR.

Table 2 shows the chi-squared test result of fPAR temporal variability between 2016 and 2019. The change of fPAR is significant from 2016 to 2019 ($p<0.05$) (Table 2). From 2017 to 2019, the daily mean fPAR at noontime in June, July, and August significantly changed the WSN-covered area ($p<0.05$).

2.3.5 Relationship between FPAR and LAI

The spatial information of LAI and mean fPAR in 2018 are presented in Figure 13. The LAI is derived from DHPs, and the fPAR is the mean value of September 2019 for each node. The spatial LAI map shows that Nodes 10 and Node 15 experienced high LAI (LAI> 3.3), and Nodes 1, 9 and 16 were located in low LAI regions (LAI<2.3) (Figure 13a). During these days, fPAR varied between 0.94 and 1.0 (Figure 13b). Three low fPAR regions were found (fPAR <0.96): Nodes 1 and 2, Node 9, and Node 13. Two high fPAR areas were present: Nodes 3 and 4, Nodes 14, 15, and 16 (fPAR>0.98).

To analyze the relationship of various factors with fPAR, a correlation between every pair of factors is presented in Figure 13. LAI and beech amount, in the correlation matrix, show a significant positive correlation with fPAR, whereas mortality rate suggests a minor and insignificant relationship to fPAR (Figure 14).

2.4 Discussion

2.4.1 Forest Inventory

Graswang forest is a temperate mixed coniferous forest site composed of Norway spruce and European beech and dominated by spruce (Fig. 4a). The trees' DBHs range from 0 cm to 45 cm at this site, with the most distributed at below 10 cm (Fig. 4c). Spruce has a broader range of DBHs and a larger mean DBH than beech (Fig. 4c). This stand DBH characteristic is consistent with a previous study in the spruce-dominated forest (Bolte et al., 2010; Hans Pretzsch et al., 2020; Rötzer et al., 2017b). Our beech trees have a relatively smaller median than Spruce. Furthermore, other studies present a larger median of mature beech than our

result. Therefore, this observation suggests a younger age of beech than spruce in our forest. The forest consisted of 47% unhealthy trees with the most DBH between 0 cm and 10 cm. This result is similar to Orman and Dobrowolska's (2017) conclusion, where a DBH of 15 cm is the line of demarcation for living and dead trees. In 2017, 40% were recorded as dead, 51% of spruce were recorded as unhealthy (Fig. 4f).

In 2017, Norway spruce had a higher amount and proportion of unhealthy trees than European beech in the Graswang forest site (Fig. 4f). Half of the spruce in the forest were recorded as unhealthy at that time. Previous studies have found that both species show high mortality under severe intraspecific competition such as drought; however, beech is more resistant and stabilizing than spruce under climate stress and therefore is less affected (H. Pretzsch et al., 2020; Pretzsch et al., 2018; Rötzer et al., 2017a). Due to the severe European drought event in 2018 (de Brito et al., 2020), a rise in the forest's mortality rate is expected (Senf et al., 2020) and a greater mortality rate of spruce compared with beech is also expected. Other studies examine the mortality of both species in monocultures and mixed culture and conclude that European beech is more resilient and resistant to climate stress in monocultures, while spruce acclimatized faster and was more resilient to climatic stress in an admixture with beech (Pretzsch et al., 2020; Pretzsch et al., 2014; Rukh et al., 2020; Schäfer et al., 2017; Vacek et al., 2019). In this context, the observed smaller DBH of beech could indicate a spruce-dominated forest transitioning towards a mixed beech and spruce environment. Because of the frequent severe drought events in 2003, 2015 and 2018 (Büntgen et al., 2021), forest management has gradually shifted from a coniferous monoculture preference to a preference for mixed and structurally diversified stands (Vacek et al., 2019) to restore and protect forest sustainability.

2.4.2 Forest Structure

TLS data were collected in September 2018 in the Graswang forest site. The results show that LAI ranges from 0.8 to 4.2, with a median of 2.1 (Fig. 6a). Spatially, the high value of LAI and shape-metrics (Cx, Cy, and RG) are mostly distributed within the WSN site, indicating more terrestrial vegetation biomass in the WSN site than outside. In the study site, LAI shows

a significant positive linear relationship with Cx and Cy (Fig. 8), indicating the forest has more plant area volume at the canopy layer than the understory, specifically at 11.6 m height.

The LAI value from DHPs in the WSN site ranges between 1.8 and 4.2, which is within the range of the TLS result. Previous studies suggest that the LAI of Norway spruce varies from 1 to 5 in the growing season (Schlerf et al., 2005; Solberg et al., 2009) and a maximum of 3 to 4 in September for European beech (Černý et al., 2020). As for a mixed spruce-dominated forest, the LAI is expected to vary between 3 and 5 during the growing season. However, our LAI range from both DHPs and TLS appears lower than the hypothesis based on previous studies and may be caused by several factors.

Firstly, spruce LAI estimations tend to decrease with forest stand age (Pokorný and Stojnič, 2012; Schlerf et al., 2005). As our spruce has a wide DBH range from 0 cm to 45 cm, the oldest stands are expected to be up to 144 years old (Bolte et al., 2010) and the corresponding LAI is between 2 and 4.5 (Pokorný and Stojnič, 2012; Schlerf et al., 2005). Environmental conditions, such as soil temperature (Öztürk et al., 2015), air temperature (Öztürk et al., 2015), and humidity index also have an effect LAI estimation. The forest tends to have a high value of LAI in a young forest with a high soil temperature and a high mean air temperature during the growing season. The humidity index based on the ground vegetation affects the LAI spatially, where the dry site has shorter trees and fewer open canopies than the wet site (Schleppi et al., 2011). In addition, Germany experienced a heatwave in 2018, resulting in unusually hot weather that led to record-breaking temperatures and a severe drought year (de Brito et al., 2020). This drought event limited water availability potentially causing the observed low LAI. Research also suggests that LAI is sensitive to drought stress (Kim et al., 2017) and tends to decrease at the end of the growing period (Baghalian et al., 2011; Schleppi et al., 2011; Süßel and Brüggemann, 2021). As our TLS data was collected in September, the LAI value could be lower due to drought effect. Intense disturbances, such as drought, often increase tree mortality (Brienen et al., 2015; Hubau et al., 2020) and elevated tree mortality can influence forest dynamics by altering the succession pattern of the forests in favor of fast-growing species (Hiltner et al., 2020). Additionally, the functional species composition and tree size

distribution are also affected by tree mortality intensity, resulting in lower LAI values (Hiltner et al., 2020; Ogaya et al., 2015). Unfortunately, a general dearth of field reporting of mortality and LAI means that it is unclear whether tree mortality intensity and LAI decline are significantly impacted by drought.

Another possible cause of the low LAI estimation seen in our analysis comes from the method used. Compared with direct methods, the indirect method, involving technologies such as TLS and DHP, underestimated LAI on average by 15.1% (Breda, 2003; Černý et al., 2020; Mussche et al., 2001; Yan et al., 2019). The reason for the underestimation is widely accepted as the non-random distribution of foliar elements within the canopy, also known as the clumping factor (Breda, 2003). TLS can effectively estimate LAI, but the measurement is affected by clumping, occlusion, voxel size, and woody material (Ma et al., 2017; Wang and Fang, 2020; Yan et al., 2019). Compare with deciduous forest, coniferous forests have a lower clumping index and are more affected by it in LAI estimation (Zhu et al., 2018). It has been suggested that a mixed stands of coniferous and deciduous tends to have a relatively high clumping index and TLS tends to underestimated LAI in mixed wood forest (Zhu et al., 2018). Study found that the estimation of LAI varies based on the instruments and methods used, but neither DHP nor TLS are seen to be superior over the other (Kuusk et al., 2018).

2.4.3 Spatiotemporal Variability of FPAR

We presented a time series of fPAR measurements for the vegetation period of 2016 to 2019 using WSNs in the temperate mixed coniferous forest site in Graswang, Germany. All fPAR estimates reflect the seasonal increase and decrease of fPAR values and show relatively high and steady fPAR above 0.80 during the growing season (Figure 9). This result is consistent with previous research on fPAR temporal variation over the course of a year (Nestola et al., 2017; Putzenlechner et al., 2020). The frequency of fPAR between 0.99-1.0 in 2019 is twice the frequency seen in 2016 (Fig. 10). Frequency rises indicate an increase of APAR over the years. Both of them can be consequent of changes in forest structure. Besides natural forest dynamics, tree mortality can also alter canopy structure. Based on the forest inventory collected in 2017, 11% of the trees were considered damaged or sick, and 36% were recorded

as dying or dead. By 2019 when TLS data was collected, the damaged/sick trees were expected to be dying/dead. In addition, drought is an essential driver of tree mortality (Senf et al., 2020), and the severe drought event happened in 2018 may have also aggravated the mortality rate. Since fPAR depends on the total amount of leaves in the canopies, increasing tree mortality potentially leads to decreasing LAI and thus causes a decline of fPAR (Ogaya et al., 2015).

In the WSN site, the change of fPAR is significant between years according to the Chi-squared test (Table 2), especially after 2017. This suggests that the forest structure has experienced a considerable amount of change since 2017. In the time series, the hotspots and coldspots of fPAR have remained in a similar position in the site (Fig. 11). This observation suggests that the spatial distribution of fPAR in the study site varies over the year, but no strong alteration has occurred. Among three fPAR coldspots, Node 13 has missing data in 2016, 2017, and 2018 and is assumed to be the same as 2019, which leads to an unchanged low fPAR region. Node 9 has the complete data recorded for all four years and experiences an increasing trend of fPAR through the year (Fig. 11). This change could be natural or anthropogenic since it has an equal variation between years (±0.01). The third low fPAR region is around Node 1, which increased in 2017 and then decreased. Since 2018, this region has experienced a decreasing trend of fPAR indicating that this could be the region where forest structure alters the most.

Temporally, fPAR distribution's skewness has shifted towards positive in 2017 and then negative in the following years (Table 1). The site map shows that fPAR values have been mainly rising from 2016 to 2018 before experiencing a decline in the years since then (Fig. 12). In the context of the drought event in 2018, we treat 2017 and 2019 as pre- and post-drought years and find the change of fPAR has varied between -0.01 and 0.02 (Fig. 12d). Studies on fPAR responses to drought conclude that drought causes significant negative trends in fPAR, especially in open forests where fPAR has severe declines over 0.2 (Jiao et al., 2020; Turco et al., 2017; Yoshida et al., 2015). These conclusions are consistent with our results, where most areas experienced a declination of fPAR since the drought year. Although

our fPAR changes in a small range, the declination is considerable in our site.

2.4.4 Influence Variables on FPAR

In our analysis, the spatial distribution of LAI from DHPs and fPAR are significantly positively correlated (Fig. 13, Fig. 14). This result is consistent with several studies where the LAI has a strong positive effect on fPAR when it is less than three and less effective when it is more than three (Dawson et al., 2003; Hu et al., 2020; Mukherjee and Sarkar, 2016; Ogaya et al., 2015). Since the estimation of fPAR can be affected by solar zenith angle (Putzenlechner et al., 2019b), the study also examined its impact on the relationship between fPAR and LAI and found that when LAI was high, there was less of an effect from solar zenith angle on fPAR (Wang et al., 2016).

In the correlation analysis, fPAR shows a statically significant positive relationship with beech proportion but not mortality rate (Fig. 14). This indicates that the tree species can influence fPAR and coniferous and deciduous tree types have different effects on fPAR. European beech (deciduous tree) has broad, flat leaves, whereas Norway spruce (a coniferous tree) has small, needle-like leaves. The coniferous tree is more clumped than the deciduous tree and its leaves have a higher angle than a deciduous tree (Zhu et al., 2018); therefore, deciduous trees absorbed more PAR than coniferous trees for the same LAI (Chen et al., 2005). Hence, the proportion of beech is positively correlated with fPAR. Tree mortality does not show a significant strong impact on fPAR in our analysis. Our result contradicts previous studies where fPAR is negatively influenced by mortality (Jiao et al., 2020; Ogaya et al., 2015). As for now, the species ratio and tree mortality are expected to be different in the forest site. An additional inventory may help to understand the impact of altering the proportion of two species and their mortality on fPAR.

2.4.5 Strength and Shortcoming

Previous studies have mainly used indirect instrument such as LAI-2000 Plant Canopy Analyzer and DHP to estimate LAI (Cutini et al., 1998; Pokorný and Marek, 2000; Solberg et al., 2009) and find that they generally underestimates LAI more than the direct methods

(Černý et al., 2020). Among all commonly used indirect methods, DHPs have been tested to be the most robust technique in estimating LAI in a large range of canopy structure and environmental conditions (Garrigues et al., 2008). Therefore, the performance of other indirect methods are often compared with DHP (Jonckheere et al., 2004; Schleppi et al., 2007). In our study, both Terrestrial LiDAR (TLS) and DHPs are used to estimated LAI. Results show that the LAI from DHPs is within the TLS LAI range. Since DHPs have less data than TLS and the collection date were earlier than TLS, the LAI range from DHPs is in the upper range of LAI acquired from TLS. Previous study conducted in similar forest suggests a good accordance of LAI estimated from DHP and TLS and stated the difference between two techniques does not indicate one is more accurate than the other (Zhu et al., 2018). Further investigation on TLS performance can be done by correlation analysis with more DHPs data in the study site.

The influence of LAI on fPAR has been previously studied in the boreal forest (Dawson et al., 2003) and mainly uses satellite data, such as MODIS (Ranga B Myneni et al., 2002; Y Tian et al., 2004; Yang et al., 2006). The relationship between LAI and fPAR shows a steep incline which becomes gradual after fPAR reaches 0.8. Instead of Landsat, our research uses ground-based LiDAR data (TLS), which provide valuable measurements of forest canopy structure in a smaller spatial coverage in a temperate forest. Hence, our study focuses on the impact of LAI on fPAR in a more confined range and presents a more detailed relationship between the two variables.

In our fPAR data set, most WSN nodes have complete continuous data recorded in the growing season. However, a few nodes were missing data in the growing season and were assumed for these periods in the analysis, such as Node 13. Incomplete data sets would affect the spatial analysis of fPAR in the interpolation process. Therefore, continuous data collection remains the main issue for long-term fPAR research. The spatiotemporal change of fPAR after forest inventory data was collected is significant. However, a comparison over a more extended period of fPAR would be more valuable to explore the effect of forest structure change and climate stress (drought).

2.5 Conclusion

This study was designed to explore the influence of LAI on fPAR and the spatiotemporal variability of fPAR in a mixed coniferous temperate forest. To approach this objective, the ground-based LiDAR TLS is used to collect the 3D point clouds of the vertical forest structure in the Graswang forest site. The daily continuous photosynthetically active radiation (PAR) is recorded by wireless sensor networks (WSNs) and further calculated to fPAR for analysis. External variables, such as wind speed, topographic shadows, and cloud effects, were considered for the long-term fPAR analysis.

This study has found that fPAR has a natural temporal variation yearly in the mixed wood forest, and the spatial distribution remains similar from 2016 to 2019. The spatiotemporal changes of fPAR were seen to be caused due to forest structure changes induced by natural dynamics, tree mortality, and climate stress. To further explore the cause of fPAR variability, we investigate several factors' impacts on fPAR, including LAI, tree species, and mortality rate. The investigation of LAI impacts on fPAR has shown a consistent result with previous studies in boreal forests, where LAI positively correlated to fPAR. Multiple correlation analyses revealed that the type of tree species presents a positive correlation with fPAR, but the impact of mortality is insignificant and minimal. Limited mortality data may cause the contrary result to previous studies.

Our study considered the sensor calibration when employing WSNs over the long term and provided a more accurate fPAR estimation. Prior to this study, satellite-derived data are commonly used in the study of LAI and fPAR interaction on a large spatial scale. This work provides insight into the use of in situ data to analyze LAI's influence on fPAR. The consistent results demonstrate the performance of TLS and WSN in estimating LAI and fPAR in the temperate forest.

A limitation of this study is the incomplete data. In the study, fPAR in the growing season is selected in the analysis; however, the daily PAR data are not completely recorded for every node. Some nodes have missing data in the analysis period, such as Node 13. Lacking

information on LAI, tree species, and mortality in the later year constrain the discovery of fPAR temporal variability. Since the estimation of fPAR can be affected by solar zenith angle (Putzenlechner et al., 2019b), some studies examined its impact on the relationship between fPAR and LAI and found that when LAI was high, there was less of an effect from solar zenith angle on fPAR (Wang et al., 2016). As our study concluded a strong influence of tree species on fPAR, further investigation on how deciduous and coniferous affect LAI and fPAR relationship are suggested. Our results suggested differently to previous studies in mortality effects on fPAR, and further work needs to be carried out in order to validate their interaction and provide a deeper insight into the long-term impacts of climate stress on fPAR in mixed coniferous forests.

The present study contributes to our understanding of fPAR variation in the mixed wood forest. The result of LAI effects on fPAR provided a deeper insight into the implication of in situ WSN on monitoring forest dynamics and further suggested the connection between LAI and fPAR and their importance. The potential transition from spruce forest to spuce and beech mixed forest is an indication of the realization of restoring and sustaining the forest ecosystem. Greater efforts are needed in understanding the role of fPAR in a mixed coniferous forest. Sufficient and suitable forest policy should therefore be plan for the long-term care of forest functions in climate mitigation while maintaining its productivity.

2.6 Tables

Table 1 Descriptive statistics of the fraction of photosynthetically active radiation (fPAR) values for all 16 wireless sensor network (WSN) nodes in June, July, and August from 2016 to 2019.

Statistics	2016	2017	2018	2019
Mean	0.96	0.97	0.97	0.97
Median	0.97	0.97	0.97	0.98
Standard Deviation	0.02	0.02	0.02	0.02
Kurtosis	2.08	1.54	2.56	6.52
Skewness	-1.35	-1.26	-1.45	-1.93
Range	0.15	0.12	0.11	0.17
Minimum	0.85	0.87	0.89	0.83
Maximum	1.00	0.99	1.00	1.00
Count	1176	1066	1018	1091

Table 2 Pearson's Chi-squared test of the fraction of photosynthetically active radiation (fPAR) from June to August between each year from 2016 to 2019. The daily mean fPAR of 16 nodes is used in the analysis.

Year	P value	Significance
2016-2017	0.0093	Significant
2017-2018	0.0053	Significant
2018-2019	0.0024	Significant
2017-2019	0.034	Significant

2.7 Figures

Figure 1 Locations of the Graswang Terrestrial Environmental Observatories (TERENO) experimental site and the reference photosynthetically active radiation (PAR) sensor located on grassland outside the forest, Southern Bavaria, Germany.

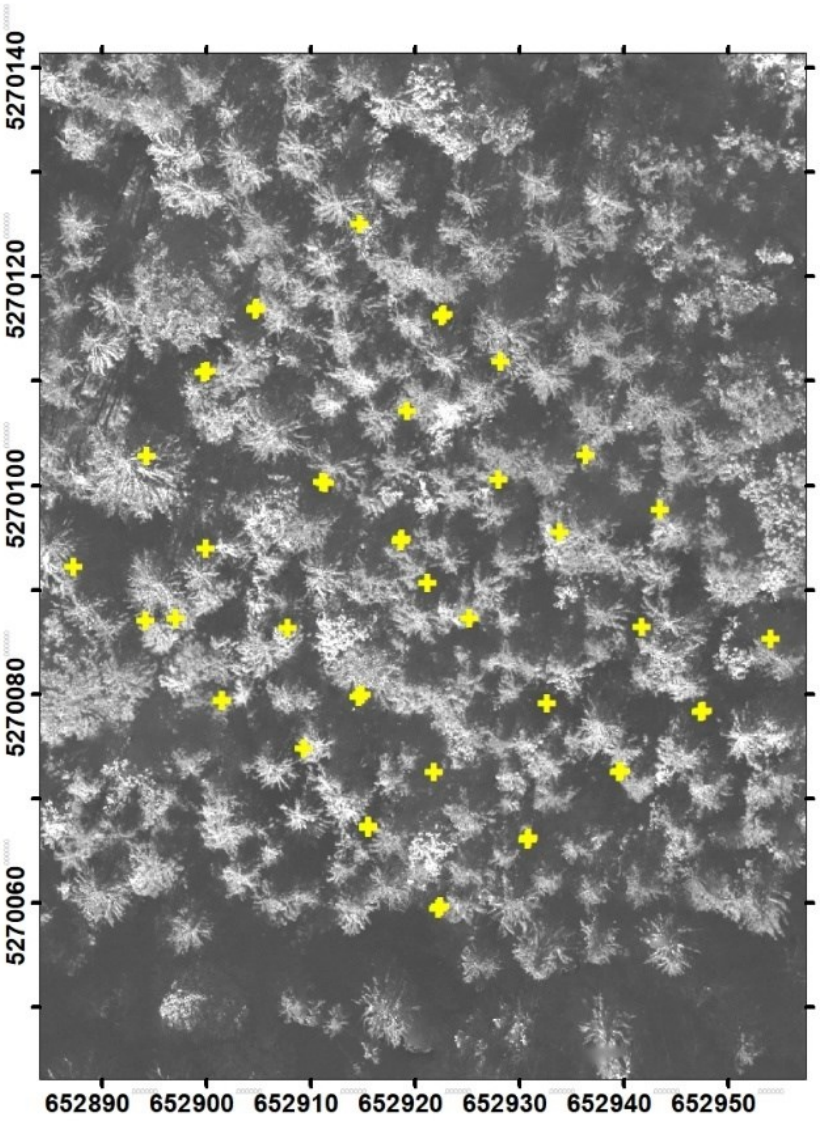

Figure 2 Top view of the 69 scans' location in Graswang forest collected by Riegl terrestrial laser scanner (TLS) during September 11th and 13th, 2018. Each position has two scans, one vertical and one horizontal, to avoid blind spots of the instrument and are shown in ETRS 1989 UTM Zone 32N Projection with latitude and longitude in meters.

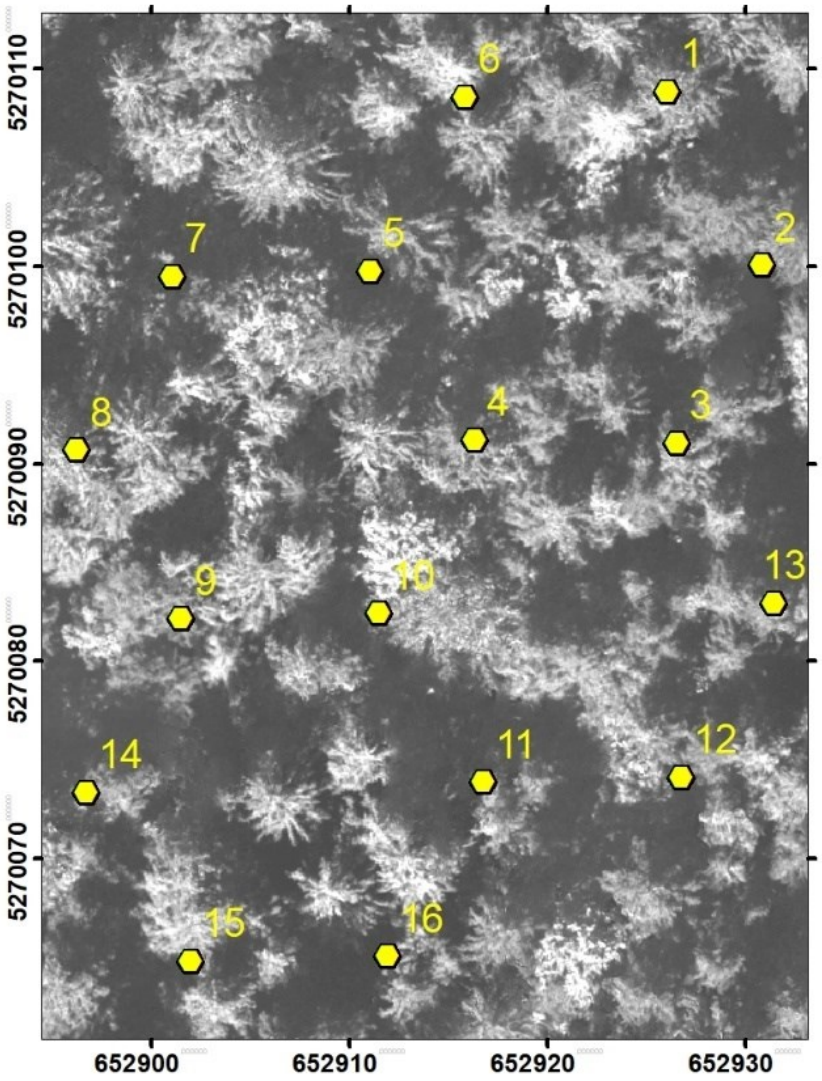

Figure 3 Experimental setup for photosynthetically active radiation (PAR) observations in the forest. Each of the 16 nodes was equipped with a PAR sensor pointed upward at 1.3 m height to perform synchronized measurements of transmitted PAR every 10 min. Viewing direction of the automated camera (Putzenlechner et al., 2019b).

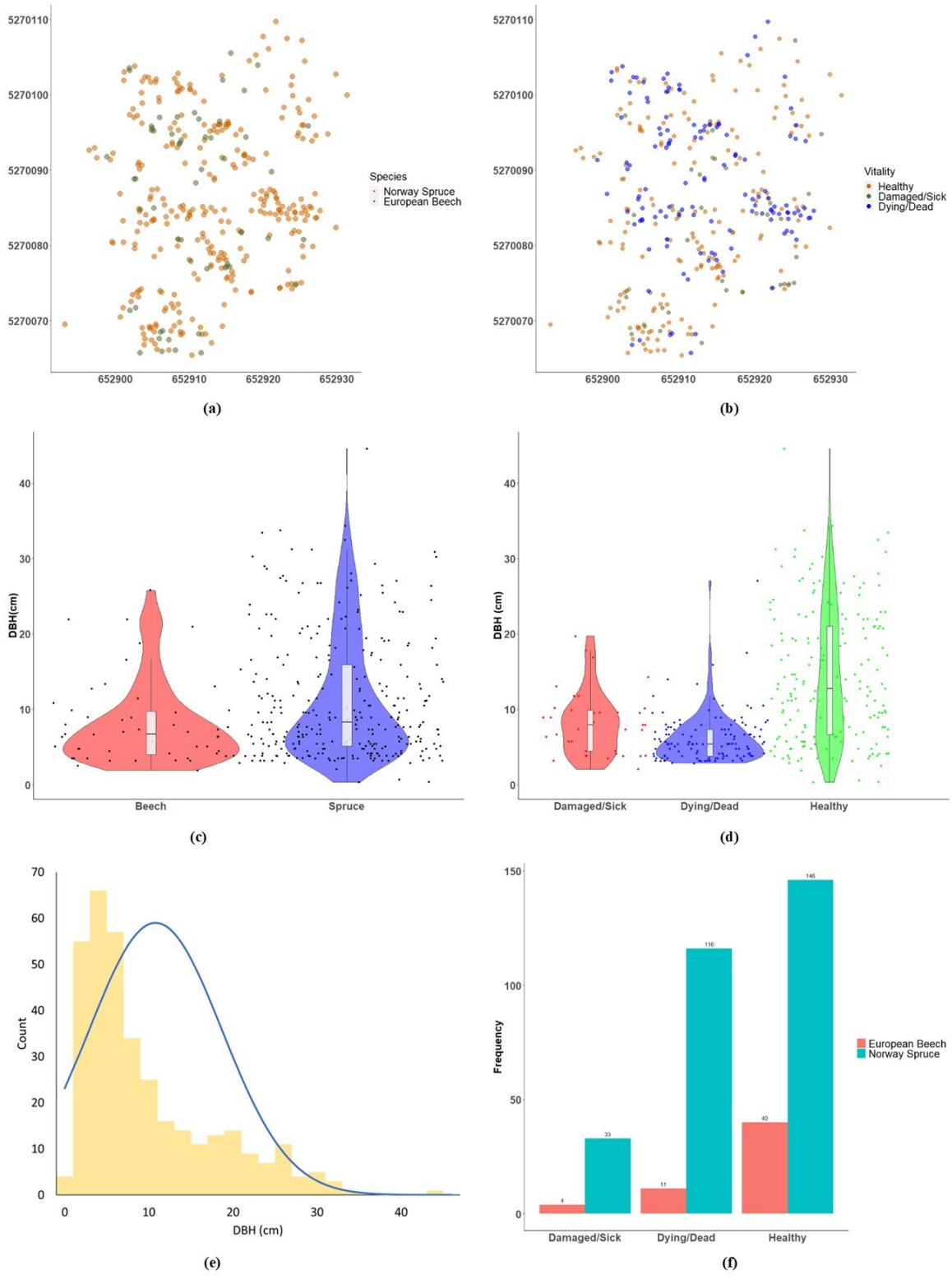

Figure 4 Position of trees categorized by (a) tree species and (b) vitality in 2017. The trees are plotted in the study site using ETRS 1989 UTM Projection. Violin plots of Tree diameter breast height (DBH) for (c) tree species and (d) vitality include the distribution of DBH and

summary statistics. The colored area presents the probability density of the DBH and the boxplot shows the median weight and interquartile ranges. (e) Tree DBH frequency distribution and normalized density curve. (f) Vitality histogram of spruce and beech: 49% of Norway spruce were healthy and 39% were dead; 73% of European beech were healthy and 20% were dead.

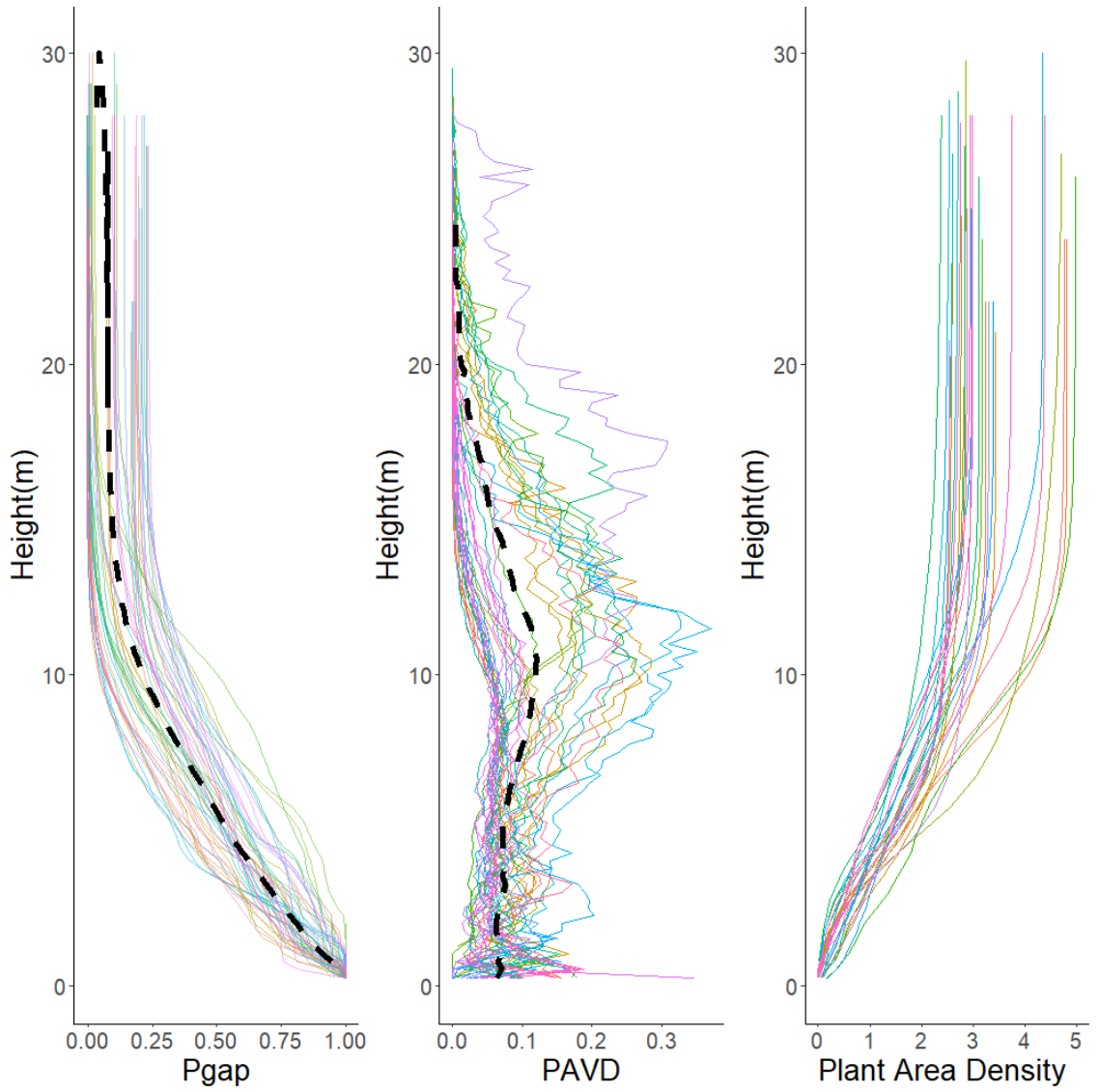

Figure 5 Waveforms for all 69 terrestrial laser scanner (TLS) scans at Graswang forest study site. The resulting waveform shows the information of probability of gap (Pgap), plant area volume density (PAVD), and plant area density. The dashed black line in each subfigure is of the average for the corresponding 69 curves.

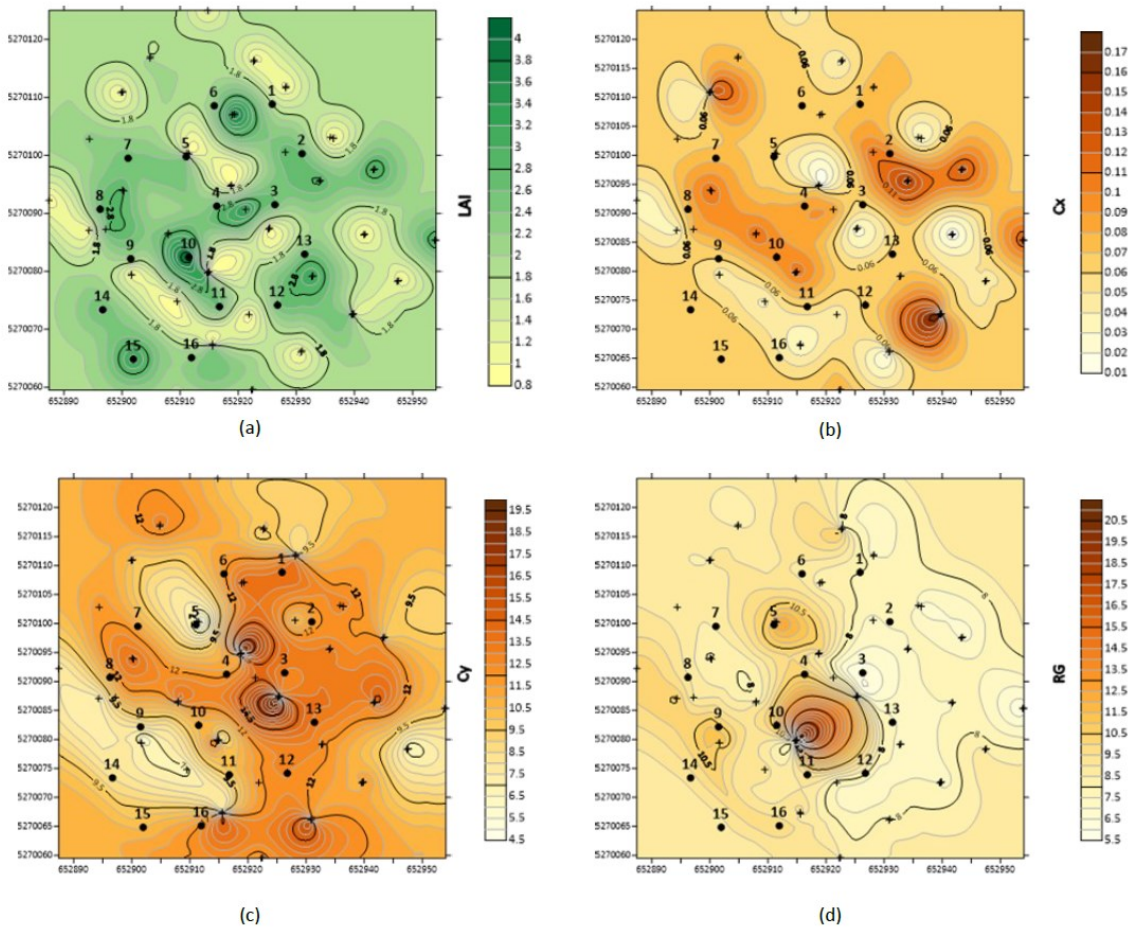

Figure 6 Spatial distribution of vertical forest structure parameters (a) leaf area index (LAI), (b) Cx, (c) Cy and (d) radius of gyration (RG) in the Graswang site on September 11st and 13rd, 2018. Contours are shown for each map. Cross indicates the terrestrial laser scanner (TLS) scans position, and dot indicates the wireless sensor network (WSN) nodes.

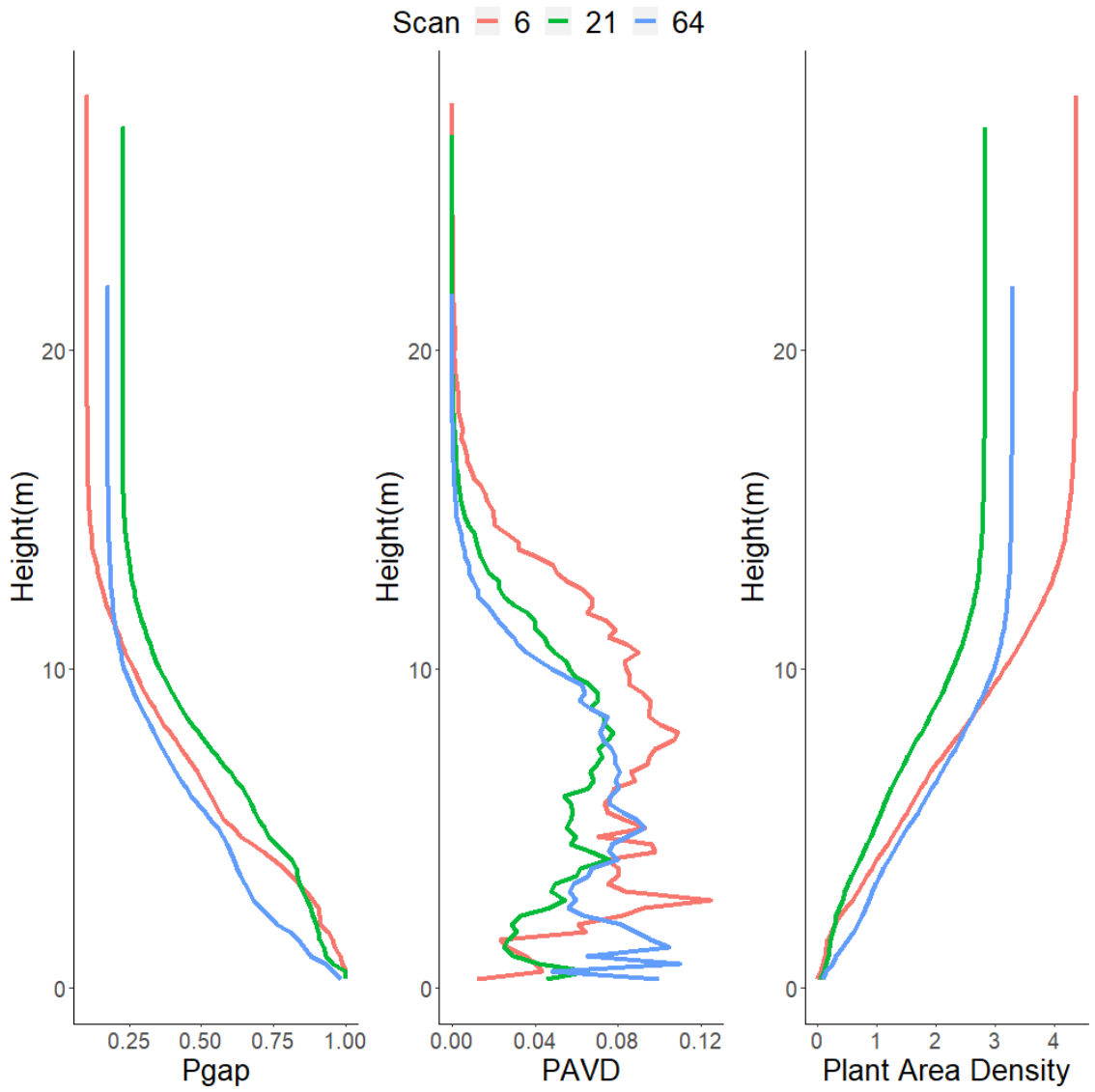

Figure 7 Waveform comparison for locations with three different radius of gyration (RG) levels in the spatial map: high RG (Scan 21), medium RG (Scan 6), and low RG (Scan 64).

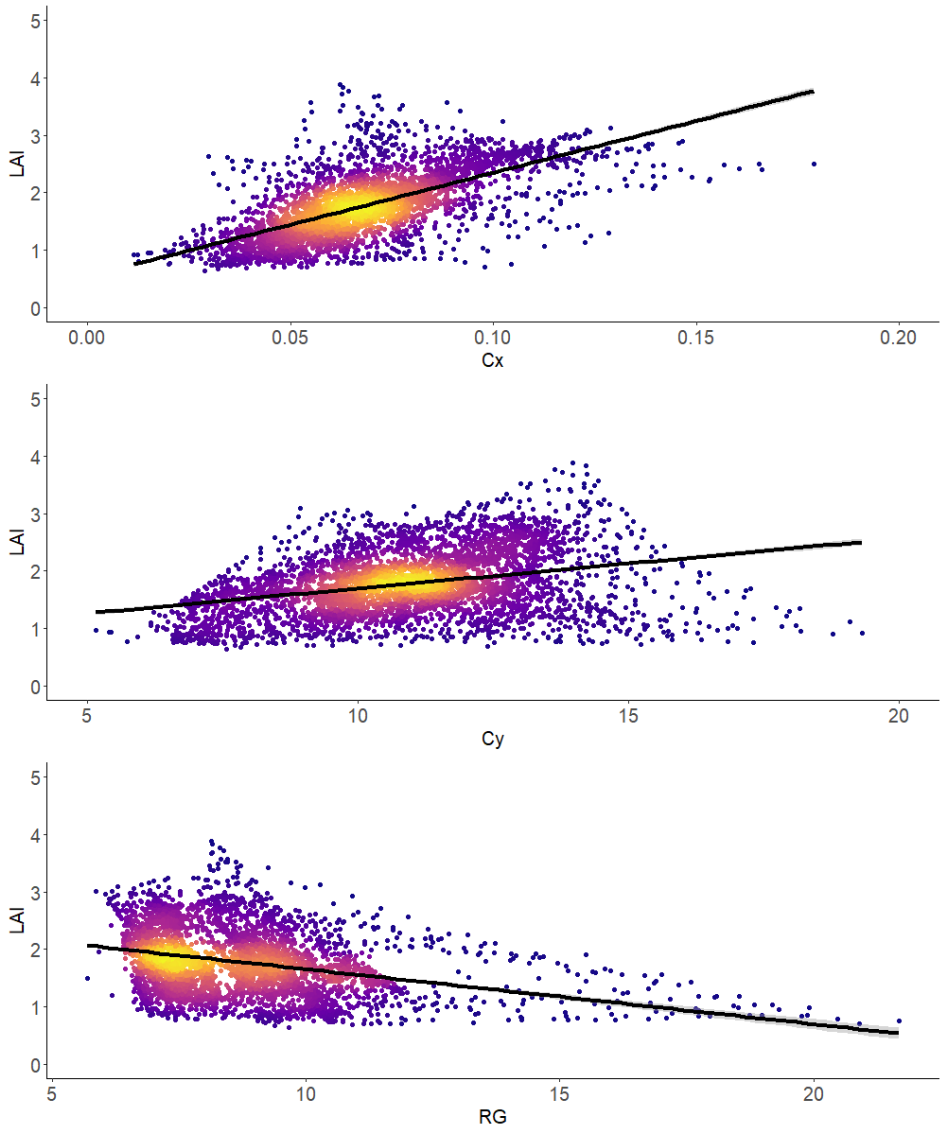

Figure 8 Density scatter plot and linear regression between leaf area index (LAI) and centroid (Cx, Cy), and radius of gyration (RG) with a 95% confidence interval present as grey area. Results shows LAI is positively correlated with Cx (correlation = 0.66, p-value <0.05) and Cy (correlation = 0.33, p-value <0.05) and negatively correlated with RG (correlation = -0.33, p-value <0.05).

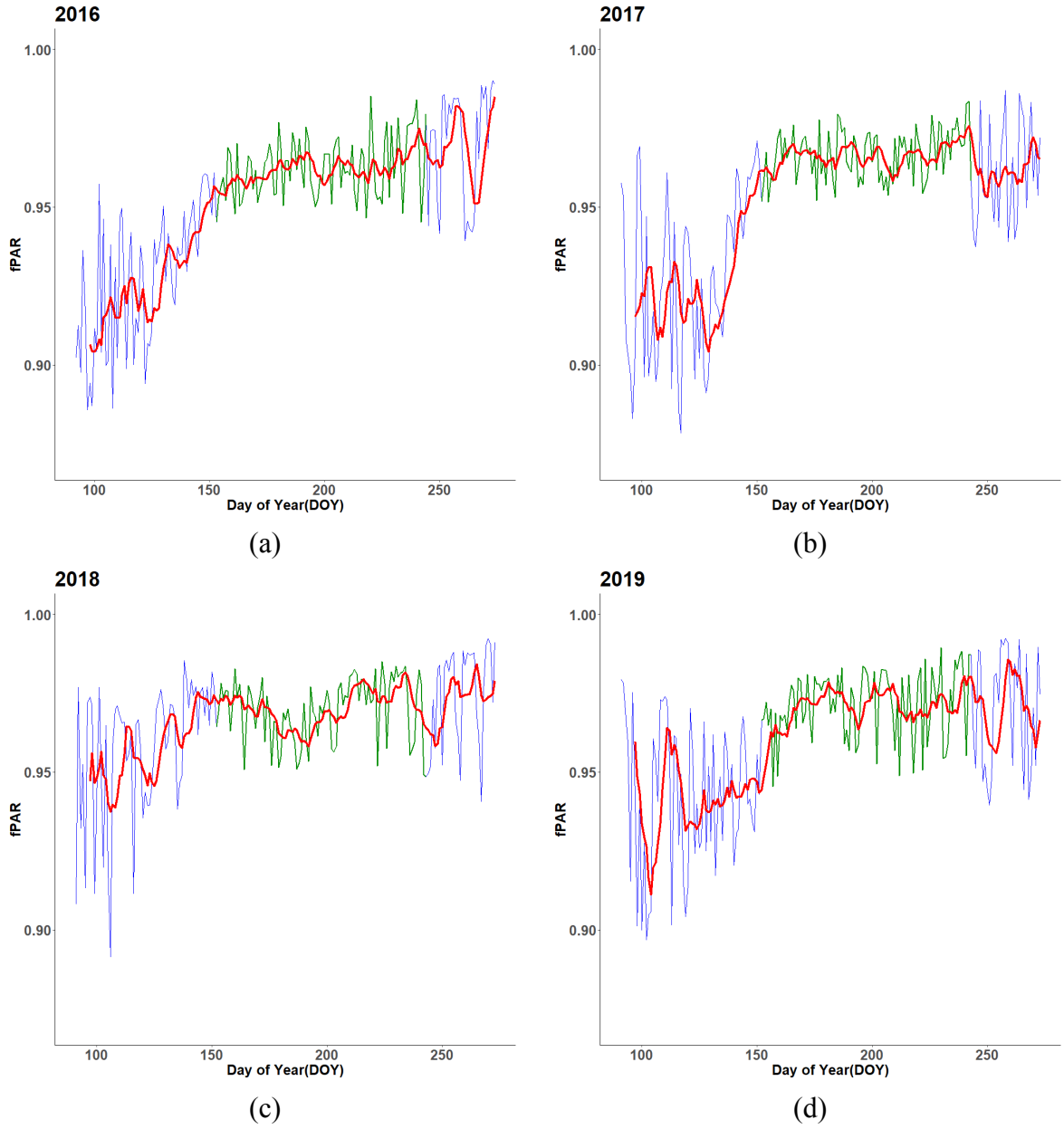

Figure 9 Seasonal changes of daily aggregated mean two-flux 10-min fraction of photosynthetically active radiation (fPAR) estimates at Graswang study site for 2016, 2017, 2018 and 2019. The blue line indicates the recorded fPAR from April to September, and the green line highlights June, July, and August. The red line 7-day moving average presents an average line over time and identifies a trend direction of fPAR for each year.

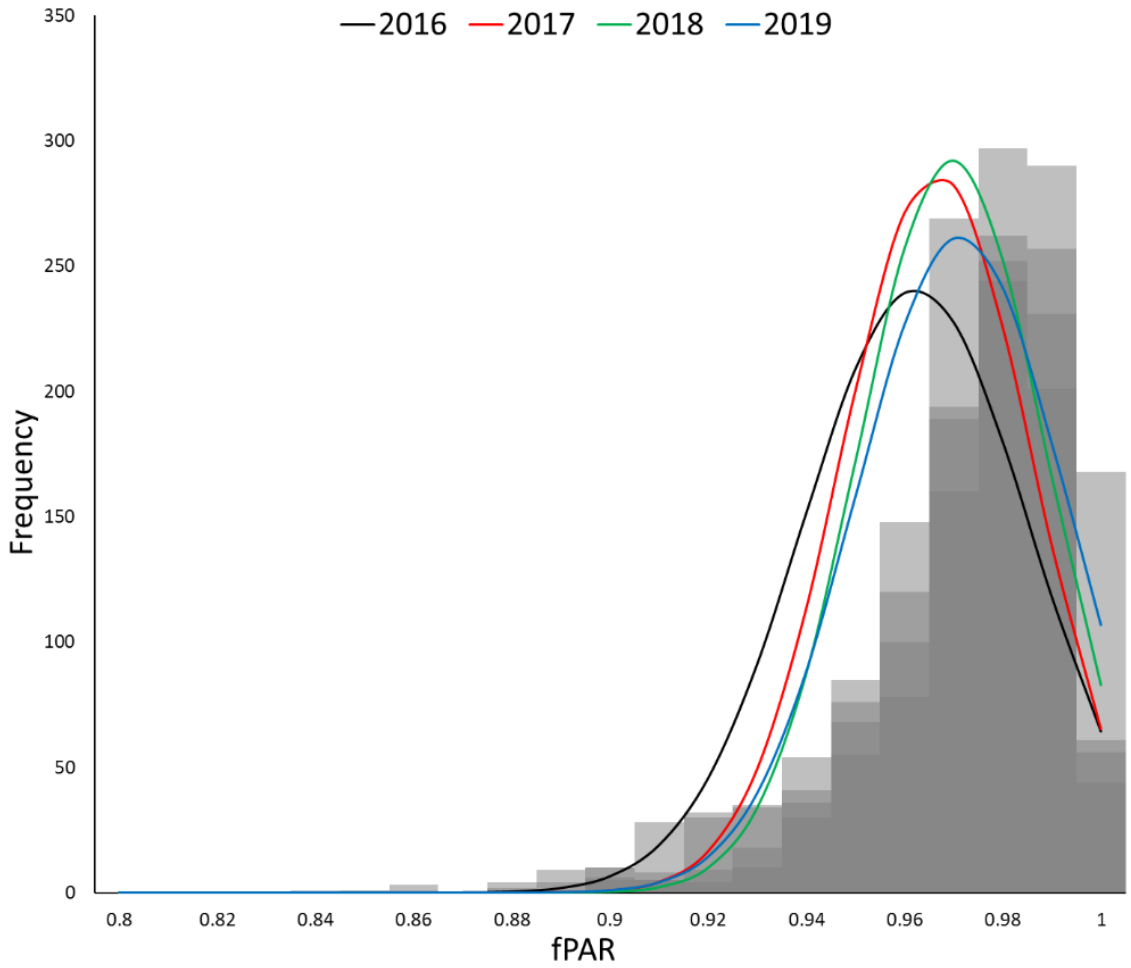

Figure 10 Frequency distribution of the fraction of photosynthetically active radiation (fPAR) with normalized density curve for each year from 2016 to 2019. FPAR values for all 16 nodes from June to August are used.

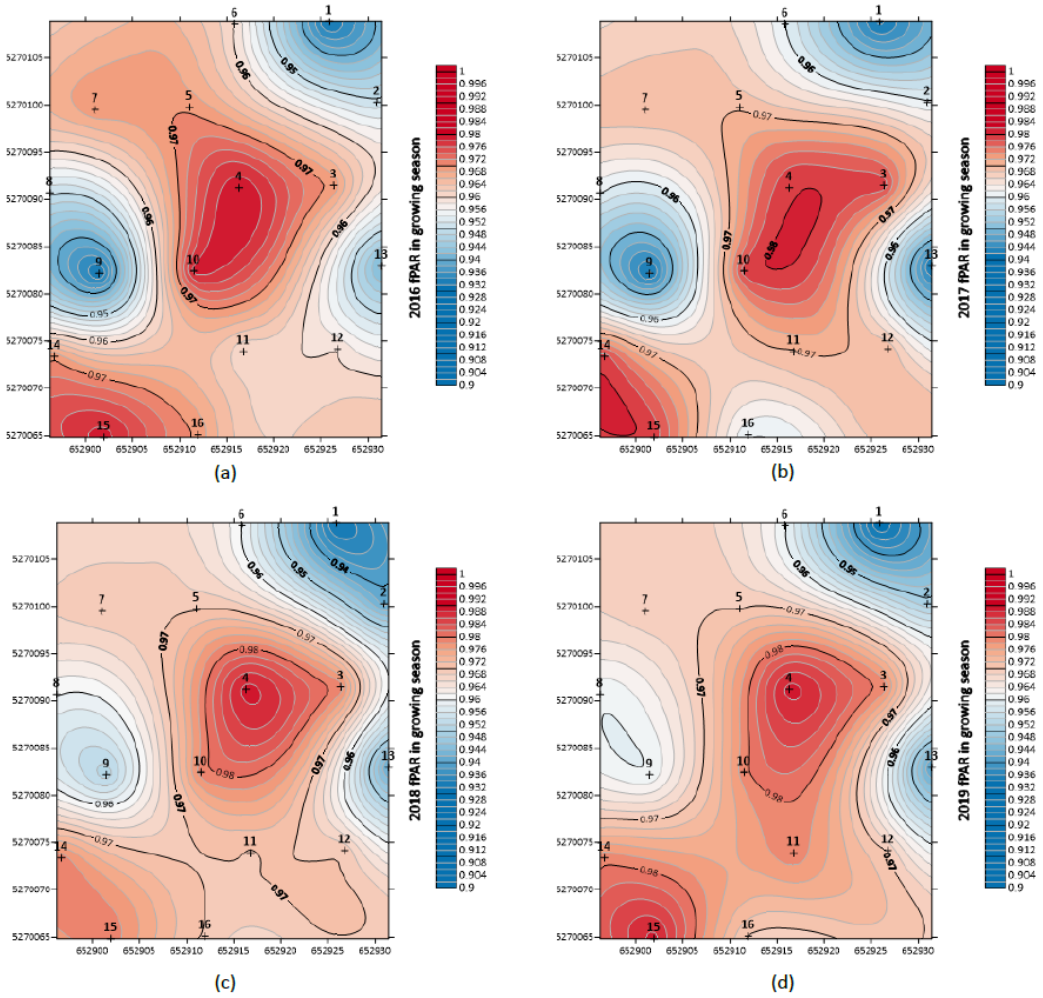

Figure 11 Spatial distribution and seasonal difference in mean fraction of photosynthetically active radiation (fPAR) in June, July, and August in 16 wireless sensor network (WSN) stations during 2016-2019. Maps are presented in ETRS 1989 UTM Zone 32N in 1x1 cell size. High fPAR values are shown in red and low fPAR values are shown in blue. Contours are also shown for each year. The crosses represent the locations of the 16 WSN nodes in the study area.

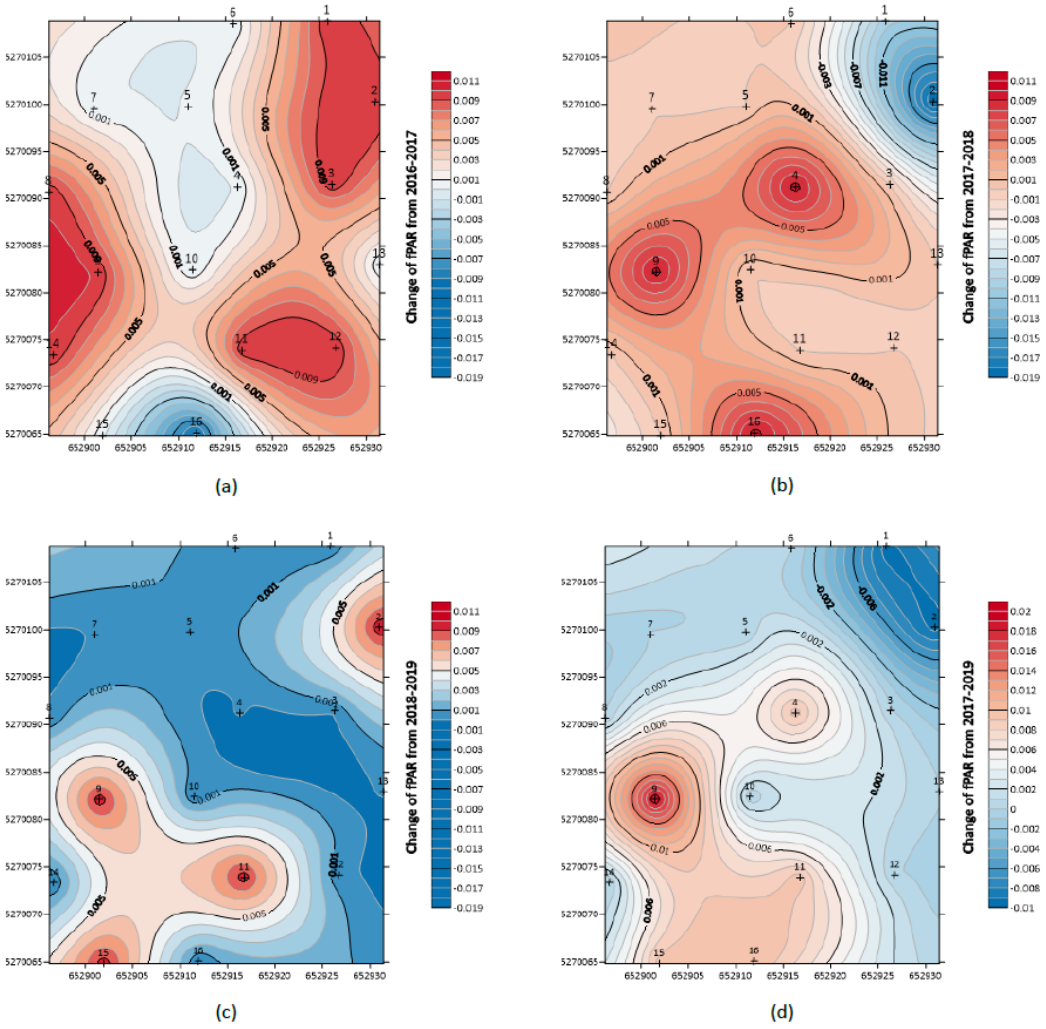

Figure 12 Spatial and temporal variation of the fraction of photosynthetically active radiation (fPAR) from 2016-2019. The mean fPAR for each nodes in June, July, and August is used in the analysis. Positive value indicates an increasing fPAR and is shown in red, and the negative value indicates a decreasing fPAR and is shown in blue. Contours are also shown for each map. The cross represents the position of 16 wireless sensor networkd (WSN) nodes in the study area.

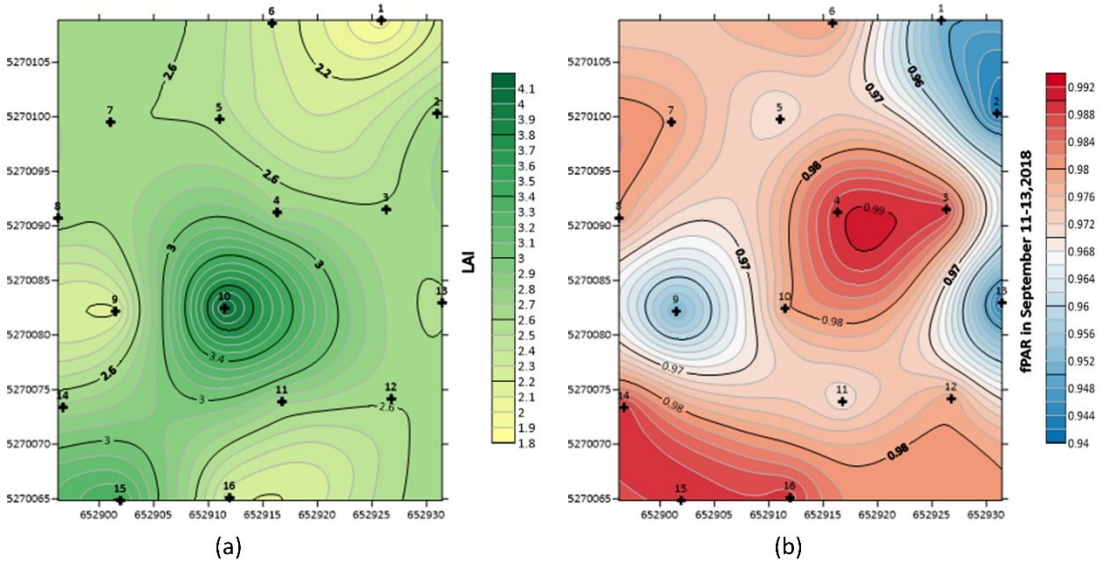

Figure 13 Spatial distribution of (a) digital hemispherical photographs (DHPs) leaf area index (LAI) and (b) the mean fraction of photosynthetically active radiation (fPAR) of each nodes in September 2019 using Kriging interpolation. The crosses indicate the node positions. The map is presented in ETRS 1989 UTM meters.

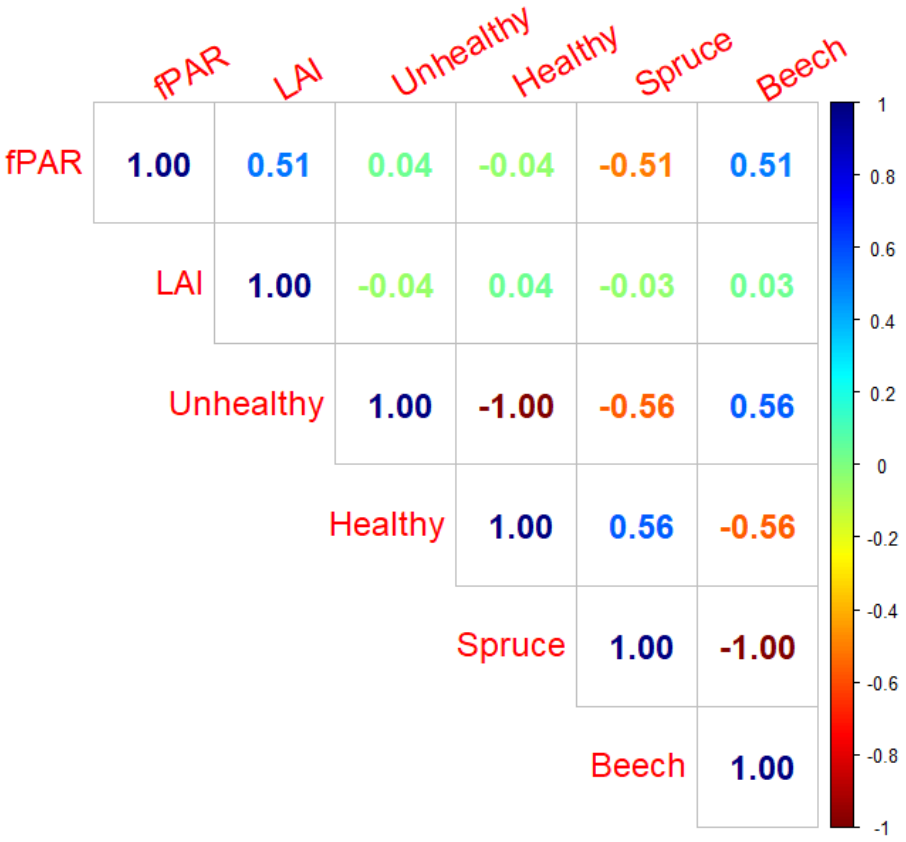

Figure 14 Correlation matrix between the fraction of photosynthetically active radiation (fPAR) and each factor (leaf area index (LAI), percentage of unhealthy and healthy trees, spruce, and beech), and between each pair of elements. Stronger correlations are denoted with darker blue and red.

2.8 References

Adeboye, O.B., Adeboye, A.P., Andero, O.S., Falana, O.B., 2019. Evaluation of AccuPAR LP 80 in estimating leaf area index of soybeans canopy in Ile-Ife, Nigeria. Agric. Res. 8, 297–308.

Anderson, K., Hancock, S., Disney, M., Gaston, K.J., 2016. Is waveform worth it? A comparison of LiDAR approaches for vegetation and landscape characterization. Remote Sens. Ecol. Conserv. 2, 5–15. https://doi.org/10.1002/rse2.8

Apogee Instrument, 2003. Owner ' s Manual Owner ' s Manual 8786, 1–11.

Baghalian, K., Abdoshah, S., Khalighi-Sigaroodi, F., Paknejad, F., 2011. Physiological and phytochemical response to drought stress of German chamomile (Matricaria recutita L.). Plant Physiol. Biochem. 49, 201–207. https://doi.org/https://doi.org/10.1016/j.plaphy.2010.11.010

Bolte, A., Hilbrig, L., Grundmann, B., Kampf, F., Brunet, J., Roloff, A., 2010. Climate change impacts on stand structure and competitive interactions in a southern Swedish spruce-beech forest. Eur. J. For. Res. 129, 261–276. https://doi.org/10.1007/s10342-009-0323-1

Bonan, G., 2015. Ecological climatology: concepts and applications. Cambridge University Press.

Breda, N.J.J., 2003. Ground- based measurements of leaf area index: a review of methods, instruments and current controversies. J. Exp. Bot. 54, 2403–2417.

Brienen, R.J.W., Phillips, O.L., Feldpausch, T.R., Gloor, E., Baker, T.R., Lloyd, J., Lopez-Gonzalez, G., Monteagudo-Mendoza, A., Malhi, Y., Lewis, S.L., 2015.

Long-term decline of the Amazon carbon sink. Nature 519, 344–348.

Büntgen, U., Urban, O., Krusic, P.J., Rybníček, M., Kolář, T., Kyncl, T., Ač, A., Koňasová, E., Čáslavský, J., Esper, J., 2021. Recent European drought extremes beyond Common Era background variability. Nat. Geosci. 14, 190–196.

Carrer, D., Roujean, J.L., Lafont, S., Calvet, J.C., Boone, A., Decharme, B., Delire, C., Gastellu-Etchegorry, J.P., 2013. A canopy radiative transfer scheme with explicit FAPAR for the interactive vegetation model ISBA-A-gs: Impact on carbon fluxes. J. Geophys. Res. Biogeosciences 118, 888–903. https://doi.org/10.1002/jgrg.20070

Černý, J., Haninec, P., Pokorný, R., 2020. Leaf area index estimated by direct, semi-direct, and indirect methods in European beech and sycamore maple stands. J. For. Res. 31, 827–836. https://doi.org/10.1007/s11676-018-0809-0

Chen, J.M., Black, T.A., 1992. Defining leaf area index for non- flat leaves. Plant. Cell Environ. 15, 421–429.

Chen, J.M., Menges, C.H., Leblanc, S.G., 2005. Global mapping of foliage clumping index using multi-angular satellite data. Remote Sens. Environ. 97, 447–457.

Chianucci, F., Cutini, A., 2012. Digital hemispherical photography for estimating forest canopy properties: Current controversies and opportunities. IForest 5, 290–295. https://doi.org/10.3832/ifor0775-005

Culvenor, D.S., Newnham, G.J., Mellor, A., Sims, N.C., Haywood, A., 2014. Automated in-situ laser scanner for monitoring forest leaf area index. Sensors 14, 14994–15008.

Dawson, T.P., North, P.R.J., Plummer, S.E., Curran, P.J., 2003. Forest ecosystem chlorophyll content: implications for remotely sensed estimates of net primary productivity. Int. J.

Remote Sens. 24, 611–617.

de Brito, M.M., Kuhlicke, C., Marx, A., 2020. Near-real-time drought impact assessment: a text mining approach on the 2018/19 drought in Germany. Environ. Res. Lett. 15, 1040a9.

Dong, T., Liu, J., Shang, J., Qian, B., Huffman, T., Zhang, Y., Champagne, C., Daneshfar, B., 2016. Assessing the impact of climate variability on cropland productivity in the Canadian Prairies using time series MODIS FAPAR. Remote Sens. 8. https://doi.org/10.3390/rs8040281

Fensholt, R., Sandholt, I., Rasmussen, M.S., 2004. Evaluation of MODIS LAI, fAPAR and the relation between fAPAR and NDVI in a semi-arid environment using in situ measurements. Remote Sens. Environ. 91, 490–507. https://doi.org/10.1016/j.rse.2004.04.009

Franklin, M., 2014. Solution to Ordinary and Universal Kriging Equations 1–5.

Frazer, G.W., Canham, C.D., Lertzman, K.P., 1999. Gap Light Analyzer (GLA), Version 2.0: Imaging software to extract canopy structure and gap light transmission indices from true-colour fisheye photographs, users manual and program documentation. Simon Fraser Univ. Burn. Br. Columbia, Inst. Ecosyst. Stud. Millbrook, New York 36.

G. Pastorello, G.A. Sanchez-Azofeifa, M.N., 2011. Enviro-Net: From Networks of Ground-Based Sensor Systems to a Web Platform for Sensor Data Management. Sensors 11, 6454.

García, E.M., Bermúdez, A., Casado, R., Quiles, F.J., 2007. Wireless sensor network localization using hexagonal intersection. IFIP Int. Fed. Inf. Process. 248, 155–166.

https://doi.org/10.1007/978-0-387-74899-3_14

Garrigues, S., Shabanov, N. V., Swanson, K., Morisette, J.T., Baret, F., Myneni, R.B., 2008. Intercomparison and sensitivity analysis of Leaf Area Index retrievals from LAI-2000, AccuPAR, and digital hemispherical photography over croplands. Agric. For. Meteorol. 148, 1193–1209. https://doi.org/10.1016/j.agrformet.2008.02.014

GCOS, 2016. The global observing system for climate: Implementation needs (GCOS- 200).

Gobron, N., Verstraete, M.M., 2009. Fraction of Absorbed Photosynthetically Active Radiation (FAPAR). Assess. status Dev. Stand. Terr. Essent. Clim. Var. 24.

Gu, Z., Cao, S., Sanchez-Azofeifa, G.A., 2018. Using LiDAR waveform metrics to describe and identify successional stages of tropical dry forests. Int. J. Appl. Earth Obs. Geoinf. 73, 482–492. https://doi.org/10.1016/j.jag.2018.07.010

Hardwick, S.R., Toumi, R., Pfeifer, M., Turner, E.C., Nilus, R., Ewers, R.M., 2015. The relationship between leaf area index and microclimate in tropical forest and oil palm plantation: Forest disturbance drives changes in microclimate. Agric. For. Meteorol. 201, 187–195. https://doi.org/10.1016/j.agrformet.2014.11.010

Hiltner, U., Huth, A., Fischer, R., 2020. Importance of succession in estimating biomass loss: Combining remote sensing and individual-based forest models. Biogeosciences Discuss. 1–23. https://doi.org/10.5194/bg-2020-264

Hu, Q., Yang, J., Xu, B., Huang, J., Memon, M.S., Yin, G., Zeng, Y., Zhao, J., Liu, K., 2020. Impact of photosynthetic active radiation on performance of tea crop under agro forestry eco system in eastern India. Remote Sens. 12, 912.

Hubau, W., Lewis, S.L., Phillips, O.L., Affum-Baffoe, K., Beeckman, H., Cuní-Sanchez, A.,

Daniels, A.K., Ewango, C.E.N., Fauset, S., Mukinzi, J.M., 2020. Asynchronous carbon sink saturation in African and Amazonian tropical forests. Nature 579, 80–87.

J. Antonio Guzmán Q., 2021. Package ‘ rTLS .’

Jiao, T., Williams, C.A., Rogan, J., De Kauwe, M.G., Medlyn, B.E., 2020. Drought Impacts on Australian Vegetation During the Millennium Drought Measured With Multisource Spaceborne Remote Sensing. J. Geophys. Res. Biogeosciences 125, 1–19. https://doi.org/10.1029/2019JG005145

Jonckheere, I., Fleck, S., Nackaerts, K., Muys, B., Coppin, P., Weiss, M., Baret, F., 2004. Review of methods for in situ leaf area index determination Part I. Theories, sensors and hemispherical photography. Agric. For. Meteorol. 121, 19–35. https://doi.org/10.1016/j.agrformet.2003.08.027

Kamnik, R., Nekrep Perc, M., Topolšek, D., 2020. Using the scanners and drone for comparison of point cloud accuracy at traffic accident analysis. Accid. Anal. Prev. 135. https://doi.org/10.1016/j.aap.2019.105391

Khaine, I., Woo, S.Y., 2015a. An overview of interrelationship between climate change and forests. Forest Sci. Technol. 11, 11–18. https://doi.org/10.1080/21580103.2014.932718

Khaine, I., Woo, S.Y., 2015b. An overview of interrelationship between climate change and forests. Forest Sci. Technol. 11, 11–18. https://doi.org/10.1080/21580103.2014.932718

Kiš, I.M., 2016. Comparison of ordinary and universal kriging interpolation techniques on a depth variable (a case of linear spatial trend), case study of the Šandrovac Field. Rud. Geol. Naft. Zb. 31, 41–58. https://doi.org/10.17794/rgn.2016.2.4

Kotamäki, N., Thessler, S., Koskiaho, J., Hannukkala, A., Huitu, H., Huttula, T., Havento, J.,

Järvenpää, M., 2009. Wireless in-situ Sensor Network for Agriculture and Water Monitoring on a River Basin Scale in Southern Finland: Evaluation from a Data User's Perspective. Sensors 9, 2862–2883. https://doi.org/10.3390/s90402862

Krelling, P.C.L., González-Jorge, H., Martínez-Sanchez, J., Arias, P., 2012. Accuracy in target center evaluation using Riegl LMS Z390i laser scanner and Riscan pro software. Opt. Appl. 42, 773–781. https://doi.org/10.5277/oa120409

Kuusk, A., Pisek, J., Lang, M., Märdla, S., 2018. Estimation of gap fraction and foliage clumping in forest canopies. Remote Sens. 10, 1153.

Li, W., Fang, H., 2015. Estimation of direct, diffuse, and total FPARs from Landsat surface reflectance data and ground- based estimates over six FLUXNET sites. J. Geophys. Res. Biogeosciences 120, 96–112.

Li, X., Liang, H., Cheng, W., 2020. Spatio-temporal variation in AOD and correlation analysis with PAR and NPP in China from 2001 to 2017. Remote Sens. 12. https://doi.org/10.3390/rs12060976

Liu, L., Zhang, X., Xie, S., Liu, X., Song, B., Chen, S., Peng, D., 2019. Global white-sky and black-sky fapar retrieval using the energy balance residual method: Algorithm and validation. Remote Sens. 11, 1004.

Lovell, J.L., Jupp, D.L.B., Gorsel, E. van, Jimenez-Berni, J., Hopkinson, C., Chasmer, L., van Gorsel, E., 2011. Foliage profiles from ground based waveform and discrete point lidar. Proc. SilviLaser 2011, 11th Int. Conf. LiDAR Appl. Assess. For. Ecosyst. Univ. Tasmania, Aust. 16-20 Oct. 2011 4, 1–10.

Ma, L., Zheng, G., Eitel, J.U.H., Magney, T.S., Moskal, L.M., 2017. Retrieving forest canopy

extinction coefficient from terrestrial and airborne lidar. Agric. For. Meteorol. 236, 1–21.

Majasalmi, T., 2015. Estimation of leaf area index and the fraction of absorbed photosynthetically active radiation in a boreal forest. Diss. For.

Majasalmi, T., Rautiainen, M., Stenberg, P., 2014. Modeled and measured fPAR in a boreal forest: Validation and application of a new model. Agric. For. Meteorol. 189, 118–124.

Mchugh, M.L., 2013. The Chi-square test of independence Lessons in biostatistics. Biochem. Medica 23, 143–9.

Mo, X., Liu, S., Chen, X., Hu, S., 2018. Variability, tendencies, and climate controls of terrestrial evapotranspiration and gross primary productivity in the recent decade over China. Ecohydrology 11, 1–13. https://doi.org/10.1002/eco.1951

Montgomery, R.A., Chazdon, R.L., 2001. Forest structure, canopy architecture, and light transmittance in tropical wet forests. Ecology 82, 2707–2718. https://doi.org/10.1890/0012-9658(2001)082[2707:FSCAAL]2.0.CO;2

Moreno, Á., García-Haro, F.J., Martínez, B., Gilabert, M.A., 2014. Noise reduction and gap filling of fAPAR time series using an adapted local regression filter. Remote Sens. 6, 8238–8260. https://doi.org/10.3390/rs6098238

Mortazavi, S.H., Salehe, M., MacGregor, M.H., 2014. Maximum WSN coverage in environments of heterogeneous path loss. Int. J. Sens. Networks 16, 185–198. https://doi.org/10.1504/IJSNET.2014.066788

Mukherjee, A., Sarkar, S., 2016. Impact of photosynthetic active radiation on performance of tea crop under agro forestry eco system in eastern India. Ital. J. Agrometeorol. Ital. DI Agrometeorol. 21, 37–46.

Muss, J.D., Aguilar-Amuchastegui, N., Mladenoff, D.J., Henebry, G.M., 2013. Analysis of waveform lidar data using shape-based metrics. IEEE Geosci. Remote Sens. Lett. 10, 106–110. https://doi.org/10.1109/LGRS.2012.2194472

Mussche, S., Samson, R., Nachtergale, L., De Schrijver, A., Lemeur, R., Lust, N., 2001. A comparison of optical and direct methods for monitoring the seasonal dynamics of leaf area index in deciduous forests. Silva Fenn. 35, 373–384. https://doi.org/10.14214/sf.575

Myneni, Ranga B, Hoffman, S., Knyazikhin, Y., Privette, J.L., Glassy, J., Tian, Y., Wang, Y., Song, X., Zhang, Y., Smith, G.R., 2002. Global products of vegetation leaf area and fraction absorbed PAR from year one of MODIS data. Remote Sens. Environ. 83, 214–231.

Myneni, R. B., Hoffman, S., Knyazikhin, Y., Privette, J.L., Glassy, J., Tian, Y., Wang, Y., Song, X., Zhang, Y., Smith, G.R., Lotsch, A., Friedl, M., Morisette, J.T., Votava, P., Nemani, R.R., Running, S.W., 2002. Global products of vegetation leaf area and fraction absorbed PAR from year one of MODIS data. Remote Sens. Environ. 83, 214–231. https://doi.org/10.1016/S0034-4257(02)00074-3

Nestola, E., Sánchez-Zapero, J., Latorre, C., Mazzenga, F., Matteucci, G., Calfapietra, C., Camacho, F., 2017. Validation of PROBA-V GEOV1 and MODIS C5 & C6 fAPAR products in a deciduous beech forest site in Italy. Remote Sens. 9, 126.

Ogaya, R., Barbeta, A., Başnou, C., Peñuelas, J., 2015. Satellite data as indicators of tree biomass growth and forest dieback in a Mediterranean holm oak forest. Ann. For. Sci. 72, 135–144.

Oliver, M.A., Webster, R., 1990. Kriging: A method of interpolation for geographical

information systems. Int. J. Geogr. Inf. Syst. 4, 313–332. https://doi.org/10.1080/02693799008941549

Orman, O., Dobrowolska, D., 2017. Gap dynamics in the Western Carpathian mixed beech old-growth forests affected by spruce bark beetle outbreak. Eur. J. For. Res. 136, 571–581.

Öztürk, M., Bolat, I., Ergün, A., 2015. Influence of air-soil temperature on leaf expansion and LAI of Carpinus betulus trees in a temperate urban forest patch. Agric. For. Meteorol. 200, 185–191. https://doi.org/10.1016/j.agrformet.2014.09.014

Parker, G.G., 2020. Tamm review: Leaf Area Index (LAI) is both a determinant and a consequence of important processes in vegetation canopies. For. Ecol. Manage. 477. https://doi.org/10.1016/j.foreco.2020.118496

Pastorello, G.Z., Sanchez-Azofeifa, G.A., Nascimento, M.A., 2011. Enviro-Net: From networks of ground-based sensor systems to a web platform for sensor data management. Sensors 11, 6454–6479.

Pokorný, R., Stojnič, S., 2012. Leaf area index of Norway spruce stands in relation to age and defoliation. Beskydy 5, 173–180. https://doi.org/10.11118/beskyd201205020173

Pretzsch, H., Grams, T., Häberle, K.H., Pritsch, K., Bauerle, T., Rötzer, T., 2020. Growth and mortality of Norway spruce and European beech in monospecific and mixed-species stands under natural episodic and experimentally extended drought. Results of the KROOF throughfall exclusion experiment. Trees - Struct. Funct. 34, 957–970. https://doi.org/10.1007/s00468-020-01973-0

Pretzsch, Hans, Hilmers, T., Biber, P., Avdagić, A., Binder, F., Bončina, A., Bosela, M., Dobor,

L., Forrester, D.I., Lévesque, M., 2020. Evidence of elevation-specific growth changes of spruce, fir, and beech in European mixed mountain forests during the last three centuries. Can. J. For. Res. 50, 689–703.

Pretzsch, H., Rötzer, T., Matyssek, R., Grams, T.E.E., Häberle, K.-H., Pritsch, K., Kerner, R., Munch, J.-C., 2014. Mixed Norway spruce (Picea abies [L.] Karst) and European beech (Fagus sylvatica [L.]) stands under drought: from reaction pattern to mechanism. Trees 28, 1305–1321.

Pretzsch, H., Schütze, G., Biber, P., 2018. Drought can favour the growth of small in relation to tall trees in mature stands of Norway spruce and European beech. For. Ecosyst. 5, 1–19.

Putzenlechner, B., Castro, S., Kiese, R., Ludwig, R., Marzahn, P., Sharp, I., Sanchez-Azofeifa, A., 2019a. Validation of Sentinel-2 fAPAR products using ground observations across three forest ecosystems. Remote Sens. Environ. 232, 111310. https://doi.org/10.1016/j.rse.2019.111310

Putzenlechner, B., Marzahn, P., Kiese, R., Ludwig, R., Sanchez-Azofeifa, A., 2019b. Assessing the variability and uncertainty of two-flux FAPAR measurements in a conifer-dominated forest. Agric. For. Meteorol. 264, 149–163. https://doi.org/10.1016/j.agrformet.2018.10.007

Putzenlechner, B., Marzahn, P., Sanchez-azofeifa, A., 2020. Accuracy assessment on the number offlux terms needed to estimate in situ fAPAR. Int J Appl Earth Obs Geoinf. 88, 102061. https://doi.org/10.1016/j.jag.2020.102061

Rankine, C.J., Sanchez-Azofeifa, G.A., Macgregor, M.H., 2014. Seasonal wireless sensor

network link performance in boreal forest phenology monitoring. 2014 11th Annu. IEEE Int. Conf. Sensing, Commun. Networking, SECON 2014 302–310. https://doi.org/10.1109/SAHCN.2014.6990366

Reiche, J., Lucas, R., Mitchell, A.L., Verbesselt, J., Hoekman, D.H., Haarpaintner, J., Kellndorfer, J.M., Rosenqvist, A., Lehmann, E.A., Woodcock, C.E., Seifert, F.M., Herold, M., 2016. Combining satellite data for better tropical forest monitoring. Nat. Clim. Chang. 6, 120–122. https://doi.org/10.1038/nclimate2919

RIEGL, 2019. VZ-400i RIEGL VZ-400i Ultra High Performance 3D Laser Scanner Redefining Productivity 1–2.

Rötzer, T., Biber, P., Moser, A., Schäfer, C., Pretzsch, H., 2017a. Stem and root diameter growth of European beech and Norway spruce under extreme drought. For. Ecol. Manage. 406, 184–195.

Rötzer, T., Häberle, K.H., Kallenbach, C., Matyssek, R., Schütze, G., Pretzsch, H., 2017b. Tree species and size drive water consumption of beech/spruce forests-a simulation study highlighting growth under water limitation. Plant Soil 418, 337–356.

Rukh, S., Poschenrieder, W., Heym, M., Pretzsch, H., 2020. Drought Resistance of Norway Spruce (Picea abies [L.] Karst) and European Beech (Fagus sylvatica [L.]) in Mixed vs. Monospecific Stands and on Dry vs. Wet Sites. From Evidence at the Tree Level to Relevance at the Stand Level. Forests 11, 639.

Ryu, Y., Lee, G., Jeon, S., Song, Y., Kimm, H., 2014. Monitoring multi-layer canopy spring phenology of temperate deciduous and evergreen forests using low-cost spectral sensors. Remote Sens. Environ. 149, 227–238.

Said, A.A., Yurtal, R., 2019. Spatial Groundwater Quality Assessment Using Geostatistics in Puntland, Somalia. Int. J. Sci. Technol. Res. 5, 84–92.

Sánchez-Azofeifa, G.A., Rankine, C., Do Espirito Santo, M.M., Fatland, R., Garcia, M., 2011. Wireless sensing networks for environmental monitoring: Two case studies from tropical forests. Proc. - 2011 7th IEEE Int. Conf. eScience, eScience 2011 70–76. https://doi.org/10.1109/eScience.2011.18

Schäfer, C., Grams, T.E.E., Rötzer, T., Feldermann, A., Pretzsch, H., 2017. Drought stress reaction of growth and Δ13C in tree rings of European beech and Norway spruce in monospecific versus mixed stands along a precipitation gradient. Forests 8, 177.

Schleppi, P., Conedera, M., Sedivy, I., Thimonier, A., 2007. Correcting non-linearity and slope effects in the estimation of the leaf area index of forests from hemispherical photographs. Agric. For. Meteorol. 144, 236–242.

Schleppi, P., Thimonier, A., Walthert, L., 2011. Estimating leaf area index of mature temperate forests using regressions on site and vegetation data. For. Ecol. Manage. 261, 601–610. https://doi.org/https://doi.org/10.1016/j.foreco.2010.11.013

Schlerf, M., Atzberger, C., Vohland, M., Buddenbaum, H., Seeling, S., Hill, J., 2005. Derivation of forest leaf area index from multi- and hyperspectral remote sensing data. EARSeL eProceedings 3, 405–413.

Senf, C., Buras, A., Zang, C.S., Rammig, A., Seidl, R., 2020. Excess forest mortality is consistently linked to drought across Europe. Nat. Commun. 11, 1–8. https://doi.org/10.1038/s41467-020-19924-1

Serbin, S.P., Ahl, D.E., Gower, S.T., 2013. Spatial and temporal validation of the MODIS

LAI and FPAR products across a boreal forest wildfire chronosequence. Remote Sens. Environ. 133, 71–84. https://doi.org/10.1016/j.rse.2013.01.022

Software, G., 2021. Surfer ® Registration Information.

Solberg, S., Brunner, A., Hanssen, K.H., Lange, H., Næsset, E., Rautiainen, M., Stenberg, P., 2009. Mapping LAI in a Norway spruce forest using airborne laser scanning. Remote Sens. Environ. 113, 2317–2327. https://doi.org/https://doi.org/10.1016/j.rse.2009.06.010

Süßel, F., Brüggemann, W., 2021. Tree water relations of mature oaks in southwest Germany under extreme drought stress in summer 2018. Plant Stress 1, 100010. https://doi.org/https://doi.org/10.1016/j.stress.2021.100010

Takruri, M., Rajasegarar, S., Challa, S., Leckie, C., Palaniswami, M., 2008. Online drift correction in wireless sensor networks using spatio-temporal modeling. Proc. 11th Int. Conf. Inf. Fusion, FUSION 2008.

Tao, X., Liang, S., He, T., Jin, H., 2016. Estimation of fraction of absorbed photosynthetically active radiation from multiple satellite data: Model development and validation. Remote Sens. Environ. 184, 539–557. https://doi.org/10.1016/j.rse.2016.07.036

Tian, F., Fensholt, R., Verbesselt, J., Grogan, K., Horion, S., Wang, Y., 2015. Evaluating temporal consistency of long-term global NDVI datasets for trend analysis. Remote Sens. Environ. 163, 326–340.

Tian, Y., Dickinson, R.E., Zhou, L., Zeng, X., Dai, Y., Myneni, R.B., Knyazikhin, Y., Zhang, X., Friedl, M., Yu, H., 2004. Comparison of seasonal and spatial variations of leaf area index and fraction of absorbed photosynthetically active radiation from Moderate Resolution Imaging Spectroradiometer (MODIS) and Common Land Model. J. Geophys.

Res. Atmos. 109.

Turco, M., Levin, N., Tessler, N., Saaroni, H., 2017. Recent changes and relations among drought, vegetation and wildfires in the Eastern Mediterranean: The case of Israel. Glob. Planet. Change 151, 28–35.

Vacek, Z., Vacek, S., Slanar, J., Bilek, L., Bulusek, D., Stefancik, I., Králíček, I., Vancura, K., 2019. Adaption of Norway spruce and European beech forests under climate change: from resistance to close-to-nature silviculture. Cent. Eur. For. JOURNAL, Vol. 65, issue 2.

Wang, Y., Fang, H., 2020. Estimation of LAI with the LiDAR technology: a review. Remote Sens. 12, 3457.

Wang, Y., Xie, D., Liu, S., Hu, R., Li, Y., Yan, G., 2016. Scaling of FAPAR from the Field to the Satellite. Remote Sens. 8, 310.

Widlowski, J.-L., 2010. On the bias of instantaneous FAPAR estimates in open-canopy forests. Agric. For. Meteorol. 150, 1501–1522.

Widlowski, J.L., 2010. On the bias of instantaneous FAPAR estimates in open-canopy forests. Agric. For. Meteorol. 150, 1501–1522. https://doi.org/10.1016/j.agrformet.2010.07.011

Xiao, Z., Liang, S., Sun, R., 2018. Evaluation of three long time series for global fraction of absorbed photosynthetically active radiation (fapar) products. IEEE Trans. Geosci. Remote Sens. 56, 5509–5524.

Xiao, Z., Liang, S., Wang, T., Jiang, B., 2016. Retrieval of leaf area index (LAI) and fraction of absorbed photosynthetically active radiation (FAPAR) from VIIRS time-series data. Remote Sens. 8. https://doi.org/10.3390/rs8040351

Yan, G., Hu, R., Luo, J., Weiss, M., Jiang, H., Mu, X., Xie, D., Zhang, W., 2019. Review of indirect optical measurements of leaf area index: Recent advances, challenges, and perspectives. Agric. For. Meteorol. 265, 390–411. https://doi.org/10.1016/j.agrformet.2018.11.033

Yang, W., Huang, D., Tan, B., Stroeve, J.C., Shabanov, N. V, Knyazikhin, Y., Nemani, R.R., Myneni, R.B., 2006. Analysis of leaf area index and fraction of PAR absorbed by vegetation products from the terra MODIS sensor: 2000-2005. IEEE Trans. Geosci. Remote Sens. 44, 1829–1842.

Yang, Z.I., Zhang, T. bin, Yi, G. hua, Li, J. ji, Qin, Y. bin, Chen, Y., 2021. Spatio-temporal variation of Fraction of Photosynthetically Active Radiation absorbed by vegetation in the Hengduan Mountains, China. J. Mt. Sci. 18, 891–906. https://doi.org/10.1007/s11629-020-6465-9

Yoshida, Y., Joiner, J., Tucker, C., Berry, J., Lee, J.-E., Walker, G., Reichle, R., Koster, R., Lyapustin, A., Wang, Y., 2015. The 2010 Russian drought impact on satellite measurements of solar-induced chlorophyll fluorescence: Insights from modeling and comparisons with parameters derived from satellite reflectances. Remote Sens. Environ. 166, 163–177.

Younis, M., Akkaya, K., 2008. Strategies and techniques for node placement in wireless sensor networks: A survey. Ad Hoc Networks 6, 621–655. https://doi.org/10.1016/j.adhoc.2007.05.003

Zacharias, S., Bogena, H., Samaniego, L., Mauder, M., Fuß, R., Pütz, T., Frenzel, M., Schwank, M., Baessler, C., Butterbach-Bahl, K., Bens, O., Borg, E., Brauer, A., Dietrich,

P., Hajnsek, I., Helle, G., Kiese, R., Kunstmann, H., Klotz, S., Munch, J.C., Papen, H., Priesack, E., Schmid, H.P., Steinbrecher, R., Rosenbaum, U., Teutsch, G., Vereecken, H., 2011. A network of terrestrial environmental observatories in Germany. Vadose Zo. J. 10, 955–973. https://doi.org/10.2136/vzj2010.0139

Zhao, P., Fan, W., Liu, Y., Mu, X., Xu, X., Peng, J., 2016. Study of the remote sensing model of FAPAR over rugged terrains. Remote Sens. 8, 10–12. https://doi.org/10.3390/rs8040309

Zhu, X., Skidmore, A.K., Wang, T., Liu, J., Darvishzadeh, R., Shi, Y., Premier, J., Heurich, M., 2018. Improving leaf area index (LAI) estimation by correcting for clumping and woody effects using terrestrial laser scanning. Agric. For. Meteorol. 263, 276–286. https://doi.org/10.1016/j.agrformet.2018.08.026

Zhu, Z., Bi, J., Pan, Y., Ganguly, S., Anav, A., Xu, L., Samanta, A., Piao, S., Nemani, R.R., Myneni, R.B., 2013. Global data sets of vegetation leaf area index (LAI)3g and fraction of photosynthetically active radiation (FPAR)3g derived from global inventory modeling and mapping studies (GIMMS) normalized difference vegetation index (NDVI3G) for the period 1981 to 2. Remote Sens. 5, 927–948. https://doi.org/10.3390/rs5020927

Chapter 3 – Conclusions

The objective of this thesis was to explore the spatiotemporal variability of the fraction of photosynthetically active radiation (fPAR) in a mixed coniferous temperate forest and better understand the influence of forest structure on fPAR using a ground-based terrestrial laser scanner (TLS) and in situ wireless sensor networks (WSNs). While the long-term fPAR variability has been studied, the data were often derived from satellite data (Fensholt et al., 2004; Liu et al., 2019; Putzenlechner et al., 2020), and research was focused on the boreal forest (Serbin et al., 2013; Tao et al., 2016; J.-L. Widlowski, 2010). The Graswang forest is part of the Terrestrial Environmental Observatories (TERENO) project investigating the long-term observation studies of climate change and global change impacts on terrestrial ecosystems across Germany (Zacharias et al., 2011). The site is already equipped with a long-term measurement system for existing research (Bogena, 2016) that offers continuous PAR data at the high spatial and temporal resolution we were interested in. In this thesis, a four-year fPAR dataset was processed using PAR data obtained from WSNs. The spatiotemporal variability of fPAR was analyzed and explored using a Kriging interpolation. Forest structure was described by LAI, centroid and radius of gyration acquired from 69 TLS scans. Information such as tree species and mortality rate were extracted from the forest inventory documented in 2017 and were correlated with fPAR to determine the influence level. Leaf area index (LAI) extracted from digital hemispherical photographs (DHPs) was examined for correlation with fPAR to study their interaction. These correlation analyses help improve the understanding of impacts of LAI, species, and mortality on fPAR.

3.1 Significance of Findings

The objectives of this thesis were to:

1. Explore the fPAR variability in a spatiotemporal scale in a temperate forest using wireless sensor networks (WSNs).
2. Study the influence of various factors in the forest on fPAR, including LAI, tree species, and tree mortality rate.

To address the first objective, the spatiotemporal variability of fPAR in a four-year time period was analyzed and compared year to year. Results showed that fPAR had a natural variation pattern through a year as expected (Nestola et al., 2017; Putzenlechner et al., 2020). The distribution of fPAR was left-skewed and was shifting towards 1.0 from 2016 to 2019. The continued rising of fPAR could be the dynamic change of forest structure, an indication of increasing tree mortality, and effects of climate stress. Spatially, two high and three low fPAR areas were discovered and remained in a similar position throughout the length of the study. During 2016 and 2019, fPAR changed in a small range but was significant between each year. The WSN site experienced its main increasing of fPAR before 2018 after which fPAR decreased. This finding indicated a disturbance event that happened in 2018 which largely altered fPAR. Due to the severe drought event discovered in 2018, this fPAR pattern can be explained by climate stress and high mortality as both factors are found to have an influence on fPAR (Jiao et al., 2020; Turco et al., 2017; Yoshida et al., 2015).

Exploring the second objective requires an illustration of the study site. According to documented forest inventory, the Graswang forest is composed of Norway spruce and European beech and is highly dominated by spruce. The DBH of beech are generally small indicating their immature stage compared with even-aged spruce. The relatively high mortality rate of spruce suggests it is susceptible characteristic when it is facing climate stress. This discovery supports previous studies on the responses of beech and spruce to climate change (H. Pretzsch et al., 2020; Pretzsch et al., 2014; Rukh et al., 2020; Schäfer et al., 2017; Vacek et al., 2019). As spruce presents better resilience and resistance in the admixture with beech, our results reveal a transition of our forest from a monoculture spruce forest to a mixed coniferous forest in order to restore and protect forest sustainability due to recent frequent climate stress in Europe. Norway spruce is considered as a native species in Europe and has experienced unprecedented declines in recent decades (Kolář et al., 2017). Beech belongs to the most socio-economically valuable European forest species and has become a forest management strategy to sustain the European forest ecosystem. In the current European forest ecosystem, even-aged spruce monocultures have been transformed into a more stable mixed coniferous and deciduous forest, where beech is the dominant species (Pretzsch et al.,

2014). Mixed stands of Norway spruce and European beech have the potential to mitigate the economic effects of climate change (Paul et al., 2019). Moreover, mixed tree species are expected to diversify stand structure with higher species, spatial and age structures to mitigate climatic change's negative effect (Vacek et al., 2019).

Forest structure metrics, leaf area index (LAI), centroid (Cx, Cy), and radius of gyration (RG) were used to describe and understand the Graswang forest vertical structure. The centroid and RG showed a statistically significant positive relationship with LAI, indicating the forest has more plant area volume at the canopy layer than the understory. This finding also supports the notion that the parameters of vertical forest structure are related to each other. The estimation of LAI is lower than the expected range. A possible explanation for this is the elder forest age, low water availability, high mortality rate and method instrument error (TLS). The bias of LAI estimation is mainly due to water limitation and tree mortality. The drought event has largely limited water availability in Europe (de Brito et al., 2020) and causes elevated tree mortality (Brienen et al., 2015; Hubau et al., 2020). Both consequences can lead to a decline of LAI in the forest growing season (Baghalian et al., 2011; Hiltner et al., 2020; Ogaya et al., 2015; Schleppi et al., 2011; Süßel and Brüggemann, 2021).

In order to understand the cause of fPAR variation, a multiple correlation analysis was conducted between LAI, tree species, mortality rate and fPAR. The statistical tests in Chapter 2 revealed a significant positive correlation between LAI and fPAR and are consistent with previous studies (Dawson et al., 2003; Hu et al., 2020; Mukherjee and Sarkar, 2016; Ogaya et al., 2015). This finding is contrary to our hypothesis, where larger fPAR indicates canopy gap and thus higher LAI. Therefore, high fPAR cannot be conclusively kinked to a more significant canopy gap in the forest, and further analysis is required to confirm the gap existence, such as the canopy height model. The significance confirms the interaction between these two biophysical variables. Tree species also found an effect on fPAR, whereas mortality shows a minor influence on fPAR. Coniferous and deciduous trees have different clumping factors and leaf angle distribution thus the PAR absorption abilities are different(Chen et al., 2005; Zhu et al., 2018). As deciduous trees have higher clumping index

than coniferous trees, they absorb more PAR than their coniferous counterparts, resulting in higher fPAR. The result of minor influence or no influence of mortality on fPAR has differed from previous research where fPAR is strongly negatively influenced by tree mortality (Jiao et al., 2020; Ogaya et al., 2015). Both previous studies used satellite-derived fPAR data, and the analysis time periods were over a decade. The mortality rate was measured annually during the term. In Chapter 2, we used in situ fPAR data and the mortality data was only for one year. The contrary conclusion of mortality effect on fPAR could be due to the spatial scale extent, temporal length, the type of fPAR data sets, or the forest selection.

3.2 Future Work

This thesis is based on the foundation for many other studies. LAI has mainly been estimated through the indirect method as the traditional methods are labour intense and time-consuming regardless of their accuracy. Many indirect methods have proven their usefulness in measuring LAI and their accuracy has been widely studied (Černý et al., 2020; Goude et al., 2019; Küßner and Mosandl, 2000; Yan et al., 2019). LAI-2000 and DHPs are the general ground-based methods used currently, and DHP has been used as a reference for determining other indirect methods' accuracy (Jonckheere et al., 2004; Zhu et al., 2018). In Chapter 2, we used both TLS and DHP and found the LAI result from DHP was within the TLS estimation. However, DHP presented a closer LAI range to the hypothetical forest LAI than TLS. Future works is needed to assess TLS performance for LAI estimation in a mixed coniferous forest.

In the correlation analysis between LAI and fPAR, our results support previous studies and suggest the usefulness of in situ WSNs in PAR measurement. However, the PAR datasets from WSNs are not fully continuous. Incomplete data reveals the issues with the outdoor performance of WSNs. Hence, the outdoor implication of WSNs and their performance evaluation in collecting continuous data require further study. Although our analysis of the LAI effects on fPAR presents consistent results with previous studies, the sample size for both datasets is limited to 16 due to the number of WSN nodes. A more detailed relationship could be explored with larger sample size. As the estimation of LAI and fPAR are related to tree mortality, a yearly recorded mortality in the forest can be used to analyze whether tree

mortality can influence the relationship between LAI and fPAR. In addition to the response of tree mortality to climate stress, we could further investigate how fPAR and LAI response to severe climate stress thus provide a useful solution for mitigating climate issue.

LAI describes forest structure through leaf area and fPAR quantifies the light absorption across an integrated plant canopy. Combine both biophysical variables, we can assess the forest function such as primary productivity and estimate the assimilation of carbon dioxide in vegetation using sufficient models. This thesis states the importance of LAI and fPAR and further investigated the interaction between each other. Chapter 2 suggested a coincident performance between satellite and in situ instrument in estimating biophysical variables in a mixed coniferous forest. The contrary result of mortality effect on fPAR brought the further investigation and experimentation into the role of tree mortality in climate mitigation.

3.3 Refrences

Baghalian, K., Abdoshah, S., Khalighi-Sigaroodi, F., Paknejad, F., 2011. Physiological and phytochemical response to drought stress of German chamomile (Matricaria recutita L.). Plant Physiol. Biochem. 49, 201–207. https://doi.org/https://doi.org/10.1016/j.plaphy.2010.11.010

Bogena, H.R., 2016. TERENO: German network of terrestrial environmental observatories. J. large-scale Res. Facil. JLSRF 2, 1–8. https://doi.org/10.17815/jlsrf-2-98

Brienen, R.J.W., Phillips, O.L., Feldpausch, T.R., Gloor, E., Baker, T.R., Lloyd, J., Lopez-Gonzalez, G., Monteagudo-Mendoza, A., Malhi, Y., Lewis, S.L., 2015. Long-term decline of the Amazon carbon sink. Nature 519, 344–348.

Černý, J., Haninec, P., Pokorný, R., 2020. Leaf area index estimated by direct, semi-direct, and indirect methods in European beech and sycamore maple stands. J. For. Res. 31, 827–836. https://doi.org/10.1007/s11676-018-0809-0

Chen, J.M., Menges, C.H., Leblanc, S.G., 2005. Global mapping of foliage clumping index using multi-angular satellite data. Remote Sens. Environ. 97, 447–457.

Dawson, T.P., North, P.R.J., Plummer, S.E., Curran, P.J., 2003. Forest ecosystem chlorophyll content: implications for remotely sensed estimates of net primary productivity. Int. J. Remote Sens. 24, 611–617.

de Brito, M.M., Kuhlicke, C., Marx, A., 2020. Near-real-time drought impact assessment: a text mining approach on the 2018/19 drought in Germany. Environ. Res. Lett. 15, 1040a9.

Fensholt, R., Sandholt, I., Rasmussen, M.S., 2004. Evaluation of MODIS LAI, fAPAR and

the relation between fAPAR and NDVI in a semi-arid environment using in situ measurements. Remote Sens. Environ. 91, 490–507. https://doi.org/10.1016/j.rse.2004.04.009

Goude, M., Nilsson, U., Holmström, E., 2019. Comparing direct and indirect leaf area measurements for Scots pine and Norway spruce plantations in Sweden. Eur. J. For. Res. 138, 1033–1047.

Hiltner, U., Huth, A., Fischer, R., 2020. Importance of succession in estimating biomass loss: Combining remote sensing and individual-based forest models. Biogeosciences Discuss. 1–23. https://doi.org/10.5194/bg-2020-264

Hu, Q., Yang, J., Xu, B., Huang, J., Memon, M.S., Yin, G., Zeng, Y., Zhao, J., Liu, K., 2020. Impact of photosynthetic active radiation on performance of tea crop under agro forestry eco system in eastern India. Remote Sens. 12, 912.

Hubau, W., Lewis, S.L., Phillips, O.L., Affum-Baffoe, K., Beeckman, H., Cuní-Sanchez, A., Daniels, A.K., Ewango, C.E.N., Fauset, S., Mukinzi, J.M., 2020. Asynchronous carbon sink saturation in African and Amazonian tropical forests. Nature 579, 80–87.

Jiao, T., Williams, C.A., Rogan, J., De Kauwe, M.G., Medlyn, B.E., 2020. Drought Impacts on Australian Vegetation During the Millennium Drought Measured With Multisource Spaceborne Remote Sensing. J. Geophys. Res. Biogeosciences 125, 1–19. https://doi.org/10.1029/2019JG005145

Jonckheere, I., Fleck, S., Nackaerts, K., Muys, B., Coppin, P., Weiss, M., Baret, F., 2004. Review of methods for in situ leaf area index determination Part I. Theories, sensors and hemispherical photography. Agric. For. Meteorol. 121, 19–35.

https://doi.org/10.1016/j.agrformet.2003.08.027

Kolář, T., Čermák, P., Trnka, M., Žid, T., Rybníček, M., 2017. Temporal changes in the climate sensitivity of Norway spruce and European beech along an elevation gradient in Central Europe. Agric. For. Meteorol. 239, 24–33.

Küßner, R., Mosandl, R., 2000. Comparison of direct and indirect estimation of leaf area index in mature Norway spruce stands of eastern Germany. Can. J. For. Res. 30, 440–447. https://doi.org/10.1139/x99-227

Liu, L., Zhang, X., Xie, S., Liu, X., Song, B., Chen, S., Peng, D., 2019. Global white-sky and black-sky fapar retrieval using the energy balance residual method: Algorithm and validation. Remote Sens. 11, 1004.

Mukherjee, A., Sarkar, S., 2016. Impact of photosynthetic active radiation on performance of tea crop under agro forestry eco system in eastern India. Ital. J. Agrometeorol. Ital. DI Agrometeorol. 21, 37–46.

Nestola, E., Sánchez-Zapero, J., Latorre, C., Mazzenga, F., Matteucci, G., Calfapietra, C., Camacho, F., 2017. Validation of PROBA-V GEOV1 and MODIS C5 & C6 fAPAR products in a deciduous beech forest site in Italy. Remote Sens. 9, 126.

Ogaya, R., Barbeta, A., Başnou, C., Peñuelas, J., 2015. Satellite data as indicators of tree biomass growth and forest dieback in a Mediterranean holm oak forest. Ann. For. Sci. 72, 135–144.

Paul, C., Brandl, S., Friedrich, S., Falk, W., Härtl, F., Knoke, T., 2019. Climate change and mixed forests: how do altered survival probabilities impact economically desirable species proportions of Norway spruce and European beech? Ann. For. Sci. 76, 1–15.

https://doi.org/10.1007/s13595-018-0793-8

Pretzsch, H., Grams, T., Häberle, K.H., Pritsch, K., Bauerle, T., Rötzer, T., 2020. Growth and mortality of Norway spruce and European beech in monospecific and mixed-species stands under natural episodic and experimentally extended drought. Results of the KROOF throughfall exclusion experiment. Trees - Struct. Funct. 34, 957–970. https://doi.org/10.1007/s00468-020-01973-0

Pretzsch, H., Rötzer, T., Matyssek, R., Grams, T.E.E., Häberle, K.-H., Pritsch, K., Kerner, R., Munch, J.-C., 2014. Mixed Norway spruce (Picea abies [L.] Karst) and European beech (Fagus sylvatica [L.]) stands under drought: from reaction pattern to mechanism. Trees 28, 1305–1321.

Putzenlechner, B., Marzahn, P., Sanchez-azofeifa, A., 2020. Accuracy assessment on the number offlux terms needed to estimate in situ fAPAR. Int J Appl Earth Obs Geoinf. 88, 102061. https://doi.org/10.1016/j.jag.2020.102061

Rukh, S., Poschenrieder, W., Heym, M., Pretzsch, H., 2020. Drought Resistance of Norway Spruce (Picea abies [L.] Karst) and European Beech (Fagus sylvatica [L.]) in Mixed vs. Monospecific Stands and on Dry vs. Wet Sites. From Evidence at the Tree Level to Relevance at the Stand Level. Forests 11, 639.

Schäfer, C., Grams, T.E.E., Rötzer, T., Feldermann, A., Pretzsch, H., 2017. Drought stress reaction of growth and Δ13C in tree rings of European beech and Norway spruce in monospecific versus mixed stands along a precipitation gradient. Forests 8, 177.

Schleppi, P., Thimonier, A., Walthert, L., 2011. Estimating leaf area index of mature temperate forests using regressions on site and vegetation data. For. Ecol. Manage. 261,

601–610. https://doi.org/https://doi.org/10.1016/j.foreco.2010.11.013

Serbin, S.P., Ahl, D.E., Gower, S.T., 2013. Spatial and temporal validation of the MODIS LAI and FPAR products across a boreal forest wildfire chronosequence. Remote Sens. Environ. 133, 71–84. https://doi.org/10.1016/j.rse.2013.01.022

Süßel, F., Brüggemann, W., 2021. Tree water relations of mature oaks in southwest Germany under extreme drought stress in summer 2018. Plant Stress 1, 100010. https://doi.org/https://doi.org/10.1016/j.stress.2021.100010

Tao, X., Liang, S., He, T., Jin, H., 2016. Estimation of fraction of absorbed photosynthetically active radiation from multiple satellite data: Model development and validation. Remote Sens. Environ. 184, 539–557. https://doi.org/10.1016/j.rse.2016.07.036

Turco, M., Levin, N., Tessler, N., Saaroni, H., 2017. Recent changes and relations among drought, vegetation and wildfires in the Eastern Mediterranean: The case of Israel. Glob. Planet. Change 151, 28–35.

Vacek, Z., Vacek, S., Slanar, J., Bilek, L., Bulusek, D., Stefancik, I., Králíček, I., Vancura, K., 2019. Adaption of Norway spruce and European beech forests under climate change: from resistance to close-to-nature silviculture. Cent. Eur. For. JOURNAL, Vol. 65, issue 2.

Widlowski, J.-L., 2010. On the bias of instantaneous FAPAR estimates in open-canopy forests. Agric. For. Meteorol. 150, 1501–1522.

Yan, G., Hu, R., Luo, J., Weiss, M., Jiang, H., Mu, X., Xie, D., Zhang, W., 2019. Review of indirect optical measurements of leaf area index: Recent advances, challenges, and perspectives. Agric. For. Meteorol. 265, 390–411.

https://doi.org/10.1016/j.agrformet.2018.11.033

Yoshida, Y., Joiner, J., Tucker, C., Berry, J., Lee, J.-E., Walker, G., Reichle, R., Koster, R., Lyapustin, A., Wang, Y., 2015. The 2010 Russian drought impact on satellite measurements of solar-induced chlorophyll fluorescence: Insights from modeling and comparisons with parameters derived from satellite reflectances. Remote Sens. Environ. 166, 163–177.

Zacharias, S., Bogena, H., Samaniego, L., Mauder, M., Fuß, R., Pütz, T., Frenzel, M., Schwank, M., Baessler, C., Butterbach-Bahl, K., Bens, O., Borg, E., Brauer, A., Dietrich, P., Hajnsek, I., Helle, G., Kiese, R., Kunstmann, H., Klotz, S., Munch, J.C., Papen, H., Priesack, E., Schmid, H.P., Steinbrecher, R., Rosenbaum, U., Teutsch, G., Vereecken, H., 2011. A network of terrestrial environmental observatories in Germany. Vadose Zo. J. 10, 955–973. https://doi.org/10.2136/vzj2010.0139

Zhu, X., Skidmore, A.K., Wang, T., Liu, J., Darvishzadeh, R., Shi, Y., Premier, J., Heurich, M., 2018. Improving leaf area index (LAI) estimation by correcting for clumping and woody effects using terrestrial laser scanning. Agric. For. Meteorol. 263, 276–286. https://doi.org/10.1016/j.agrformet.2018.08.026

References for Entire Thesis

Adeboye, O.B., Adeboye, A.P., Andero, O.S., Falana, O.B., 2019. Evaluation of AccuPAR LP 80 in estimating leaf area index of soybeans canopy in Ile-Ife, Nigeria. Agric. Res. 8, 297–308.

Anderson, K., Hancock, S., Disney, M., Gaston, K.J., 2016. Is waveform worth it? A comparison of LiDAR approaches for vegetation and landscape characterization. Remote Sens. Ecol. Conserv. 2, 5–15. https://doi.org/10.1002/rse2.8

Apogee Instrument, 2003. Owner ' s Manual Owner ' s Manual 8786, 1–11.

Aslan, Y.E., Korpeoglu, I., Ulusoy, özgür, 2012. A framework for use of wireless sensor networks in forest fire detection and monitoring. Comput. Environ. Urban Syst. 36, 614–625. https://doi.org/10.1016/j.compenvurbsys.2012.03.002

Baghalian, K., Abdoshah, S., Khalighi-Sigaroodi, F., Paknejad, F., 2011. Physiological and phytochemical response to drought stress of German chamomile (Matricaria recutita L.). Plant Physiol. Biochem. 49, 201–207. https://doi.org/https://doi.org/10.1016/j.plaphy.2010.11.010

Baret, F., Andrieu, B., Folmer, J.C., Hanocq, J.F., Sarrouy, C., 1993. Gap fraction measurement from hemispherical infrared photography and its use to evaluate PAR interception efficiency. Crop Struct. Microclim. Charact. Appl. INRA Ed. Paris 359–372.

Baslam, M., Mitsui, T., Hodges, M., Priesack, E., Herritt, M.T., Aranjuelo, I., Sanz-Sáez, Á.,

2020. Photosynthesis in a changing global climate: Scaling up and scaling down in crops. Front. Plant Sci. 11, 882.

Bauer, J., Jarmer, T., Schittenhelm, S., Siegmann, B., Aschenbruck, N., 2019. Processing and filtering of leaf area index time series assessed by in-situ wireless sensor networks. Comput. Electron. Agric. 165, 104867. https://doi.org/10.1016/j.compag.2019.104867

Bindoff, N.L., Willebrand, J., Artale, V., Cazenave, A., Gregory, J.M., Gulev, S., Hanawa, K., Le Quere, C., Levitus, S., Nojiri, Y., 2007. Observations: oceanic climate change and sea level.

Bogena, H.R., 2016. TERENO: German network of terrestrial environmental observatories. J. large-scale Res. Facil. JLSRF 2, 1–8. https://doi.org/10.17815/jlsrf-2-98

Bolte, A., Hilbrig, L., Grundmann, B., Kampf, F., Brunet, J., Roloff, A., 2010. Climate change impacts on stand structure and competitive interactions in a southern Swedish spruce-beech forest. Eur. J. For. Res. 129, 261–276. https://doi.org/10.1007/s10342-009-0323-1

Bonan, G., 2015. Ecological climatology: concepts and applications. Cambridge University Press.

Breda, N.J.J., 2003. Ground- based measurements of leaf area index: a review of methods, instruments and current controversies. J. Exp. Bot. 54, 2403–2417.

Brienen, R.J.W., Phillips, O.L., Feldpausch, T.R., Gloor, E., Baker, T.R., Lloyd, J.,

Lopez-Gonzalez, G., Monteagudo-Mendoza, A., Malhi, Y., Lewis, S.L., 2015. Long-term decline of the Amazon carbon sink. Nature 519, 344–348.

Büntgen, U., Urban, O., Krusic, P.J., Rybníček, M., Kolář, T., Kyncl, T., Ač, A., Koňasová, E., Čáslavský, J., Esper, J., 2021. Recent European drought extremes beyond Common Era background variability. Nat. Geosci. 14, 190–196.

Camacho, F., Fuster, B., Li, W., Weiss, M., Ganguly, S., Lacaze, R., Baret, F., 2021. Crop specific algorithms trained over ground measurements provide the best performance for GAI and fAPAR estimates from Landsat-8 observations. Remote Sens. Environ. 260, 112453.

Carrer, D., Roujean, J.L., Lafont, S., Calvet, J.C., Boone, A., Decharme, B., Delire, C., Gastellu-Etchegorry, J.P., 2013. A canopy radiative transfer scheme with explicit FAPAR for the interactive vegetation model ISBA-A-gs: Impact on carbon fluxes. J. Geophys. Res. Biogeosciences 118, 888–903. https://doi.org/10.1002/jgrg.20070

Černý, J., Haninec, P., Pokorný, R., 2020. Leaf area index estimated by direct, semi-direct, and indirect methods in European beech and sycamore maple stands. J. For. Res. 31, 827–836. https://doi.org/10.1007/s11676-018-0809-0

Chen, J.M., Black, T.A., 1992. Defining leaf area index for non- flat leaves. Plant. Cell Environ. 15, 421–429.

Chen, J.M., Menges, C.H., Leblanc, S.G., 2005. Global mapping of foliage clumping index using multi-angular satellite data. Remote Sens. Environ. 97, 447–457.

Chen, Y., Sun, K., Chen, C., Bai, T., Park, T., Wang, W., Nemani, R.R., Myneni, R.B., 2019. Generation and evaluation of LAI and FPAR products from Himawari-8 advanced Himawari imager (AHI) data. Remote Sens. 11. https://doi.org/10.3390/rs11131517

Chianucci, F., Cutini, A., 2012. Digital hemispherical photography for estimating forest canopy properties: Current controversies and opportunities. IForest 5, 290–295. https://doi.org/10.3832/ifor0775-005

Claverie, M., Matthews, J.L., Vermote, E.F., Justice, C.O., 2016. A 30+ year AVHRR LAI and FAPAR climate data record: Algorithm description and validation. Remote Sens. 8, 1–12. https://doi.org/10.3390/rs8030263

Corke, P., Wark, T., Jurdak, R., Hu, W., Valencia, P., Moore, D., 2010. Environmental wireless sensor networks. Proc. IEEE 98, 1903–1917. https://doi.org/10.1109/JPROC.2010.2068530

Culvenor, D.S., Newnham, G.J., Mellor, A., Sims, N.C., Haywood, A., 2014. Automated in-situ laser scanner for monitoring forest leaf area index. Sensors 14, 14994–15008.

Danson, F.M., Hetherington, D., Morsdorf, F., Koetz, B., Allgöwer, B., 2007. Forest canopy gap fraction from terrestrial laser scanning. IEEE Geosci. Remote Sens. Lett. 4, 157–160. https://doi.org/10.1109/LGRS.2006.887064

Dawson, T.P., North, P.R.J., Plummer, S.E., Curran, P.J., 2003. Forest ecosystem chlorophyll content: implications for remotely sensed estimates of net primary productivity. Int. J. Remote Sens. 24, 611–617.

de Brito, M.M., Kuhlicke, C., Marx, A., 2020. Near-real-time drought impact assessment: a text mining approach on the 2018/19 drought in Germany. Environ. Res. Lett. 15, 1040a9.

Díaz-Ramírez, A., Tafoya, L.A., Atempa, J.A., Mejía-Alvarez, P., 2012. Wireless Sensor Networks and Fusion Information Methods for Forest Fire Detection. Procedia Technol. 3, 69–79. https://doi.org/10.1016/j.protcy.2012.03.008

Diffey, B., 2004. Climate change, ozone depletion and the impact on ultraviolet exposure of human skin. Phys. Med. Biol. 49. https://doi.org/10.1088/0031-9155/49/1/R01

Dong, T., Liu, J., Shang, J., Qian, B., Huffman, T., Zhang, Y., Champagne, C., Daneshfar, B., 2016. Assessing the impact of climate variability on cropland productivity in the Canadian Prairies using time series MODIS FAPAR. Remote Sens. 8. https://doi.org/10.3390/rs8040281

Dong, T., Meng, J., Shang, J., Liu, J., Wu, B., 2015. Evaluation of chlorophyll-related vegetation indices using simulated Sentinel-2 data for estimation of crop fraction of absorbed photosynthetically active radiation. IEEE J. Sel. Top. Appl. Earth Obs. Remote Sens. 8, 4049–4059.

Ellison, D., Morris, C.E., Locatelli, B., Sheil, D., Cohen, J., Murdiyarso, D., Gutierrez, V., Noordwijk, M. van, Creed, I.F., Pokorny, J., Gaveau, D., Spracklen, D. V., Tobella, A.B., Ilstedt, U., Teuling, A.J., Gebrehiwot, S.G., Sands, D.C., Muys, B., Verbist, B., Springgay, E., Sugandi, Y., Sullivan, C.A., 2017. Trees, forests and water: Cool insights

for a hot world. Glob. Environ. Chang. https://doi.org/10.1016/j.gloenvcha.2017.01.002

Fan, W., Liu, Y., Xu, X., Chen, G., Zhang, B., 2014. A new FAPAR analytical model based on the law of energy conservation: A case study in China. IEEE J. Sel. Top. Appl. Earth Obs. Remote Sens. 7, 3945–3955.

Fensholt, R., Sandholt, I., Rasmussen, M.S., 2004. Evaluation of MODIS LAI, fAPAR and the relation between fAPAR and NDVI in a semi-arid environment using in situ measurements. Remote Sens. Environ. 91, 490–507. https://doi.org/10.1016/j.rse.2004.04.009

Ferre, J.A., Pawlowski, A., Guzman, J.L., Rodriguez, F., Berenguel, M., 2010. A wireless sensor network for greenhouse climate monitoring, in: 2010 Fifth International Conference on Broadband and Biomedical Communications. IEEE, pp. 1–5.

Francis, J.A., Wu, B., 2020. Why has no new record-minimum Arctic sea-ice extent occurred since September 2012? Environ. Res. Lett. 15, 114034.

Franklin, M., 2014. Solution to Ordinary and Universal Kriging Equations 1–5.

Frazer, G.W., Canham, C.D., Lertzman, K.P., 1999. Gap Light Analyzer (GLA), Version 2.0: Imaging software to extract canopy structure and gap light transmission indices from true-colour fisheye photographs, users manual and program documentation. Simon Fraser Univ. Burn. Br. Columbia, Inst. Ecosyst. Stud. Millbrook, New York 36.

Friedlingstein, P., 2015. Carbon cycle feedbacks and future climate change. Philos. Trans. R.

Soc. A Math. Phys. Eng. Sci. 373, 20140421.

Friedlingstein, P., Bopp, L., Ciais, P., Dufresne, J., Fairhead, L., LeTreut, H., Monfray, P., Orr, J., 2001. Positive feedback between future climate change and the carbon cycle. Geophys. Res. Lett. 28, 1543–1546.

Friedlingstein, P., Dufresne, J.-L., Cox, P.M., Rayner, P., 2003. How positive is the feedback between climate change and the carbon cycle? Tellus B Chem. Phys. Meteorol. 55, 692–700.

Fritsch, S., Machwitz, M., Ehammer, A., Conrad, C., Dech, S., 2012. Validation of the collection 5 MODIS FPAR product in a heterogeneous agricultural landscape in arid Uzbekistan using multitemporal RapidEye imagery. Int. J. Remote Sens. 33, 6818–6837.

Fu, G., Wu, J.-S., 2017. Validation of MODIS collection 6 FPAR/LAI in the alpine grassland of the Northern Tibetan Plateau. Remote Sens. Lett. 8, 831–838.

G. Pastorello, G.A. Sanchez-Azofeifa, M.N., 2011. Enviro-Net: From Networks of Ground-Based Sensor Systems to a Web Platform for Sensor Data Management. Sensors 11, 6454.

García, E.M., Bermúdez, A., Casado, R., Quiles, F.J., 2007. Wireless sensor network localization using hexagonal intersection. IFIP Int. Fed. Inf. Process. 248, 155–166. https://doi.org/10.1007/978-0-387-74899-3_14

Garrigues, S., Shabanov, N. V., Swanson, K., Morisette, J.T., Baret, F., Myneni, R.B., 2008.

Intercomparison and sensitivity analysis of Leaf Area Index retrievals from LAI-2000, AccuPAR, and digital hemispherical photography over croplands. Agric. For. Meteorol. 148, 1193–1209. https://doi.org/10.1016/j.agrformet.2008.02.014

GCOS, 2016. The global observing system for climate: Implementation needs (GCOS- 200).

Geoffrey Craggs, 2016. Photosynthesis and its Role in Climate Change and Soil Regeneration - Future Directions International.

Gobron, N., Verstraete, M.M., 2009. Fraction of Absorbed Photosynthetically Active Radiation (FAPAR). Assess. status Dev. Stand. Terr. Essent. Clim. Var. 24.

Goude, M., Nilsson, U., Holmström, E., 2019. Comparing direct and indirect leaf area measurements for Scots pine and Norway spruce plantations in Sweden. Eur. J. For. Res. 138, 1033–1047.

Gu, Z., Cao, S., Sanchez-Azofeifa, G.A., 2018. Using LiDAR waveform metrics to describe and identify successional stages of tropical dry forests. Int. J. Appl. Earth Obs. Geoinf. 73, 482–492. https://doi.org/10.1016/j.jag.2018.07.010

Hardwick, S.R., Toumi, R., Pfeifer, M., Turner, E.C., Nilus, R., Ewers, R.M., 2015. The relationship between leaf area index and microclimate in tropical forest and oil palm plantation: Forest disturbance drives changes in microclimate. Agric. For. Meteorol. 201, 187–195. https://doi.org/10.1016/j.agrformet.2014.11.010

Hiltner, U., Huth, A., Fischer, R., 2020. Importance of succession in estimating biomass loss:

Combining remote sensing and individual-based forest models. Biogeosciences Discuss. 1–23. https://doi.org/10.5194/bg-2020-264

Hovi, A., Lukeš, P., Rautiainen, M., 2017. Seasonality of albedo and FAPAR in a boreal forest. Agric. For. Meteorol. 247, 331–342.

Hu, J., Su, Y., Tan, B., Huang, D., Yang, W., Schull, M., Bull, M.A., Martonchik, J. V., Diner, D.J., Knyazikhin, Y., Myneni, R.B., 2007. Analysis of the MISR LAI/FPAR product for spatial and temporal coverage, accuracy and consistency. Remote Sens. Environ. 107, 334–347. https://doi.org/10.1016/j.rse.2006.06.020

Hu, Q., Yang, J., Xu, B., Huang, J., Memon, M.S., Yin, G., Zeng, Y., Zhao, J., Liu, K., 2020. Impact of photosynthetic active radiation on performance of tea crop under agro forestry eco system in eastern India. Remote Sens. 12, 912.

Hubau, W., Lewis, S.L., Phillips, O.L., Affum-Baffoe, K., Beeckman, H., Cuní-Sanchez, A., Daniels, A.K., Ewango, C.E.N., Fauset, S., Mukinzi, J.M., 2020. Asynchronous carbon sink saturation in African and Amazonian tropical forests. Nature 579, 80–87.

Imbach, P., Molina, L., Locatelli, B., Roupsard, O., Mahé, G., Neilson, R., Corrales, L., Scholze, M., Ciais, P., 2012. Modeling potential equilibrium states of vegetation and terrestrial water cycle of Mesoamerica under climate change scenarios. J. Hydrometeorol. 13, 665–680.

J. Antonio Guzmán Q., 2021. Package ‘ rTLS .’

Jiao, T., Williams, C.A., Rogan, J., De Kauwe, M.G., Medlyn, B.E., 2020. Drought Impacts on Australian Vegetation During the Millennium Drought Measured With Multisource Spaceborne Remote Sensing. J. Geophys. Res. Biogeosciences 125, 1–19. https://doi.org/10.1029/2019JG005145

Jonckheere, I., Fleck, S., Nackaerts, K., Muys, B., Coppin, P., Weiss, M., Baret, F., 2004. Review of methods for in situ leaf area index determination Part I. Theories, sensors and hemispherical photography. Agric. For. Meteorol. 121, 19–35. https://doi.org/10.1016/j.agrformet.2003.08.027

Kamnik, R., Nekrep Perc, M., Topolšek, D., 2020. Using the scanners and drone for comparison of point cloud accuracy at traffic accident analysis. Accid. Anal. Prev. 135. https://doi.org/10.1016/j.aap.2019.105391

Khaine, I., Woo, S.Y., 2015a. An overview of interrelationship between climate change and forests. Forest Sci. Technol. 11, 11–18. https://doi.org/10.1080/21580103.2014.932718

Khaine, I., Woo, S.Y., 2015b. An overview of interrelationship between climate change and forests. Forest Sci. Technol. 11, 11–18. https://doi.org/10.1080/21580103.2014.932718

Kiš, I.M., 2016. Comparison of ordinary and universal kriging interpolation techniques on a depth variable (a case of linear spatial trend), case study of the Šandrovac Field. Rud. Geol. Naft. Zb. 31, 41–58. https://doi.org/10.17794/rgn.2016.2.4

Knorr, W., Gobron, N., Scholze, M., Kaminski, T., Pinty, B., 2005. Global drought conditions causing recent atmospheric carbon dioxide increase. Eos Trans. AGU 86, 178–181.

Kolář, T., Čermák, P., Trnka, M., Žid, T., Rybníček, M., 2017. Temporal changes in the climate sensitivity of Norway spruce and European beech along an elevation gradient in Central Europe. Agric. For. Meteorol. 239, 24–33.

Kotamäki, N., Thessler, S., Koskiaho, J., Hannukkala, A., Huitu, H., Huttula, T., Havento, J., Järvenpää, M., 2009. Wireless in-situ Sensor Network for Agriculture and Water Monitoring on a River Basin Scale in Southern Finland: Evaluation from a Data User's Perspective. Sensors 9, 2862–2883. https://doi.org/10.3390/s90402862

Krelling, P.C.L., González-Jorge, H., Martínez-Sanchez, J., Arias, P., 2012. Accuracy in target center evaluation using Riegl LMS Z390i laser scanner and Riscan pro software. Opt. Appl. 42, 773–781. https://doi.org/10.5277/oa120409

Küßner, R., Mosandl, R., 2000. Comparison of direct and indirect estimation of leaf area index in mature Norway spruce stands of eastern Germany. Can. J. For. Res. 30, 440–447. https://doi.org/10.1139/x99-227

Kuusk, A., Pisek, J., Lang, M., Märdla, S., 2018. Estimation of gap fraction and foliage clumping in forest canopies. Remote Sens. 10, 1153.

Li, W., Fang, H., 2015. Estimation of direct, diffuse, and total FPARs from Landsat surface reflectance data and ground- based estimates over six FLUXNET sites. J. Geophys. Res. Biogeosciences 120, 96–112.

Li, W., Weiss, M., Waldner, F., Defourny, P., Demarez, V., Morin, D., Hagolle, O., Baret, F., 2015. A generic algorithm to estimate LAI, FAPAR and FCOVER variables from

SPOT4_HRVIR and landsat sensors: Evaluation of the consistency and comparison with ground measurements. Remote Sens. 7, 15494–15516. https://doi.org/10.3390/rs71115494

Li, X., Liang, H., Cheng, W., 2020. Spatio-temporal variation in AOD and correlation analysis with PAR and NPP in China from 2001 to 2017. Remote Sens. 12. https://doi.org/10.3390/rs12060976

Liang, S., Hou, X., Sui, X., Wang, M., 2017. Deciduous broadleaf forests green FPAR and its relationship with spectral vegetation indices, in: 2017 10th International Congress on Image and Signal Processing, BioMedical Engineering and Informatics (CISP-BMEI). IEEE, pp. 1–5.

Liang, X., Hyyppä, J., Kaartinen, H., Holopainen, M., Melkas, T., 2012. Detecting changes in forest structure over time with bi-temporal terrestrial laser scanning data. ISPRS Int. J. Geo-Information 1, 242–255.

Liu, L., Zhang, X., Xie, S., Liu, X., Song, B., Chen, S., Peng, D., 2019. Global white-sky and black-sky fapar retrieval using the energy balance residual method: Algorithm and validation. Remote Sens. 11, 1004.

Lovell, J.L., Jupp, D.L.B., Gorsel, E. van, Jimenez-Berni, J., Hopkinson, C., Chasmer, L., van Gorsel, E., 2011. Foliage profiles from ground based waveform and discrete point lidar. Proc. SilviLaser 2011, 11th Int. Conf. LiDAR Appl. Assess. For. Ecosyst. Univ. Tasmania, Aust. 16-20 Oct. 2011 4, 1–10.

Luo, S., Wang, C., Xi, X., Pan, F., 2014. Estimating FPAR of maize canopy using airborne discrete-return LiDAR data. Opt. Express 22, 5106–5117.

Luoma, V., Yrttimaa, T., Kankare, V., Saarinen, N., Pyörälä, J., Kukko, A., Kaartinen, H., Hyyppä, J., Holopainen, M., Vastaranta, M., 2021. Revealing changes in the stem form and volume allocation in diverse boreal forests using two-date terrestrial laser scanning. Forests 12, 835.

Ma, L., Zheng, G., Eitel, J.U.H., Magney, T.S., Moskal, L.M., 2017. Retrieving forest canopy extinction coefficient from terrestrial and airborne lidar. Agric. For. Meteorol. 236, 1–21.

Majasalmi, T., 2015. Estimation of leaf area index and the fraction of absorbed photosynthetically active radiation in a boreal forest. Diss. For.

Majasalmi, T., Rautiainen, M., Stenberg, P., 2014. Modeled and measured fPAR in a boreal forest: Validation and application of a new model. Agric. For. Meteorol. 189, 118–124.

Matin, M.A., Islam, M.M., 2012. Overview of wireless sensor network. Wirel. Sens. networks-technology Protoc. 1–3.

Mchugh, M.L., 2013. The Chi-square test of independence Lessons in biostatistics. Biochem. Medica 23, 143–9.

Medlyn, B.E., Dreyer, E., Ellsworth, D., Forstreuter, M., Harley, P.C., Kirschbaum, M.U.F., Le Roux, X., Montpied, P., Strassemeyer, J., Walcroft, A., 2002. Temperature response of parameters of a biochemically based model of photosynthesis. II. A review of

experimental data. Plant. Cell Environ. 25, 1167–1179.

Mitchard, E.T.A., 2018. The tropical forest carbon cycle and climate change. Nature 559, 527–534. https://doi.org/10.1038/s41586-018-0300-2

Mo, X., Liu, S., Chen, X., Hu, S., 2018. Variability, tendencies, and climate controls of terrestrial evapotranspiration and gross primary productivity in the recent decade over China. Ecohydrology 11, 1–13. https://doi.org/10.1002/eco.1951

Montgomery, R.A., Chazdon, R.L., 2001. Forest structure, canopy architecture, and light transmittance in tropical wet forests. Ecology 82, 2707–2718. https://doi.org/10.1890/0012-9658(2001)082[2707:FSCAAL]2.0.CO;2

Moreno, Á., García-Haro, F.J., Martínez, B., Gilabert, M.A., 2014. Noise reduction and gap filling of fAPAR time series using an adapted local regression filter. Remote Sens. 6, 8238–8260. https://doi.org/10.3390/rs6098238

Mortazavi, S.H., Salehe, M., MacGregor, M.H., 2014. Maximum WSN coverage in environments of heterogeneous path loss. Int. J. Sens. Networks 16, 185–198. https://doi.org/10.1504/IJSNET.2014.066788

Mõttus, M., Sulev, M., Baret, F., Lopez-Lozano, R., Reinart, A., 2012. Photosynthetically active radiation: measurement and modeling, in: Encyclopedia of Sustainability Science and Technology. Springer, pp. 7970–8000.

Mukherjee, A., Sarkar, S., 2016. Impact of photosynthetic active radiation on performance of

tea crop under agro forestry eco system in eastern India. Ital. J. Agrometeorol. Ital. DI Agrometeorol. 21, 37–46.

Murphy, G.E., Acuna, M.A., Dumbrell, I., 2010. Tree value and log product yield determination in radiata pine (Pinus radiata) plantations in Australia: comparisons of terrestrial laser scanning with a forest inventory system and manual measurements. Can. J. For. Res. 40, 2223–2233.

Muss, J.D., Aguilar-Amuchastegui, N., Mladenoff, D.J., Henebry, G.M., 2013. Analysis of waveform lidar data using shape-based metrics. IEEE Geosci. Remote Sens. Lett. 10, 106–110. https://doi.org/10.1109/LGRS.2012.2194472

Mussche, S., Samson, R., Nachtergale, L., De Schrijver, A., Lemeur, R., Lust, N., 2001. A comparison of optical and direct methods for monitoring the seasonal dynamics of leaf area index in deciduous forests. Silva Fenn. 35, 373–384. https://doi.org/10.14214/sf.575

Myneni, R.B., 2001. Retrieving LAI and FPAR from MERIS Data With Advanced Algorithms.

Myneni, Ranga B, Hoffman, S., Knyazikhin, Y., Privette, J.L., Glassy, J., Tian, Y., Wang, Y., Song, X., Zhang, Y., Smith, G.R., 2002. Global products of vegetation leaf area and fraction absorbed PAR from year one of MODIS data. Remote Sens. Environ. 83, 214–231.

Myneni, R. B., Hoffman, S., Knyazikhin, Y., Privette, J.L., Glassy, J., Tian, Y., Wang, Y., Song, X., Zhang, Y., Smith, G.R., Lotsch, A., Friedl, M., Morisette, J.T., Votava, P.,

Nemani, R.R., Running, S.W., 2002. Global products of vegetation leaf area and fraction absorbed PAR from year one of MODIS data. Remote Sens. Environ. 83, 214–231. https://doi.org/10.1016/S0034-4257(02)00074-3

National Academies of Sciences and Medicine, E., 2016. Attribution of extreme weather events in the context of climate change. National Academies Press.

Nestola, E., Sánchez-Zapero, J., Latorre, C., Mazzenga, F., Matteucci, G., Calfapietra, C., Camacho, F., 2017. Validation of PROBA-V GEOV1 and MODIS C5 & C6 fAPAR products in a deciduous beech forest site in Italy. Remote Sens. 9, 126.

Ogaya, R., Barbeta, A., Başnou, C., Peñuelas, J., 2015. Satellite data as indicators of tree biomass growth and forest dieback in a Mediterranean holm oak forest. Ann. For. Sci. 72, 135–144.

Oliver, M.A., Webster, R., 1990. Kriging: A method of interpolation for geographical information systems. Int. J. Geogr. Inf. Syst. 4, 313–332. https://doi.org/10.1080/02693799008941549

Orman, O., Dobrowolska, D., 2017. Gap dynamics in the Western Carpathian mixed beech old-growth forests affected by spruce bark beetle outbreak. Eur. J. For. Res. 136, 571–581.

Öztürk, M., Bolat, I., Ergün, A., 2015. Influence of air-soil temperature on leaf expansion and LAI of Carpinus betulus trees in a temperate urban forest patch. Agric. For. Meteorol. 200, 185–191. https://doi.org/10.1016/j.agrformet.2014.09.014

Parker, G.G., 2020. Tamm review: Leaf Area Index (LAI) is both a determinant and a consequence of important processes in vegetation canopies. For. Ecol. Manage. 477. https://doi.org/10.1016/j.foreco.2020.118496

Pastorello, G.Z., Sanchez-Azofeifa, G.A., Nascimento, M.A., 2011. Enviro-Net: From networks of ground-based sensor systems to a web platform for sensor data management. Sensors 11, 6454–6479.

Paul, C., Brandl, S., Friedrich, S., Falk, W., Härtl, F., Knoke, T., 2019. Climate change and mixed forests: how do altered survival probabilities impact economically desirable species proportions of Norway spruce and European beech? Ann. For. Sci. 76, 1–15. https://doi.org/10.1007/s13595-018-0793-8

Pawlowski, A., Guzman, J.L., Rodríguez, F., Berenguel, M., Sánchez, J., Dormido, S., 2009. Simulation of greenhouse climate monitoring and control with wireless sensor network and event-based control. Sensors 9, 232–252. https://doi.org/10.3390/s90100232

Peng, D., Zhang, B., Liu, Liangyun, Fang, H., Chen, D., Hu, Y., Liu, Lingling, 2012. Characteristics and drivers of global NDVI- based FPAR from 1982 to 2006. Global Biogeochem. Cycles 26.

Pickett-Heaps, C.A., Canadell, J.G., Briggs, P.R., Gobron, N., Haverd, V., Paget, M.J., Pinty, B., Raupach, M.R., 2014. Evaluation of six satellite-derived Fraction of Absorbed Photosynthetic Active Radiation (FAPAR) products across the Australian continent. Remote Sens. Environ. 140, 241–256. https://doi.org/10.1016/j.rse.2013.08.037

Pokorný, R., Stojnič, S., 2012. Leaf area index of Norway spruce stands in relation to age and defoliation. Beskydy 5, 173–180. https://doi.org/10.11118/beskyd201205020173

Pretzsch, H., Grams, T., Häberle, K.H., Pritsch, K., Bauerle, T., Rötzer, T., 2020. Growth and mortality of Norway spruce and European beech in monospecific and mixed-species stands under natural episodic and experimentally extended drought. Results of the KROOF throughfall exclusion experiment. Trees - Struct. Funct. 34, 957–970. https://doi.org/10.1007/s00468-020-01973-0

Pretzsch, Hans, Hilmers, T., Biber, P., Avdagić, A., Binder, F., Bončina, A., Bosela, M., Dobor, L., Forrester, D.I., Lévesque, M., 2020. Evidence of elevation-specific growth changes of spruce, fir, and beech in European mixed mountain forests during the last three centuries. Can. J. For. Res. 50, 689–703.

Pretzsch, H., Rötzer, T., Matyssek, R., Grams, T.E.E., Häberle, K.-H., Pritsch, K., Kerner, R., Munch, J.-C., 2014. Mixed Norway spruce (Picea abies [L.] Karst) and European beech (Fagus sylvatica [L.]) stands under drought: from reaction pattern to mechanism. Trees 28, 1305–1321.

Pretzsch, H., Schütze, G., Biber, P., 2018. Drought can favour the growth of small in relation to tall trees in mature stands of Norway spruce and European beech. For. Ecosyst. 5, 1–19.

Pu, J., Yan, K., Zhou, G., Lei, Y., Zhu, Y., Guo, D., Li, H., Xu, L., Knyazikhin, Y., Myneni, R.B., 2020. Evaluation of the MODIS LAI/FPAR algorithm based on 3D-RTM

simulations: A case study of grassland. Remote Sens. 12, 3391.

Putzenlechner, B., Castro, S., Kiese, R., Ludwig, R., Marzahn, P., Sharp, I., Sanchez-Azofeifa, A., 2019a. Validation of Sentinel-2 fAPAR products using ground observations across three forest ecosystems. Remote Sens. Environ. 232, 111310. https://doi.org/10.1016/j.rse.2019.111310

Putzenlechner, B., Marzahn, P., Kiese, R., Ludwig, R., Sanchez-Azofeifa, A., 2019b. Assessing the variability and uncertainty of two-flux FAPAR measurements in a conifer-dominated forest. Agric. For. Meteorol. 264, 149–163. https://doi.org/10.1016/j.agrformet.2018.10.007

Putzenlechner, B., Marzahn, P., Sanchez-azofeifa, A., 2020. Accuracy assessment on the number offlux terms needed to estimate in situ fAPAR. Int J Appl Earth Obs Geoinf. 88, 102061. https://doi.org/10.1016/j.jag.2020.102061

Qin, H., Wang, C., Pan, F., Lin, Y., Xi, X., Luo, S., 2017. Estimation of FPAR and FPAR profile for maize canopies using airborne LiDAR. Ecol. Indic. 83, 53–61.

Qu, Y., Zhu, Y., Han, W., Wang, J., Ma, M., 2014. Crop leaf area index observations with a wireless sensor network and its potential for validating remote sensing products. IEEE J. Sel. Top. Appl. Earth Obs. Remote Sens. 7, 431–444. https://doi.org/10.1109/JSTARS.2013.2289931

Rankine, C.J., Sanchez-Azofeifa, G.A., Macgregor, M.H., 2014. Seasonal wireless sensor network link performance in boreal forest phenology monitoring. 2014 11th Annu. IEEE

Int. Conf. Sensing, Commun. Networking, SECON 2014 302–310. https://doi.org/10.1109/SAHCN.2014.6990366

Reiche, J., Lucas, R., Mitchell, A.L., Verbesselt, J., Hoekman, D.H., Haarpaintner, J., Kellndorfer, J.M., Rosenqvist, A., Lehmann, E.A., Woodcock, C.E., Seifert, F.M., Herold, M., 2016. Combining satellite data for better tropical forest monitoring. Nat. Clim. Chang. 6, 120–122. https://doi.org/10.1038/nclimate2919

RIEGL, 2019. VZ-400i RIEGL VZ-400i Ultra High Performance 3D Laser Scanner Redefining Productivity 1–2.

Rötzer, T., Biber, P., Moser, A., Schäfer, C., Pretzsch, H., 2017a. Stem and root diameter growth of European beech and Norway spruce under extreme drought. For. Ecol. Manage. 406, 184–195.

Rötzer, T., Häberle, K.H., Kallenbach, C., Matyssek, R., Schütze, G., Pretzsch, H., 2017b. Tree species and size drive water consumption of beech/spruce forests-a simulation study highlighting growth under water limitation. Plant Soil 418, 337–356.

Rukh, S., Poschenrieder, W., Heym, M., Pretzsch, H., 2020. Drought Resistance of Norway Spruce (Picea abies [L.] Karst) and European Beech (Fagus sylvatica [L.]) in Mixed vs. Monospecific Stands and on Dry vs. Wet Sites. From Evidence at the Tree Level to Relevance at the Stand Level. Forests 11, 639.

Ryu, Y., Lee, G., Jeon, S., Song, Y., Kimm, H., 2014. Monitoring multi-layer canopy spring phenology of temperate deciduous and evergreen forests using low-cost spectral sensors.

Remote Sens. Environ. 149, 227–238.

Said, A.A., Yurtal, R., 2019. Spatial Groundwater Quality Assessment Using Geostatistics in Puntland, Somalia. Int. J. Sci. Technol. Res. 5, 84–92.

Sánchez-Azofeifa, G.A., Rankine, C., Do Espirito Santo, M.M., Fatland, R., Garcia, M., 2011. Wireless sensing networks for environmental monitoring: Two case studies from tropical forests. Proc. - 2011 7th IEEE Int. Conf. eScience, eScience 2011 70–76. https://doi.org/10.1109/eScience.2011.18

Sanz- Sáez, Á., Koester, R.P., Rosenthal, D.M., Montes, C.M., Ort, D.R., Ainsworth, E.A., 2017. Leaf and canopy scale drivers of genotypic variation in soybean response to elevated carbon dioxide concentration. Glob. Chang. Biol. 23, 3908–3920.

Schäfer, C., Grams, T.E.E., Rötzer, T., Feldermann, A., Pretzsch, H., 2017. Drought stress reaction of growth and Δ13C in tree rings of European beech and Norway spruce in monospecific versus mixed stands along a precipitation gradient. Forests 8, 177.

Schleppi, P., Conedera, M., Sedivy, I., Thimonier, A., 2007. Correcting non-linearity and slope effects in the estimation of the leaf area index of forests from hemispherical photographs. Agric. For. Meteorol. 144, 236–242.

Schleppi, P., Thimonier, A., Walthert, L., 2011. Estimating leaf area index of mature temperate forests using regressions on site and vegetation data. For. Ecol. Manage. 261, 601–610. https://doi.org/https://doi.org/10.1016/j.foreco.2010.11.013

Schlerf, M., Atzberger, C., Vohland, M., Buddenbaum, H., Seeling, S., Hill, J., 2005. Derivation of forest leaf area index from multi- and hyperspectral remote sensing data. EARSeL eProceedings 3, 405–413.

Senf, C., Buras, A., Zang, C.S., Rammig, A., Seidl, R., 2020. Excess forest mortality is consistently linked to drought across Europe. Nat. Commun. 11, 1–8. https://doi.org/10.1038/s41467-020-19924-1

Senna, M.C.A., Costa, M.H., Shimabukuro, Y.E., 2005. Fraction of photosynthetically active radiation absorbed by Amazon tropical forest: A comparison of field measurements, modeling, and remote sensing. J. Geophys. Res. Biogeosciences 110.

Serbin, S.P., Ahl, D.E., Gower, S.T., 2013. Spatial and temporal validation of the MODIS LAI and FPAR products across a boreal forest wildfire chronosequence. Remote Sens. Environ. 133, 71–84. https://doi.org/10.1016/j.rse.2013.01.022

Shabanov, N. V., Wang, Y., Buermann, W., Dong, J., Hoffman, S., Smith, G.R., Tian, Y., Knyazikhin, Y., Myneni, R.B., 2003. Effect of foliage spatial heterogeneity in the MODIS LAI and FPAR algorithm over broadleaf forests. Remote Sens. Environ. 85, 410–423. https://doi.org/10.1016/S0034-4257(03)00017-8

Sieber, M.H., Thomsen, M.B., Spradling, A.C., 2016. Electron transport chain remodeling by GSK3 during oogenesis connects nutrient state to reproduction. Cell 164, 420–432.

Software, G., 2021. Surfer ® Registration Information.

Solberg, S., Brunner, A., Hanssen, K.H., Lange, H., Næsset, E., Rautiainen, M., Stenberg, P., 2009. Mapping LAI in a Norway spruce forest using airborne laser scanning. Remote Sens. Environ. 113, 2317–2327. https://doi.org/https://doi.org/10.1016/j.rse.2009.06.010

Somerville, R.C.J., 2020. Facts and opinions about climate change. Bull. At. Sci. 76, 331–335.

Sonnentag, O., Talbot, J., Chen, J.M., Roulet, N.T., 2007. Using direct and indirect measurements of leaf area index to characterize the shrub canopy in an ombrotrophic peatland. Agric. For. Meteorol. 144, 200–212.

Srinivasan, S., Popescu, S.C., Eriksson, M., Sheridan, R.D., Ku, N.-W., 2014. Multi-temporal terrestrial laser scanning for modeling tree biomass change. For. Ecol. Manage. 318, 304–317.

Sun, B., Gao, Z., Li, Z., Wang, B., Bai, L., Wu, J., Li, C., Ding, X., 2014. Construction of Monthly Time-Series NPP Datasets over Chinese Terrestrial Based on MERIS FPAR Data During 2002-2012. Dragon 3Mid Term Results 724, 140.

Sun, Y., Qin, Q., Ren, H., Zhang, Y., 2021. Decameter Cropland LAI/FPAR Estimation From Sentinel-2 Imagery Using Google Earth Engine. IEEE Trans. Geosci. Remote Sens.

Süßel, F., Brüggemann, W., 2021. Tree water relations of mature oaks in southwest Germany under extreme drought stress in summer 2018. Plant Stress 1, 100010. https://doi.org/https://doi.org/10.1016/j.stress.2021.100010

Takruri, M., Rajasegarar, S., Challa, S., Leckie, C., Palaniswami, M., 2008. Online drift correction in wireless sensor networks using spatio-temporal modeling. Proc. 11th Int. Conf. Inf. Fusion, FUSION 2008.

Tao, F., Yokozawa, M., Hayashi, Y., Lin, E., 2003. Terrestrial water cycle and the impact of climate change. AMBIO A J. Hum. Environ. 32, 295–301.

Tao, X., Liang, S., He, T., Jin, H., 2016. Estimation of fraction of absorbed photosynthetically active radiation from multiple satellite data: Model development and validation. Remote Sens. Environ. 184, 539–557. https://doi.org/10.1016/j.rse.2016.07.036

Tao, X., Liang, S., Wang, D., 2015. Assessment of five global satellite products of fraction of absorbed photosynthetically active radiation: Intercomparison and direct validation against ground-based data. Remote Sens. Environ. 163, 270–285. https://doi.org/10.1016/j.rse.2015.03.025

Thomas, V., Finch, D.A., McCaughey, J.H., Noland, T., Rich, L., Treitz, P., 2006. Spatial modelling of the fraction of photosynthetically active radiation absorbed by a boreal mixedwood forest using a lidar–hyperspectral approach. Agric. For. Meteorol. 140, 287–307.

Tian, F., Fensholt, R., Verbesselt, J., Grogan, K., Horion, S., Wang, Y., 2015. Evaluating temporal consistency of long-term global NDVI datasets for trend analysis. Remote Sens. Environ. 163, 326–340.

Tian, Y, Dickinson, R.E., Zhou, L., Zeng, X., Dai, Y., Myneni, R.B., Knyazikhin, Y., Zhang,

X., Friedl, M., Yu, H., 2004. Comparison of seasonal and spatial variations of leaf area index and fraction of absorbed photosynthetically active radiation from Moderate Resolution Imaging Spectroradiometer (MODIS) and Common Land Model. J. Geophys. Res. Atmos. 109.

Tian, Y., Dickinson, R.E., Zhou, L., Zeng, X., Dai, Y., Myneni, R.B., Knyazikhin, Y., Zhang, X., Friedl, M., Yu, H., Wu, W., Shaikh, M., 2004. Comparison of seasonal and spatial variations of leaf area index and fraction of absorbed photosynthetically active radiation from Moderate Resolution Imaging Spectroradiometer (MODIS) and Common Land Model. J. Geophys. Res. D Atmos. 109, 1–14. https://doi.org/10.1029/2003jd003777

Turco, M., Levin, N., Tessler, N., Saaroni, H., 2017. Recent changes and relations among drought, vegetation and wildfires in the Eastern Mediterranean: The case of Israel. Glob. Planet. Change 151, 28–35.

Urban, O., 2003. Physiological impacts of elevated CO 2 concentration ranging from molecular to whole plant responses. Photosynthetica 41, 9–20.

Vacek, Z., Vacek, S., Slanar, J., Bilek, L., Bulusek, D., Stefancik, I., Králíček, I., Vancura, K., 2019. Adaption of Norway spruce and European beech forests under climate change: from resistance to close-to-nature silviculture. Cent. Eur. For. JOURNAL, Vol. 65, issue 2.

Vastaranta, M., Melkas, T., Holopainen, M., Kaartinen, H., Hyyppä, J., Hyyppä, H., 2009. Laser-based field measurements in tree-level forest data acquisition. Photogramm. J.

Finl 21, 51–61.

Vose, J.M., Dougherty, P.M., Long, J.N., Smith, F.W., Gholz, H.L., Curran, P.J., 1994. Factors influencing the amount and distribution of leaf area of pine stands. Ecol. Bull. 102–114.

Wang, Y., Fang, H., 2020. Estimation of LAI with the LiDAR technology: a review. Remote Sens. 12, 3457.

Wang, Y., Tian, Y., Zhang, Y., El-Saleous, N., Knyazikhin, Y., Vermote, E., Myneni, R.B., 2001. Investigation of product accuracy as a function of input and model uncertainties: Case study with SeaWiFS and MODIS LAI/FPAR algorithm. Remote Sens. Environ. 78, 299–313.

Wang, Y., Xie, D., Liu, S., Hu, R., Li, Y., Yan, G., 2016. Scaling of FAPAR from the Field to the Satellite. Remote Sens. 8, 310.

Whitmore, T.C., Brown, N.D., Swaine, M.D., Kennedy, D., Goodwin-Bailey, C.I., Gong, W.-K., 1993. Use of hemispherical photographs in forest ecology: measurement of gap size and radiation totals in a Bornean tropical rain forest. J. Trop. Ecol. 9, 131–151.

Widlowski, J.-L., 2010. On the bias of instantaneous FAPAR estimates in open-canopy forests. Agric. For. Meteorol. 150, 1501–1522.

Widlowski, J.L., 2010. On the bias of instantaneous FAPAR estimates in open-canopy forests. Agric. For. Meteorol. 150, 1501–1522. https://doi.org/10.1016/j.agrformet.2010.07.011

Xiao, Z., Liang, S., Sun, R., 2018. Evaluation of three long time series for global fraction of

absorbed photosynthetically active radiation (fapar) products. IEEE Trans. Geosci. Remote Sens. 56, 5509–5524.

Xiao, Z., Liang, S., Wang, T., Jiang, B., 2016. Retrieval of leaf area index (LAI) and fraction of absorbed photosynthetically active radiation (FAPAR) from VIIRS time-series data. Remote Sens. 8. https://doi.org/10.3390/rs8040351

Xu, B., Park, T., Yan, K., Chen, C., Zeng, Y., Song, W., Yin, G., Li, J., Liu, Q., Knyazikhin, Y., Myneni, R.B., 2018. Analysis of global LAI/FPAR products from VIIRS and MODIS sensors for spatio-temporal consistency and uncertainty from 2012-2016. Forests 9, 1–21. https://doi.org/10.3390/f9020073

Yan, G., Hu, R., Luo, J., Weiss, M., Jiang, H., Mu, X., Xie, D., Zhang, W., 2019. Review of indirect optical measurements of leaf area index: Recent advances, challenges, and perspectives. Agric. For. Meteorol. 265, 390–411. https://doi.org/10.1016/j.agrformet.2018.11.033

Yang, F., Ren, H., Li, X., Hu, M., Yang, Y., 2014. Assessment of MODIS, MERIS, GEOV1 FPAR products over Northern China with ground measured data and by analyzing residential effect in mixed pixel. Remote Sens. 6, 5428–5451.

Yang, W., Huang, D., Tan, B., Stroeve, J.C., Shabanov, N. V, Knyazikhin, Y., Nemani, R.R., Myneni, R.B., 2006. Analysis of leaf area index and fraction of PAR absorbed by vegetation products from the terra MODIS sensor: 2000-2005. IEEE Trans. Geosci. Remote Sens. 44, 1829–1842.

Yang, Z.I., Zhang, T. bin, Yi, G. hua, Li, J. ji, Qin, Y. bin, Chen, Y., 2021. Spatio-temporal variation of Fraction of Photosynthetically Active Radiation absorbed by vegetation in the Hengduan Mountains, China. J. Mt. Sci. 18, 891–906. https://doi.org/10.1007/s11629-020-6465-9

Yoshida, Y., Joiner, J., Tucker, C., Berry, J., Lee, J.-E., Walker, G., Reichle, R., Koster, R., Lyapustin, A., Wang, Y., 2015. The 2010 Russian drought impact on satellite measurements of solar-induced chlorophyll fluorescence: Insights from modeling and comparisons with parameters derived from satellite reflectances. Remote Sens. Environ. 166, 163–177.

Younis, M., Akkaya, K., 2008. Strategies and techniques for node placement in wireless sensor networks: A survey. Ad Hoc Networks 6, 621–655. https://doi.org/10.1016/j.adhoc.2007.05.003

Zacharias, S., Bogena, H., Samaniego, L., Mauder, M., Fuß, R., Pütz, T., Frenzel, M., Schwank, M., Baessler, C., Butterbach-Bahl, K., Bens, O., Borg, E., Brauer, A., Dietrich, P., Hajnsek, I., Helle, G., Kiese, R., Kunstmann, H., Klotz, S., Munch, J.C., Papen, H., Priesack, E., Schmid, H.P., Steinbrecher, R., Rosenbaum, U., Teutsch, G., Vereecken, H., 2011. A network of terrestrial environmental observatories in Germany. Vadose Zo. J. 10, 955–973. https://doi.org/10.2136/vzj2010.0139

Zhao, P., Fan, W., Liu, Y., Mu, X., Xu, X., Peng, J., 2016. Study of the remote sensing model of FAPAR over rugged terrains. Remote Sens. 8, 10–12. https://doi.org/10.3390/rs8040309

Zhu, X., Skidmore, A.K., Wang, T., Liu, J., Darvishzadeh, R., Shi, Y., Premier, J., Heurich, M., 2018. Improving leaf area index (LAI) estimation by correcting for clumping and woody effects using terrestrial laser scanning. Agric. For. Meteorol. 263, 276–286. https://doi.org/10.1016/j.agrformet.2018.08.026

Zhu, Z., Bi, J., Pan, Y., Ganguly, S., Anav, A., Xu, L., Samanta, A., Piao, S., Nemani, R.R., Myneni, R.B., 2013. Global data sets of vegetation leaf area index (LAI)3g and fraction of photosynthetically active radiation (FPAR)3g derived from global inventory modeling and mapping studies (GIMMS) normalized difference vegetation index (NDVI3G) for the period 1981 to 2. Remote Sens. 5, 927–948. https://doi.org/10.3390/rs5020927